



0 1160 0038190 9

LOAD ANALYSIS OF HIGHER
ORDER CORRECTION ELEMENTS

Carmen Rotolo

September 30, 1982

I. INTRODUCTION

There are eleven higher order correction element circuits which can be broken up into seven different equivalent circuits. Figure (1) is a summary of the characteristics of the seven circuits to be analyzed. The tune quad circuit requirements are the most stringent and also have ninety elements with a total inductance of 41 H. Hence, the tune quad circuit is analyzed in much greater depth than the others and is done so within the body of this report. Appendix A contains graphs pertinent to the other six circuits.

It is desired to find several characteristics of the load which are important to the overall system. It is necessary to know the impedance seen by the power supply (P. S.) to determine the stability of the system. The effects of P. S. ripple voltage and common mode voltage are necessary to know so as not to exceed the current specifications.

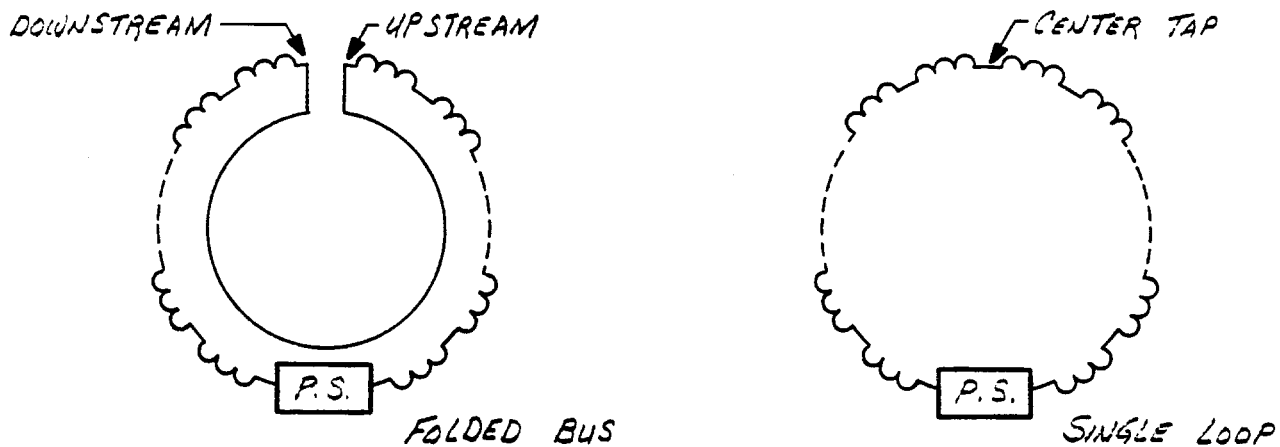
The field producing or excitation currents are not the same as the P. S. current, and it is necessary to know the relationship between them as well as how these currents differ along the bus. It is desired to know the maximum voltage to ground that will occur during a dump.

Lastly, it is desired to know the effect of placing a damping resistor across each magnet which may be necessary to meet some criteria.

II. BACKGROUND

A. Folded Bus/Single Loop

Some of the circuits to be analyzed are identified as having a folded bus and others as being a single loop. The sketch below shows these two different bus configurations.



This paper does not attempt to deal with noise pick-up in either of these configurations. The single loop is used to save money in the circuits which do not require as much accuracy.

B. SPICE Simulation

The circuit analysis program SPICE, which is available on the Cyber, was used to simulate the load. Figure (2) shows a typical SPICE model for the tune quad circuit.

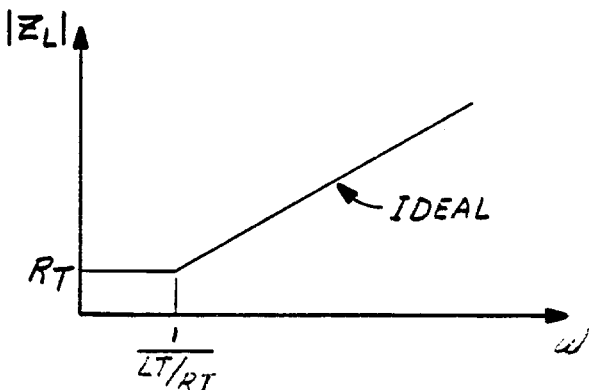
The numbering of nodes in the coil bus and return bus is consistant throughout the analysis so as to easily identify the location of a particular voltage or current along the bus. In some cases, C_1 was placed in parallel with C_2 and the split inductive portion of the model was combined. In other cases, the wire resistance RWCB and RWRB were placed at the opposite end of the subcircuit so that capacitances would be at external nodes of the subcircuit so that initial conditions could be set. The frequency response of the model changes above a few kilohertz when the number of cells are reduced by using multi-valued cells. In cases where frequencies above 1 KHZ were not of interest, as many as four magnets were combined in a single cell. Figure (3) is a table which was developed to help identify the various file names associated with each analysis.

C. Load Without Capacitance

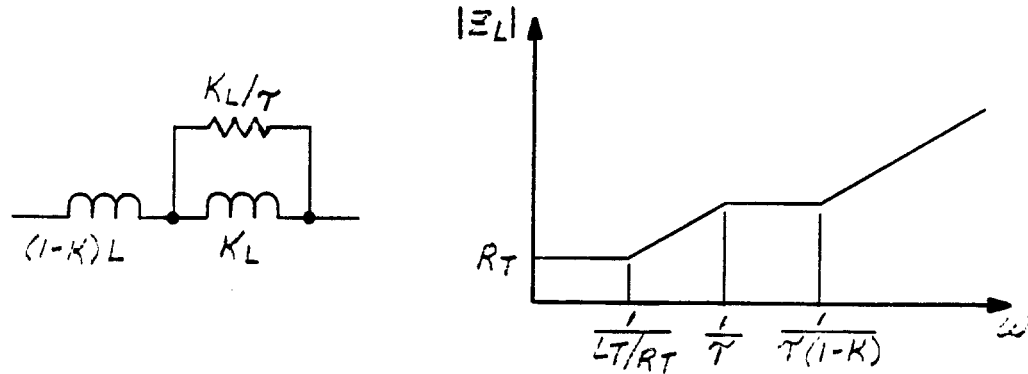
A Bode plot of an ideal load without eddy currents, capacitances, or damping resistors is just a series, R/L .

R_T = TOTAL WIRE RESISTANCE

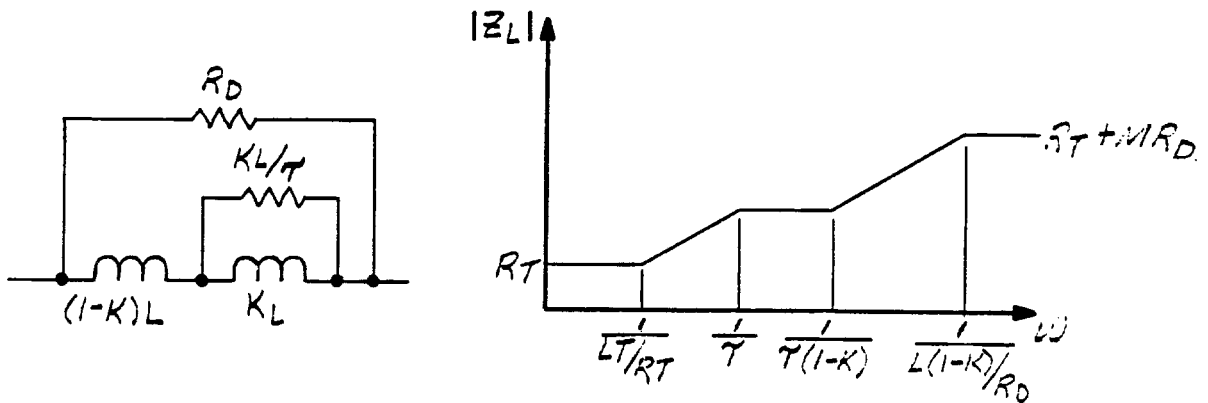
L_T = TOTAL DC INDUCTANCE



If the magnets have eddy currents modeled as shown, the Bode plot becomes:



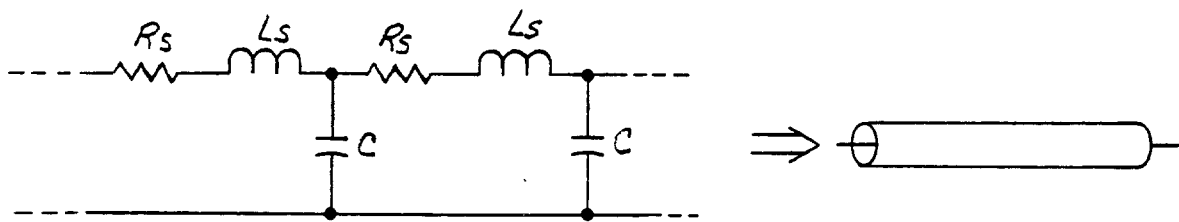
and if a damping resistors R_D were placed across each magnet, and m = total number of magnets.



D. Transmission Line Characteristics

The capacitances associated with each magnet tend to make the load at relatively low frequencies look like a transmission line. This is true of both the folded bus and the single loop since the capacitance to ground is dominant.

Here we will review some of the general equations and characteristics associated with transmission line theory. The references used here and throughout this analysis are indicated at the end of this paper. For a transmission line model:



Let,

$$(1) \quad Z_s = R_s + j\omega L_s$$

$$(2) \quad Y = j\omega C$$

where R_s , L_s , and C are per magnet values. Then, the characteristic impedance Z_0 , and propagation constant, γ are:

$$(3) \quad Z_0 = \sqrt{Z_s/Y} = \frac{\gamma}{Y}$$

$$(4) \quad \gamma = \sqrt{Z_s \cdot Y} = Z_0 \cdot Y = \alpha + j\beta \text{ (magnets}^{-1}\text{)}$$

where, α = attenuation constant

β = phase constant

and the velocity of propagation v is:

$$(5) \quad v = \omega/\beta \text{ (magnets/sec.)}$$

also,

$$(6) \quad \lambda = v/f \text{ (magnets)}$$

where, λ = wavelength in units of magnets for excitation frequency, f .

Substituting (1) and (2) into (4) and separating real and imaginary components yield:

$$(7) \quad \alpha = \frac{R_s}{\sqrt{L_s/C}} \sqrt{\frac{1}{2(1 + \sqrt{1 + 1/Q^2})}}$$

$$(8) \quad \beta = \omega \sqrt{L_s C} \sqrt{\frac{1 + \sqrt{1 + 1/Q^2}}{2}}$$

from which (7) and (8) into (3) yields:

$$(9) \quad |z_0| = \sqrt{\frac{L_s}{C}} \sqrt{\frac{1}{Q^2(1 + \sqrt{1 + 1/Q^2})}}$$

where,

$$Q = \omega L_s / R_s$$

If losses are small such that $Q^2 \gg 1$

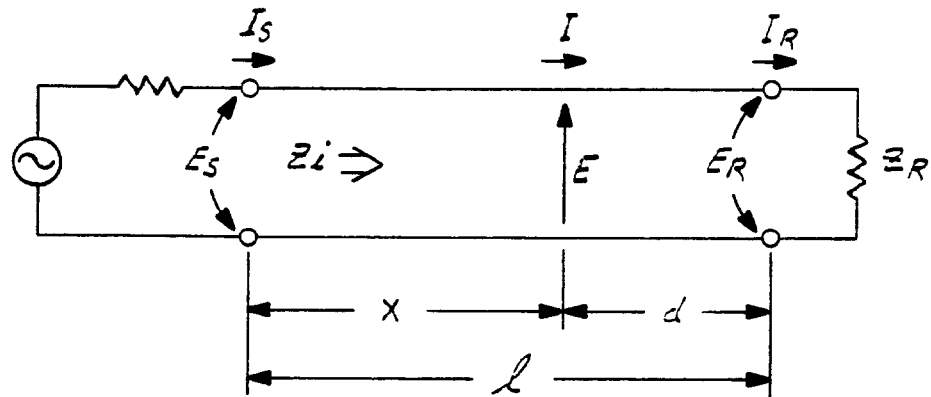
$$(10) \quad \alpha = R_s / 2 \sqrt{L_s / C} = R_s / 2 z_0$$

$$(11) \quad \beta = \omega \sqrt{L_s C}$$

$$(12) \quad z_0 = \sqrt{L_s / C}$$

Actually, a Q as low as 2 yields only a few percent error.

Consider a large uniform transmission line corresponding to a long string of identical magnets of length ℓ in units of magnets.



The general solution of the steady-state differential equations for E and I are²:

$$(13) \quad E = A_1 e^{-\gamma x} + A_2 e^{\gamma x}$$

$$(14) \quad I = \frac{1}{Z_0} (A_1 e^{-\gamma x} - A_2 e^{\gamma x})$$

To express the constant A_1 and A_2 in terms of sending-end quantities, set $E = I_s Z_i$ and $I = I_s$ at $x = 0$. Solving for A_1 and A_2 yields:

$$A_1 = I_s (Z_i + Z_0)/Z$$

$$A_2 = I_s (Z_i - Z_0)/Z$$

Substituting back into (13) and (14), yields E and I in terms of sending-end quantities.

$$(15) \quad E(x) = E = \frac{I_s}{2} \left[(z_i + z_0) e^{-\gamma x} + (z_i - z_0) e^{\gamma x} \right]$$

$$(16) \quad I(x) = I = \frac{I_s}{2z_0} \left[(z_i + z_0) e^{-\gamma x} - (z_i - z_0) e^{\gamma x} \right]$$

For the case where the line is terminated in a short, $z_R = 0$ and hence $E_R = 0$. By setting $E = 0$ and $x = l$ in (15), the sending-end impedance for a shorted line, z_{is} is found to be:

$$(17) \quad z_{is} = \frac{z_0 (e^{\gamma l} - e^{-\gamma l})}{e^{\gamma l} + e^{-\gamma l}} = z_0 \tanh \gamma l$$

Substituting z_{is} for z_i in (15) and (16), E and I for a shorted line of length l in terms of I_s using hyperbolic notation becomes:

$$(18) \quad E = I_s z_0 \left[\tanh \gamma l \cosh \gamma x - \sinh \gamma x \right]$$

$$(19) \quad I = I_s \left[\cosh \gamma x - \tanh \gamma l \sinh \gamma x \right]$$

or in terms of the sending-end voltage E_s , noting that

$$E_s = I_s z_{is}$$

$$(20) \quad E = E_s \left[\cosh \gamma x - \sinh \gamma x / \tanh \gamma l \right]$$

$$(21) \quad I = \frac{E_s}{z_0} \left[\cosh \gamma x / \tanh \gamma l - \sinh \gamma x \right]$$

The Impedance Z at point x is:

$$(22) \quad Z = E/I = z_0 \left[\frac{\tanh \gamma l - \tanh \gamma x}{1 - \tanh \gamma l \tanh \gamma x} \right]$$

Setting $\gamma = \alpha + j\beta$ in (17), the sending-end impedance, Z_{is} becomes:

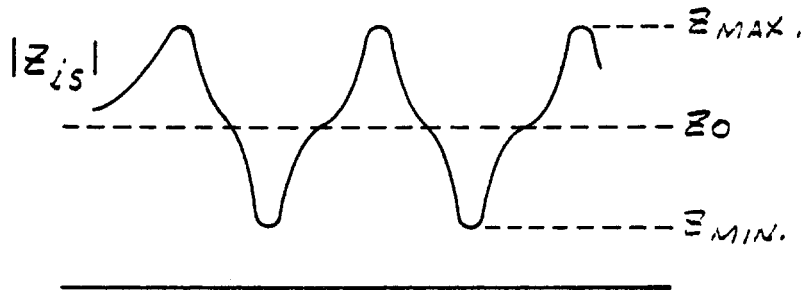
$$(23) \quad Z_{is} = Z_0 \tanh(\alpha l + j\beta l) = Z_0 \frac{\tanh \alpha l + j \tan \beta l}{1 + j \tanh \alpha l \tan \beta l}$$

Since β is nearly a linear function of ω , maximum and minimum occur at odd and even multiples of $\beta l = n/2$, respectively. Z_{is} as a function of frequency is repetitive such that:

$$(24) \quad Z_{max} = Z_0 / \tanh \alpha l \text{ at } f_1, f_3, f_5, \text{ etc.}$$

and

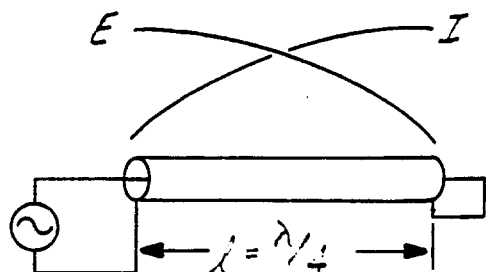
$$(25) \quad Z_{min} = Z_0 \tanh \alpha l \text{ at } f_2, f_4, f_6, \text{ etc.}$$



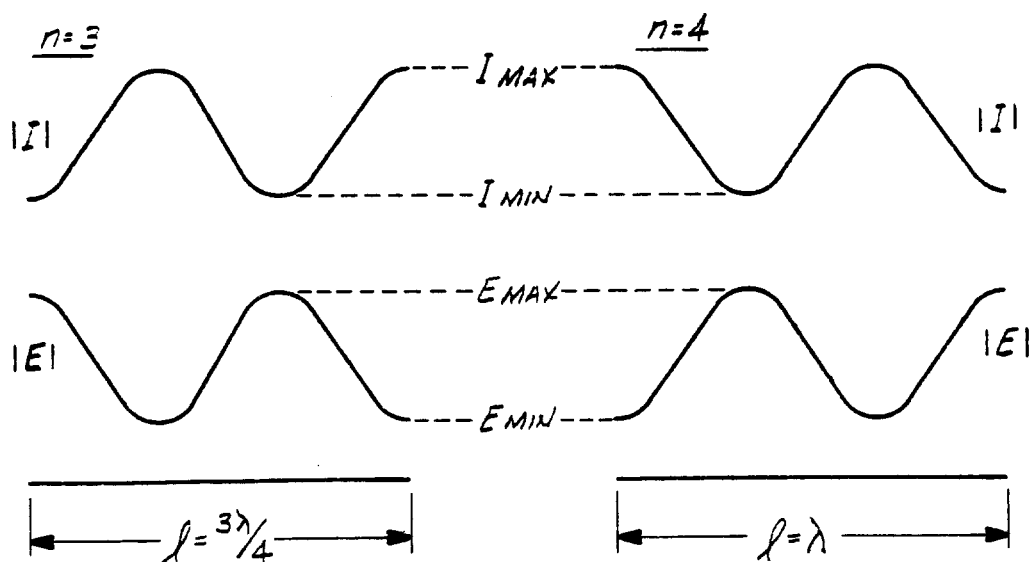
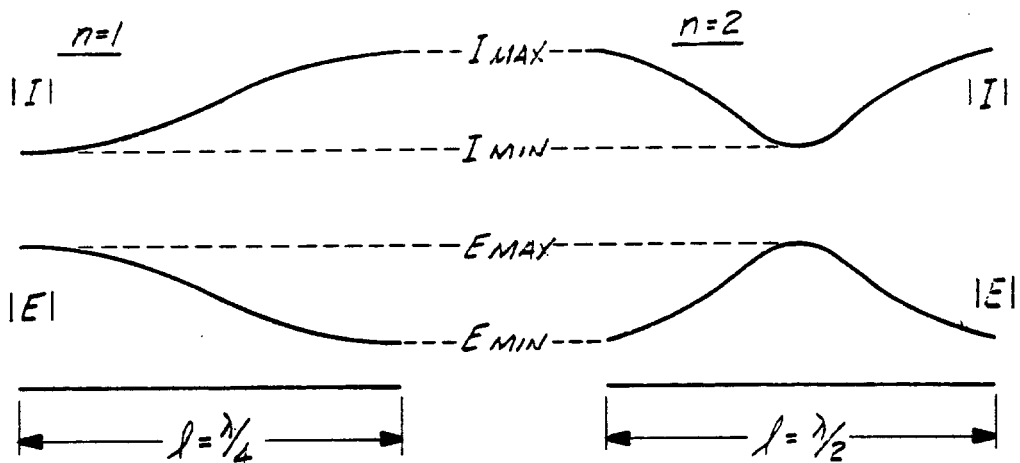
where the frequency of these resonances occur at:

$$(26) \quad f_n = nv/4l = n/4l \sqrt{L_s C}$$

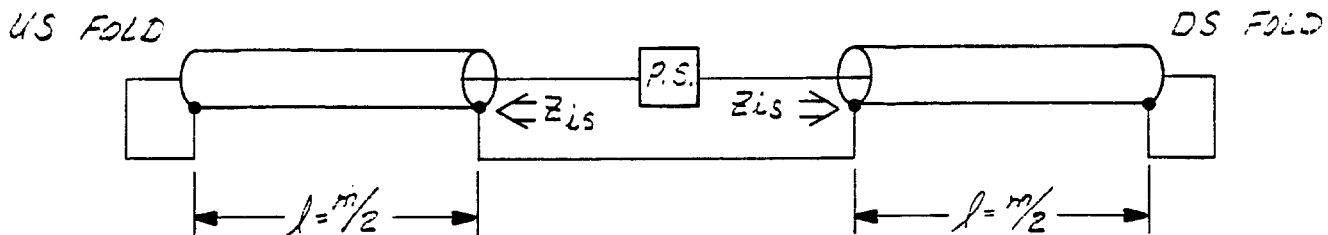
The lowest resonant mode of excitation ($n = 1$) occurs when $l = \lambda/4$ (l = quarter wavelength), and a standing wave pattern of voltage and current would be:



When losses are small, but not negligible, the standing waves of voltage and current at various higher modes of excitation are not uniform along the line. The standing wave patterns are skewed such that the maximums and minimums of $|E|$ and $|I|$ are larger toward the sending end. For the shorted line under consideration $E_{\min} = 0$ at the far end of the line. The standing wave patterns of $|E|$ and $|I|$ for the first few modes of excitation are,



Consider the P. S. to be located at the center of the magnet string. Due to the symmetrical nature of the circuit, the equivalent transmission line model where m is the total number of magnets is:



Due to the series connection of the P. S., it sees a load impedance of $2 z_{is}$ or the sum of sending-end impedance of each segment of the line. Hence,

$$(27) \quad Z_L = 2 z_{is} = 2 z_0 \tanh \gamma \frac{m}{2}$$

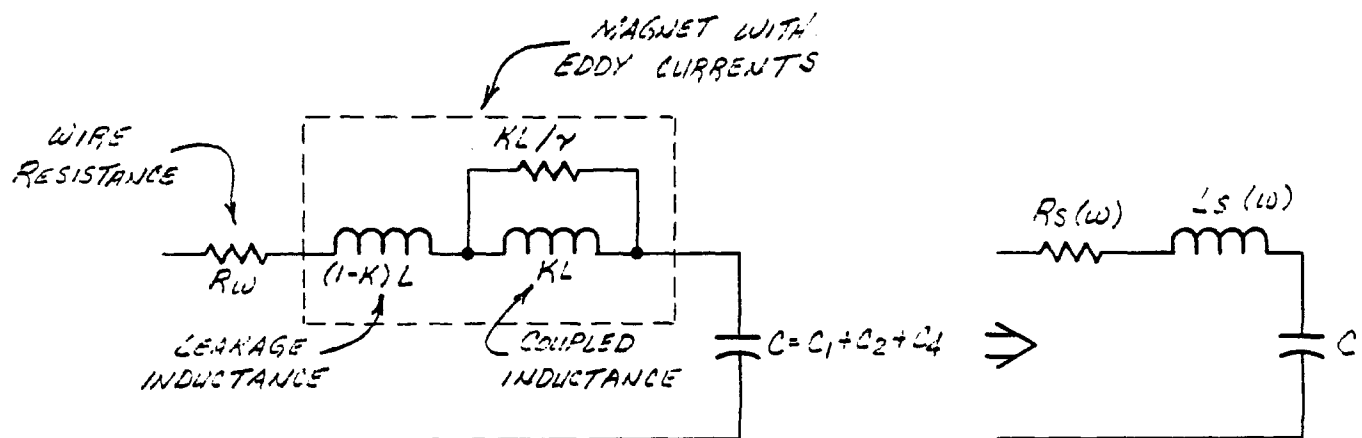
and from (24) and (25):

$$(28) \quad Z_L \text{ max} = 2 z_0 / \tanh \alpha \frac{m}{2}$$

$$(29) \quad Z_L \text{ min} = 2 z_0 \tanh \alpha \frac{m}{2}$$

Thus far, the equations presented have assumed R_S , L_S , and C were constant valued for each magnet. However, due to the effects of eddy currents, the equivalent series R_S and L_S will be functions of frequency.

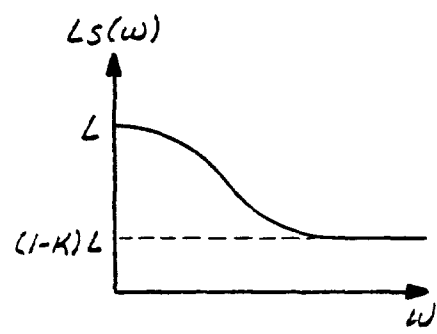
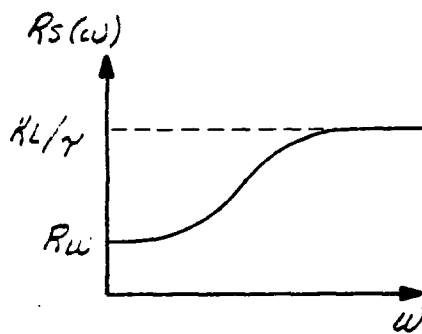
The equivalent per magnet circuit for the correction elements with eddy currents is:¹



$R_S(\omega)$ and $L_S(\omega)$ can be shown to be:

$$(30) \quad R_S(\omega) = R_S = R_W + \frac{K L \tau \omega^2}{1 + \omega^2 \tau^2} \quad 0 < K < 1$$

$$(31) \quad L_S(\omega) = L_S = (1-K)L + \frac{K L}{1 + \omega^2 \tau^2}$$



For a given frequency R_S and L_S could be calculated and substituted into the previously presented equations for α , β , Z_0 , etc. However, an explicit equation for Q is:

$$(32) \quad Q = \frac{\omega L_S}{R_S} = \frac{1 + \omega^2 \tau^2 (1-K)}{(R_w/\omega L)(1 + \omega^2 \tau^2) + K\omega\tau}$$

neglecting the wire resistance R_w ,

$$(33) \quad Q = \frac{1 + \omega^2 \tau^2 (1-K)}{K\tau\omega}$$

For $\omega^2 \tau^2 (1-K) \gg 1$, $L_S = (1-K)L$, $R_S = KL/\tau$, as shown in the sketch and $Q = \omega\tau(1-K)/K$. Examination of equation (33) indicates that at low frequency Q is large, and as frequency is increased Q decreases to a minimum then begins to increase.

The minimum value of $Q = 2\sqrt{1-K}/K$ at $\omega = 1/\tau\sqrt{1-K}$ (e.g., at $K = .9$, $Q_{min} = .7$). Hence, the frequencies at which resonances occur can drastically change the shape of $Z_L(f)$ being damped if resonances occur prior to Q_{min} .

Since both L_S and Q are both functions of frequency, it is difficult to find an explicit equation for the resonant frequency. However, if the parameters of the circuit are known, a trial and error method of solution can be used. From (23) and (27) it can be seen that the resonances in Z_L occur at $\beta l = n\pi/2$. Hence,

$$(34) \quad \beta m/2 = n\pi/2 = \frac{m}{2} \cdot \omega_n \cdot \sqrt{L_S C} \cdot \sqrt{(1 + \sqrt{1 + 1/Q^2})/2}$$

Rearranging and solving for f_n

$$(35) \quad f_n = n/2 m \sqrt{L_s C} \sqrt{(1 + \sqrt{1 + 1/Q^2})/2}$$

For $K < .9$ a lower bound for f_1 is:

$$(36) \quad f_{1\min} = 1/2 m \sqrt{L_s C} (1.17)$$

and an upper bound for f_1 is:

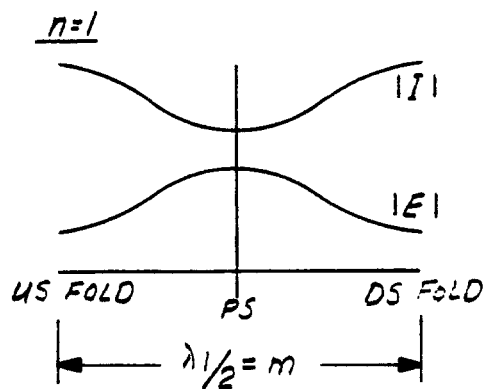
$$(37) \quad f_{1\max} = 1/2 m \sqrt{(1-K)L_s C}$$

If the resonances occur such that $\omega^2 \tau^2 (1-K) > > 1$ i.e., L_s

and R_s are constant

$$(38) \quad f_n = n/2m \sqrt{(1-K) L C}$$

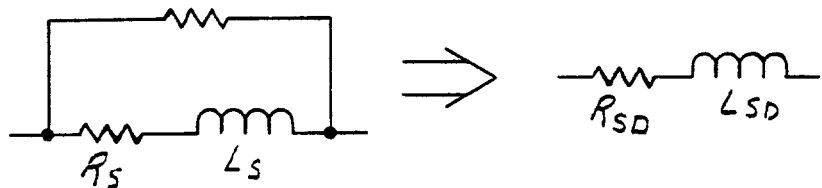
and standing waves of voltage and current will exist at these frequencies, similar to those previously shown. The lowest resonant mode ($n = 1$) will look like:



E. Effect of Damping Resistor Across Each Magnet

If a damping resistor is placed across a series R_s, L_s

$$R_D = R_{DAMP}$$



The equivalent series R_{SD} and L_{SD} at a given frequency are:

$$(39) \quad L_{SD} = \frac{L_S (1-K_D)^2}{1 + Q^2 K_D^2}$$

and,

$$(40) \quad R_{SD} = R_S (1-K_D) \frac{1 + Q^2 K_D}{1 + Q^2 K_D^2}$$

where, $K_D = R_S / (R_S + R_D)$ and $Q = \omega L_S / R_S$

and Q with damping, Q_D is

$$(41) \quad Q_D = \omega L_{SD} / R_{SD} = Q(1-K_D) / (1 + Q^2 K_D)$$

Then L_{SD} , R_{SD} , and Q_D could be used in place of L_S , R_S , and Q in the previously developed equations. Examination of (39) through (41) shows that for frequency such L_S , R_S are constant and $QK_D \gg 1$ i.e., ($\omega \gg (R_D + R_S)/L_S$)

$$(42) \quad L_{SD} = R_D^2 / \omega^2 L_S, \quad R_{SD} = R_D, \quad Q_{SD} = R_D / \omega L_S$$

Substituting (42) into (7) and (8) yields,

$$(43) \quad \alpha = \beta = \sqrt{\frac{\omega C R_D}{2}}$$

and from (3)

$$(44) \quad Z_0 = \sqrt{\frac{R_D}{\omega C}} < -45^\circ$$

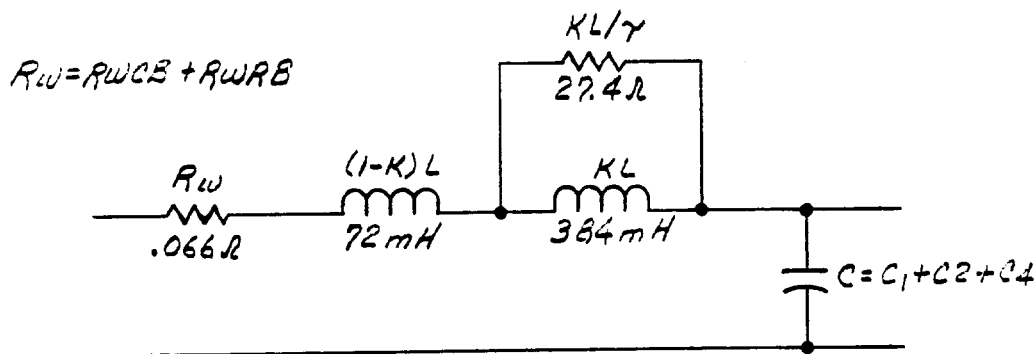
As ω is increased $\tanh \alpha \rightarrow 1$ and from (28) and (29) it could be seen that Z_L will be damped and in the limit.

$$(45) \quad Z_L \max = Z_L \min = 2 Z_0 = 2 \sqrt{R_D / \omega C} \angle -45^\circ$$

III. ANALYSIS OF TUNE QUAD CIRCUIT

A. $Z_L(f)$ - Impedance seen by the P. S.

The equivalent transmission line model per magnet for the tune quad referring to Fig. (1) is:



where $L = .456$ H, $K = .842$, and $\tau = 14$ mS; also $m = 90$.

Figure (4) is the result of a SPICE simulation of the Tune Quad circuit using the model shown in Fig. (2) with soft ground resistors $R_{G_1} = R_{G_2} = 1$ MEG. Since $I_{PS} = 1 \angle 0^\circ$, the plot of V_{PS} is equivalent to the load impedance Z_L .

The Plot shows

$$Z_L \max = 87.8 \text{ db} = 24.5 \text{ K}$$

$$Z_L \min = 61.9 \text{ db} = 1.24 \text{ K}$$

and

$$f_1 = 200 \text{ Hz}$$

At $f = 200$ Hz, $\omega^2 \tau^2 (1-K) = 49 > > 1$, hence

$$L_S = (1-K)L = .072 \text{ H}$$

$$R_S = KL/\tau = 27.4 \Omega$$

$$Q = \omega \tau (1-K)/K = 3.3$$

Using (38) to calculate f_1

$$f_1 = 1/2 \pi \sqrt{(1-K)LC} = 207 \text{ Hz}$$

then from (10), (11), and (12) for $f \geq 200$ Hz

$$\alpha = R_S / 2 \sqrt{L_S / C} = 5.1 \times 10^{-3}$$

$$\beta = \omega \sqrt{L_S C} = \omega 2.68 \times 10^{-5}$$

$$Z_0 = \sqrt{L_S / C} = 2.68 \text{ K}$$

and from (5) and (6)

$$v = \omega / \beta = 1 / \sqrt{L_S C} = 3.73 \times 10^4 \text{ mag./sec.}$$

$$\lambda_1 = v/f_1 = 180 \text{ magnets}$$

then using these values in (28) and (29) to calculate

Z_L max and Z_L min

$$Z_L \text{ max (CALC)} = 2 Z_0 / \tanh \alpha \frac{m}{2} = 23.7 \text{ K} = 87.5 \text{ db}$$

$$Z_L \text{ min (CALC)} = 2 Z_0 \tanh \alpha \frac{m}{2} = 1.21 \text{ K} = 61.7 \text{ db}$$

Figure (5) is the same as Fig. (4) except, $R_{G_1} = R_{G_2} = 10 \text{ K}$.

Since $R_{G_1} + R_{G_2}$ is across the P. S. and in parallel with

Z_L' ,

$$Z_L' = \frac{Z_L \cdot 20 \text{ K}}{Z_L + 20 \text{ K}}$$

and,

$$Z_{L' \max} (\text{CALC}) = \frac{(23.7 \text{ K}) \cdot (20 \text{ K})}{23.7 \text{ K} + 20 \text{ K}} = 10.9 \text{ K} = 80.7 \text{ db}$$

$$Z_{L' \min} (\text{CALC}) = \frac{(1.21 \text{ K}) \cdot (20 \text{ K})}{1.21 \text{ K} + 20 \text{ K}} = 1.14 \text{ K} = 61.1 \text{ db}$$

Figure (5) shows:

$$Z_{L' \max} = 80.9 \text{ db} = 11.1 \text{ K}$$

$$Z_{L' \min} = 61.3 \text{ db} = 1.16 \text{ K}$$

The agreement between the calculated values and the SPICE simulation is very good except that at higher frequencies ($\approx 10 \text{ KHz}$) the simulation deviates from the calculated response. This is believed to be caused by the discretes of the model, whereas when 90 single-valued elements were used in the simulation, this phenomenon did not occur for frequencies up to 10 KHz. In any event, the load characteristic beyond a few kilohertz is of little interest due to the response of the system.

The effect on Z_L of adding a damping resistor across each magnet can be seen in Figures (6), (7), and (8) for damping resistors of 1 K, 500Ω , and 100Ω , respectively. To get a better feeling for the effect of the damping resistor, Z_L will be calculated at two different frequencies for a damping resistor, $R_D = 500\Omega$. For $R_D = 500\Omega$, $K_D = .052$.

at $f = 200$ HZ: $Q = 3.3$ and from (39), (40), and (41)

$$L_{SD} = .066 \text{ H}, R_{SD} = 39.5\Omega, Q_{SD} = 2.0$$

from (10), (11), and (12)

$$\alpha = 7.7 \times 10^{-3} \quad \beta = 3.2 \times 10^{-2} \quad Z_0 = 2.6 \text{ K}$$

and from (23) and (27)

$$Z_L = 15.6 \text{ K} = 83.9 \text{ db}$$

$$Z_L (\text{plot}) = 15.3 \text{ K} = 83.7 \text{ db}$$

at $f = 2$ KHZ: $Q = 33$ and from (39), (40), and (41)

$$L_{SD} = .016 \text{ H} \quad R_{SD} = 380\Omega \quad Q_{SD} = .543$$

from (7), (8), and (3)

$$\alpha = .121 \quad \beta = .198 \quad Z_0 = 1.85 \text{ K} < -31^\circ$$

and from (23) and (27)

$$|Z_L| = 3.7 \text{ K} = 71.4 \text{ db} \quad \phi_L = -31^\circ$$

$$|Z_L| (\text{plot}) = 3.6 \text{ K} = 71 \text{ db} \quad \phi_L = -30^\circ$$

Summarizing, the Tune Quad load without damping resistors has resonances at multiples of 200 HZ alternately reaching maximum and minimum values of 24 K and 1 K.

At 200 HZ and beyond, the equivalent series resistance, R_S and inductance, L_S can be considered constants independent of frequency. The soft ground resistors used to center the power supply voltage about ground are in parallel with the load and hence have an impact on the overall magnitude of load seen by the supply.

When damping resistors are added across each magnet, the equivalent series inductance and resistance become functions of frequencies resulting in the magnitude of the load being damped as frequency increases approaching $2 Z_0$. At higher frequencies, Z_0 is itself a function of frequency proportional to $1/\sqrt{\omega}$.

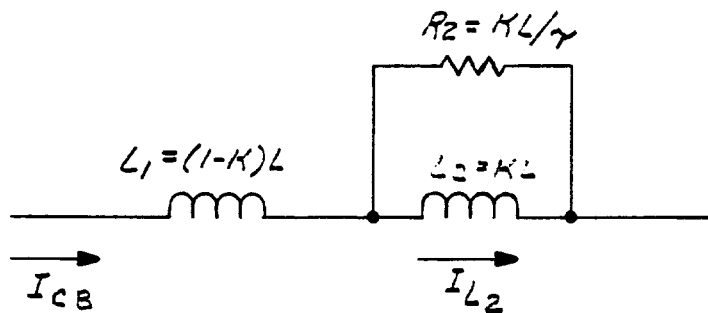
B. Bus and field excitation current vs. frequency.

For the power supply considered as an ideal current source, (19) could be used at a given frequency to compute the current at any point along the bus. It is expected that at the first resonance mode ($f = 200$ HZ) the bus current will be maximum at each of the folds. Using (19) with the Tune Quad parameters at $f = 200$ HZ for which $\beta l = \pi/2$; and for $X = l = 45$, $I = I_{DS FOLD}$

$$\begin{array}{l|l} I_{DS FOLD} & = I_S / j \sinh \alpha l = 4.32 I_S < -90^\circ \\ & f = 200 \text{ Hz} \\ & l = 45 \end{array}$$

Figure (9) is a plot derived from SPICE of the magnitude of $I_{DS\ FOLD}$ for a P. S. current of unity and shows that at 200 HZ it reaches a maximum value of 4.2 A. Fortunately, the P. S. current will be rolled off at a much lower frequency.

In a magnet with eddy currents modeled by:



the field producing current is the current in the coupled inductance, I_{L_2} ⁴. The relationship between I_{L_2} and the coil bus current I_{CB} using Laplace notation is:

$$(46) \quad I_{L_2} / I_{CB} = 1/(1 + s \tau)$$

which is a single low pass filter with a corner frequency of $1/2 \pi \tau = 11.4$ HZ for the Tune Quad.

Figure (10) is a plot derived from SPICE for the Tune Quad of various currents at low frequency. It can be seen that the I_{L_2} current will be 1% lower than the corresponding bus current at a frequency of 1.6 HZ. The bus current at the fold and near the midpoint are less than 1% higher than the P. S. current for frequencies below 10 HZ.

C. Effect of Power Supply Ripple Voltage

In order to evaluate the effect of P. S. ripple voltage, consider the P. S. to be an ideal voltage source, V_{PS} . Then

(21) can be used with $E_S = V_{PS}/2$ to compute the current at any point along the bus. The bus current at the P. S., I_{CB_6} is simply V_{PS}/Z_L , hence the $I_{CB_6}/V_{PS} = Y_L$, the load admittance. For the case without any damping resistor,

At 200 Hz,

$$I_{CB_6}/V_{PS} = 1/Z_{L \text{ max}} = 1/24.5 \text{ K} = .04 \text{ ma/V}$$

and at 400 Hz

$$I_{CB_6}/V_{PS} = 1/Z_{L \text{ min}} = 1/1.24 \text{ K} = .8 \text{ ma/V}$$

From (21) with $E_S = V_{PS}/2$ and $X = \ell$

$$I_{DS \text{ FOLD}}/V_{PS} = 1/2 Z_0 \sinh \gamma \ell$$

from which

$$I_{DS \text{ FOLD}}/V_{PS} \left| \begin{array}{l} = 1/j 2 Z_0 \cosh \alpha \ell = .18 \text{ ma/V} \angle -90^\circ \\ f = 200 \text{ Hz } (\beta \ell = \pi/2) \end{array} \right.$$

$$I_{DS \text{ FOLD}}/V_{PS} \left| \begin{array}{l} = -1/2 Z_0 \sinh \alpha \ell = .81 \text{ ma/V} \angle 180^\circ \\ f = 400 \text{ Hz } (\beta \ell = \pi) \end{array} \right.$$

Figure (11) is a plot derived from SPICE of I_{CB_6} and $I_{DS \text{ FOLD}}$ for V_{PS} equal unity and hence represents the gain I/V_{PS} from which the above points can easily be verified.

For the Tune Quad circuit, a goal for the ripple current specification is $\Delta I/I_{FS} < 10^{-5}/f$ which in terms of the ripple voltage means:

$$V_{PS} < \frac{10^{-5} \cdot I_{FS}}{f \cdot (I/V_{PS})}$$

If it were necessary to maintain the coil bus current such that $I_{CB}/I_{FS} < 10^{-5}/f$, the limits on V_{PS} could be obtained by using I/V_{PS} from Figure (11) realizing that $I_{FS} = 50$ A. For example, near the P. S. using I_{CB_6}/V_{PS} at 60 Hz,

$$V_{PS} < \frac{10^{-5} \cdot 50}{60 \cdot (.25 \text{ ma/V})} = 33 \text{ mv}$$

and at 400 Hz

$$V_{PS} < \frac{10^{-5} \cdot 50}{400 \cdot (.8 \text{ ma/V})} = 1.6 \text{ mv}$$

In general, for $I_{CB_6}/I_{FS} < 10^{-5}/f$

$$V_{PS} < \frac{10^{-5} \cdot 50}{f \cdot (I_{CB_6}/V_{PS})} = \frac{10^{-5} \cdot 50}{f \cdot Y_L}$$

and the maximum tolerable V_{PS} would continually decrease with frequency the worst cases being at the maximums of Y_L . Note that if the load were 90 ideal magnets where $Y_L = 1/90 \omega L$

$$V_{PS} < 10^{-5} \cdot 50 \cdot 2\pi L$$

which is independent of frequency.

Since it is only necessary for the excitation current I_{L_2} to be such that $I_{L_2} / I_{FS} < 10^{-5}/f$, the maximum P. S. ripple need not be as small. Substituting $s = j\omega$ in (46) yields,

$$|I_{L_2} / I_{CB}| = 1 / \sqrt{1 + \omega^2 \tau^2} \approx 1/\omega\tau \text{ for } \omega^2\tau^2 \gg 1$$

Hence, near the P. S. for $I_{L_2(6)} / I_{FS} < 10^{-5}/f$

$$V_{PS} < \frac{10^{-5} \cdot I_{FS}}{f \cdot I_{L_2} / I_{CB} \cdot (Y_L)} = \frac{10^{-5} \cdot I_{FS} \cdot 2\pi\tau}{Y_L}$$

using Y_L from Figure (11) or $1/Z_L$ from Figure (4)

$$V_{PS} < 176 \text{ mv at 60 HZ}$$

$$V_{PS} < 360 \text{ mv at 120 HZ}$$

For frequencies beyond 400 HZ and $Y_L = Y_{L \max}$, $V_{PS} < 55 \text{ mv}$

to insure $I_{L_2(6)} / I_{FS} < 10^{-5}/f$.

If damping resistors are added across each magnet, two phenomenon occur so as to improve the ripple characteristics. First, from Figures (6), (7), and (8) which are plots of Z_L for various damping resistors, it could be seen that $Y_{L \max}(@ Z_{L \min})$ is generally lower tending to make the coil bus current smaller. This is true except at very high frequencies ($\omega > > (R_D + R_S)/L_S$) where Y_L increases as $\sqrt{\omega}$. Secondly, the relationship between I_{L_2} and I_{CB} becomes second order where,

$$(47) \quad I_{L_2} / I_{CB} = 1 / (s^2\tau(1-K)L/R_D + s(\tau + L/R_D) + 1)$$

For values of R_D being considered, (47) has two real poles and at low frequency is similar to (46) and at high frequency decreases as $1/\omega^2$ negating the effect of increasing Y_L .

For comparison, to maintain $I_{L_2(6)} / I_{FS} < 10^{-5}/f$ using (47) with $R_D = 1K$, and Y_L from Figure (11):

$$V_{PS} < 184 \text{ mv at } 60 \text{ Hz}$$

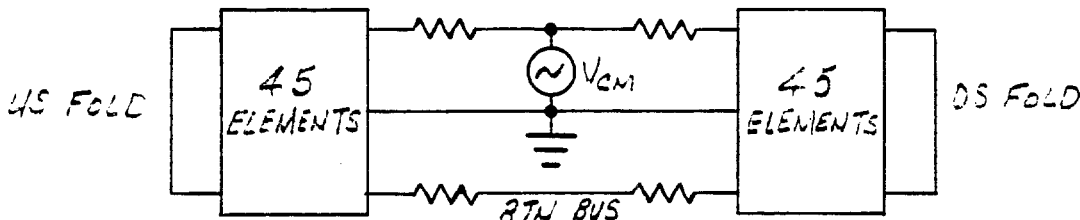
$$V_{PS} < 373 \text{ mv at } 120 \text{ Hz}$$

and

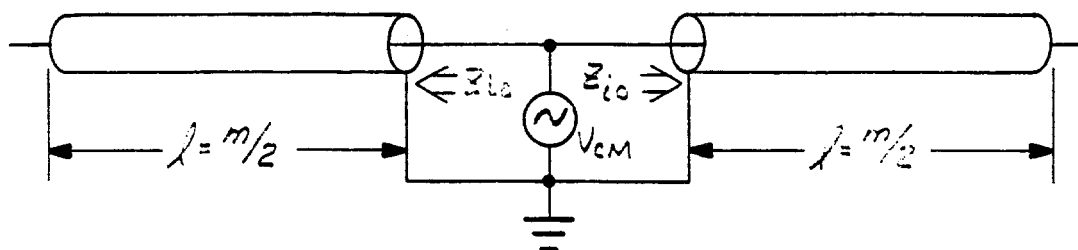
$$V_{PS} < 721 \text{ mv at } 400 \text{ Hz}$$

D. Common Mode Voltage Effects

The equivalent circuit used for common mode analysis is:



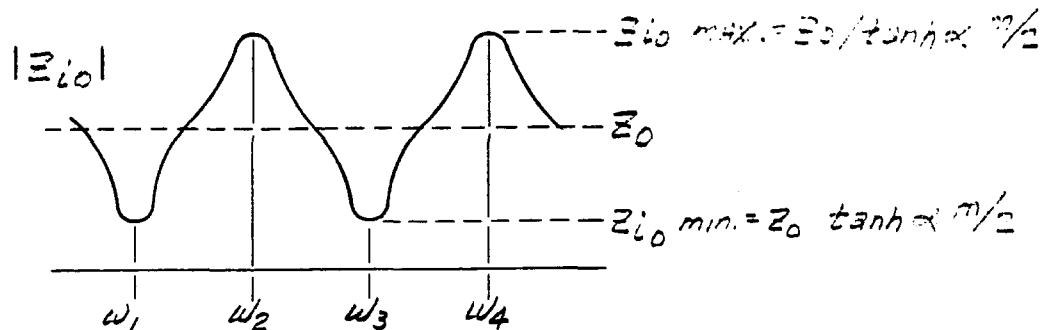
From symmetry, the voltage to ground, at the downstream fold, and upstream fold, are equal and only small currents will flow in the return bus. Hence, this can be approximated as two open circuit lines in parallel.



Setting $I = 0$ and $x = m/2$ in (16), the sending end impedance for an open circuit line, Z_{i_0} , is found to be:

$$(48) \quad Z_{i_0} = Z_0 / \tanh \gamma m/2$$

which with frequency looks like:



Note that this is similar to Z_L in the normal mode except that Z_{i_0} max and Z_{i_0} min occur at even and odd multiples of ω_1 , respectively. Standing waves of voltage and current will also exist on the bus similar to the normal mode except that $|I|$ will be near zero at the downstream fold (see sketch in Figure (12)). Furthermore, if the same line characteristics are assumed (this may not be a good assumption), Z_{i_0} max and min are half of that Z_L in the normal mode.

$$Z_{i_0 \text{ max}} \Big|_{\text{CM}} = \frac{Z_L \text{ max} \Big|_{\text{NM}}}{2} = \frac{24.5 \text{ K}}{2} = 12.3 \text{ K}$$

$$Z_{i_0 \text{ min}} \Big|_{\text{CM}} = \frac{Z_L \text{ min} \Big|_{\text{NM}}}{2} = \frac{1.24 \text{ K}}{2} = 620 \Omega$$

From which,

$$Y_{i_0 \text{ max}} = \frac{1}{Z_{i_0 \text{ min}}} = \frac{1}{620} = 1.6 \times 10^{-3} \text{ u}$$

$$Y_{i_0 \text{ min}} = \frac{1}{Z_{i_0 \text{ max}}} = \frac{1}{12.3 \text{ K}} = .081 \times 10^{-3} \text{ u}$$

From the graph of Y_{i_0} in Figure (12) derived from SPICE analysis:

$$Y_{i_0 \text{ max}} = 1.37 \times 10^{-3} \text{ u}$$

$$Y_{i_0 \text{ min}} = .1 \times 10^{-3} \text{ u}$$

The first resonant frequency f_1 occurs at 180 HZ as compared to 200 HZ in the normal mode (the reason for which is not understood).

$$Y_{i_0} = I_{CB_6} / V_{CM}$$

Hence, at 180 HZ, 540 HZ, etc., coil bus current at the P. S. will be 1.37 ma/V of common mode voltage at those frequencies which should be the worst case effect of coil bus current due to common mode voltages. However, the currents of interest are excitation currents (i.e., I_{L_2}).

Figure (13) is a graph of $I_{L_2(146)} / V_{CM}$ which reaches a maximum at 180 HZ. From the graph:

$$I_{L_2(146)} / V_{CM} \Big|_{180 \text{ Hz}} = -81.4 \text{ db} = .085 \times 10^{-3} \text{ u}$$

Since, at higher frequencies ($\omega^2 \tau^2 > > 1$)

$$I_{L_2} = I_{CB} / \omega \tau$$

I_{L_2} / V_{Cm} at 180 Hz is predicted to be:

$$I_{L_2} / V_{Cm} \Big|_{180 \text{ Hz}} = \frac{Y_{i_0 \text{ max}}}{\omega \tau} = \frac{1.37 \times 10^{-3}}{15.8} = .086 \times 10^{-3} \text{ u}$$

Note the attenuation of I_{L_2} / V_{Cm} as ω increases.

For $I_{L_2} / I_{FS} < 10^{-5}/f$ and $\omega^2 \tau^2 > > 1$,

$$V_{Cm} < \frac{10^{-5} \cdot 50}{f \cdot I_{L_2} / V_{Cm}} = \frac{10^{-5} \cdot 50 \cdot 2\pi\tau}{Y_{i_0}}$$

For frequencies beyond 180 Hz and $Y_{i_0} = Y_{i_0 \text{ max}}$

$V_{Cm} < 32 \text{ mv}$ to insure $I_{L_2} / I_{FS} < 10^{-5}/f$.

Note that at 60 Hz from Figure (13):

$$I_{L_2} / V_{Cm} = -88.9 \text{ db} = .036 \times 10^{-3} \text{ u}$$

Hence,

$$V_{Cm} \Big|_{60 \text{ Hz}} < 232 \text{ mv}$$

If damping resistors are used, I_{CB} / V_{Cm} and I_{L_2} / I_{CB} will both be smaller as in the case of the ripple voltage, resulting in improved common mode characteristic.

E. Time Domain Analysis

The maximum current ramp rate which the P. S. is expected to achieve is 5A/sec. However, the tight specification of $.02\% \text{ FS}$ and $\Delta I / I_{FS} < 10^{-5}/f$ need only be achieved at ramp rates of $\leq .1\% \text{ FS/sec.} = 50 \text{ ma/sec.}$

If the C's which produce the transmission line effect were neglected, the coil bus current, I_{CB} would equal the P. S. current I_{PS} .

For I_{PS} a ramp where $i_{PS}(t) = At$

$$I_{PS}(s) = A/s^2$$

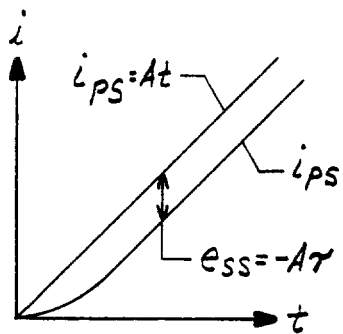
and from (46) $I_{L_2}(s)$ without damping resistor would be:

$$I_{L_2}(s) = A/s^2 (1 + s\tau)$$

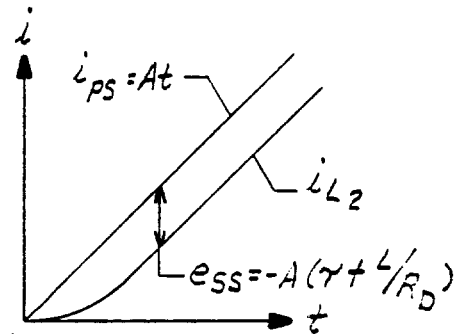
and from (47) with damping resistor, R_D

$$I_{L_2}(s) = A/s^2 [s^2 \tau (1-K)L/R_D + s (\tau + L/R_D) + 1]$$

which have steady-state errors, e_{SS} of:



WITHOUT DAMPING



WITH DAMPING

Figure (14) and Figure (15) are SPICE transient analyses of the Tune Quad circuit including all the C's which produce the transmission line effects. Figure (14) is for $I_{PS} = 5A/S$ without a damping resistor and Figure (15) is for $I_{PS} = 5A/S$ with various damping resistors. On this scale very little transmission line effect can be observed in the I_{L_2} currents. Note that the current at the downstream fold $I_{DS FOLD}$ initially lags I_{PS} , but quickly (5 ms) catches up to I_{PS} .

Figure (16) is a plot of the difference in coil bus currents at the PS (I_{CB_6}) and at the downstream fold ($I_{DS\ FOLD}$) for various damping resistors with the same ramp of 5A/S.

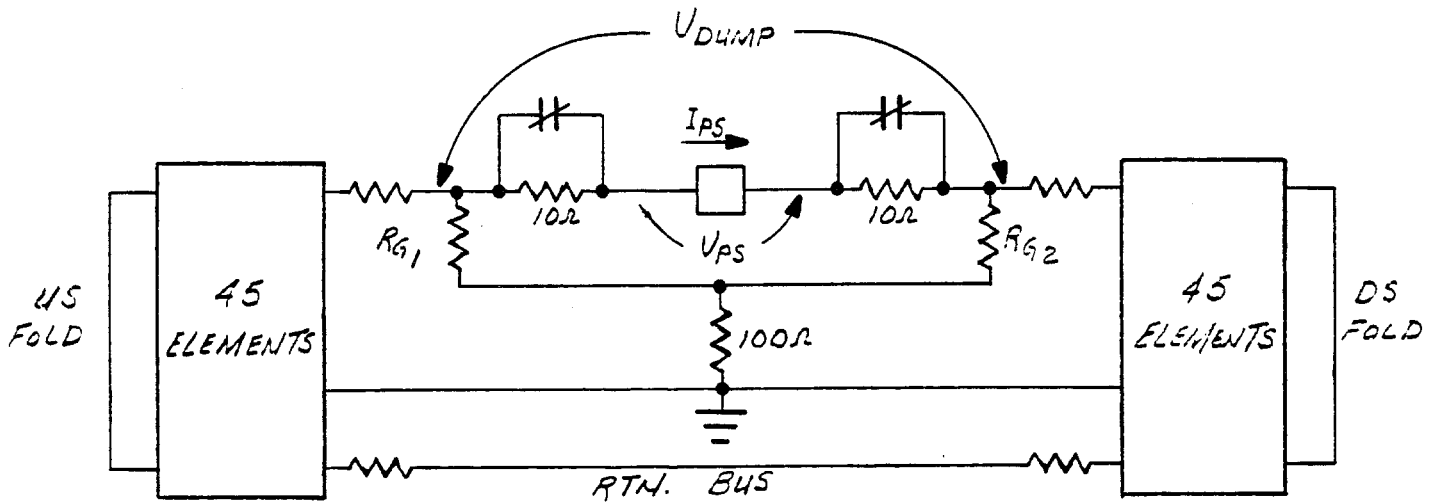
Note that the frequency of oscillation is 200 HZ, the lowest resonant mode ($n = 1$). Since $I_{CB}(6)$ is nearly identical to I_{PS} , the graph essentially is the error at the downstream ($I_{DS\ FOLD}$) current compared to I_{PS} .

From transmission line theory, the first resonant mode produces maximum current at the folds. Hence, the maximum coil bus current errors are at the folds and not somewhere in the middle of the bus.

The difference in excitation currents at the closest magnet to the P. S. $[I_{L_2(146)}]$ and the furthest magnet, $[I_{L_2(190)}]$ is shown in Figure (17) for various damping resistors. The maximum difference is < .7 ma which is .0014% FS at $I_{PS} = 5A/S$ without a damping resistor. Note that at $I_{PS} = 1A/S$ this error is reduced to < .15 ma.

F. Dump Analysis

Whenever the P. S. is turned off because of a quench, P. S. failure, or in fact any reason, the P. S. will go to zero volts and two (2) ten ohm resistors will be placed in series with the load.



If a dump occurs when $I_{PS} = 50A$, V_{DUMP} will look like a 1,000 V step and the voltage to ground at the dump resistors will be ± 500 V. Of interest here, are the voltages to ground along the bus which will exceed 500 V due to the transmission line effects.

The SPICE model used to simulate the P. S./DUMP network uses non-linear dependent sources. The initial conditions are such that $I_{PS} = 50A$ and $V_{PS} = 50 R_{TOT}$ (301 V). At $t = 0$ V_{PS} goes to 0 V in 0.1 ms and after 10 ms the PS/DUMP model looks like a 20 ohm resistor in 0.1 ms. The SPICE model used for the correction element string differs from that for $Z_L(f)$ in Figure (2) in two respects. First, the wire resistances RWCB and RWRB for each magnet was placed at the upstream side of each cell in order to set initial conditions on the capacitors, and secondly, the damping resistor R_{DAMP} was

changed from 10 MEG (OPEN) to 10 K. R_{DAMP} was made 10 K in order to run a SPICE transient analysis and maintain the same number of SPICE subcircuits. The lower R_{DAMP} causes the 200 HZ resonances to be damping beyond 1 KHZ which will tend to indicate a lower maximum voltage than would otherwise occur.

Figure (18) shows the overall dump which is an exponential decay with time constant $L/R = 90 \times .456 \text{ H}/26\Omega = 1.58 \text{ sec}$. Figure (19) is V_{DUMP} and I_{PS} during the first 15 ms of the dump. The dominant frequency in I_{PS} is 400 HZ ($n = 2$) which is expected from the AC analysis.

The voltage to ground along the bus is such that the upstream side is positive and the downstream side is negative ($I = +50A$). Figure (20) shows the downstream side voltages to ground near the P. S., at the downstream folded, and near the midpoint. The voltage near the midpoint, V(168), shows a 400 HZ oscillation as expected. A maximum voltage to ground of -611 V occurs at the first magnet downstream of the P. S. (node 6). From symmetry, a maximum voltage of +611 V is expected at the first magnet upstream of the P. S. Figures (21), (22), and (23) are for $R_{DAMP} = 1 \text{ K}, 500\Omega$, and 100Ω , respectively. In all cases, the maximum voltage to ground occurs at node (6) as follows:

$V_{max} = 611 \text{ V}$ $W/RDAMP = 10 \text{ K}$

$V_{max} = 584 \text{ V}$ $W/RDAMP = 1 \text{ K}$

$V_{max} = 572 \text{ V}$ $W/RDAMP = 500\Omega$

$V_{max} = 538 \text{ V}$ $W/RDAMP = 100\Omega$

III. CONCLUSION

Although the preceding analysis involves only the Tune Quad circuit, impedance plots ($Z_L(f)$) for various damping resistors and a dump analysis have been run for all of the circuits using SPICE and can be found in Appendix A. All of them look similar to those for the Tune Quad except f_n , $Z_{L max}$, $Z_{L min}$, etc., are of different values. Further analysis using these plots will be required to determine if a damping resistor is necessary for P. S. stability considerations.

It is believed that if ripple and common mode specifications can be met for the Tune Quad circuit, it should be more than adequate for the other circuits which have less tighter specifications. However, the information required to determine the specific ripple and common mode requirements for each circuit can be obtained from the $Z_L(f)$ plots. The addition of damping resistors would result in improved ripple and common mode specifications.

It should be noted that it is the capacitance associated with each magnet and not the eddy current effect which causes the load to look like a transmission line at higher frequencies.

In fact, the eddy current effect causes a reduction in the oscillations of the field excitation currents as compared to the coil bus current. For ramp rates of $< 5\text{A/S}$, the resulting differences in the field excitation currents along the bus become insignificantly small. The penalty that is paid for this reduction is that the excitation current will lag the P. S. current causing a constant steady state error for a given ramp rate. The amount of this error is significant and should be taken into consideration when programming the P. S. current. The effect of adding a damping resistor tends to further reduce the oscillations in the field excitation current and produces a larger steady state error for the same ramp rate.

The dump analysis for the Tune Quad indicates the maximum voltage to ground would be 611 V with $R_{DAMP} = 10 \text{ K}$, but it is expected that this voltage would be somewhat higher had no damping resistor been used. Of the circuits other than the Tune Quad, the maximum voltage to ground reached 650 V in some cases. The addition of a 1 K damping resistor in the Tune Quad circuit reduces the maximum voltage to 584, and in the other circuits to $< 550 \text{ V}$.

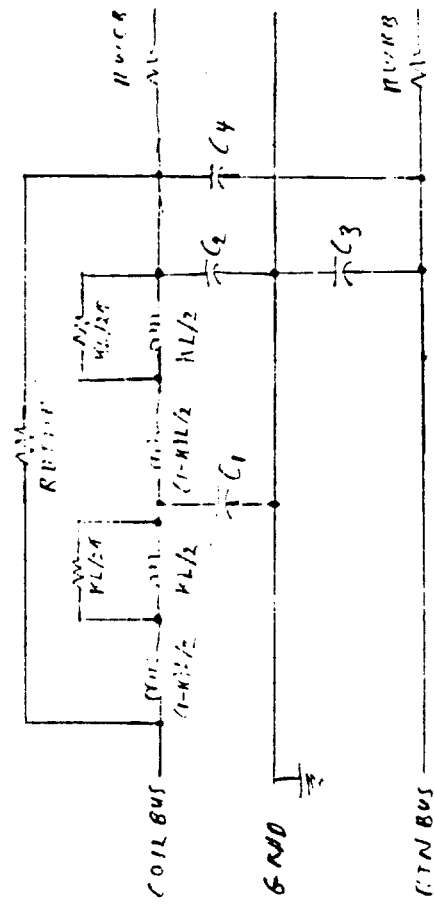
The benefits derived by adding a damping resistor across each magnet seems to outweigh the drawbacks. From what is known thus far, it would seem that a 1 K damping resistors should be used.

1. R. E. Shafer, "Transmission Line Characteristics of Energy Doubler Dipole Strings," Design Report #UPC-37.
2. W. C. Johnson, "Transmission Lines and Networks," McGraw Hill (1950).
3. R. E. Matick, "Transmission Lines for Digital and Communication Networks," McGraw Hill (1969).
4. R. E. Shafer, "Eddy Currents, Dispersion Relations, and Transient Effects in Superconducting Magnets," Technical Memorandum #TM-991.
5. R. E. Shafer, Memorandum to Raymond Yarema, dated August 31, 1981.

000 > 320 m/s ~ 5
solo hazard ~ 2

FOLDED OVER
SINCE LOOP

m	$\frac{e^2 \rho}{m}$	$\frac{L}{\text{mm}}$	K	$\frac{C_1}{(n+1)F}$	C_2	C_3	$\frac{C_4}{(n+1)F}$	P_{WCR}	Current	$\frac{\partial C_1}{\partial m}$	$\frac{\partial C_2}{\partial m}$	$\frac{\partial C_3}{\partial m}$	$\frac{\partial C_4}{\partial m}$
A	2	TUNE QUAD	20	0.458	1.4	0.2	1.2	1.2	1.6	36	30	5	-0.2%
B	2	EXTEND HARMONIC QUAD	4	0.416	1.4	0.2	0.2	0.2	0.5	230	230	F	-0.2%
C	1	2END HARMONICS OF FOCUSING	48	0.416	0.2	14	7.3	0.1	0	72	72	J	2.9%
D	2	SEXTAPOLE	20	0.523	0.47	9.1	7.3	1.2	0	36	0	5	-0.2%
E	2	39th HARMONIC OCTOPOLE	16	0.452	2.62	6.7	9.2	3.4	2.4	17	16	J	1.2%
F	1	ZERO ORDER HARMONIC OCT. AT FOCUSING LOC. (E3)	18	0.356	6.7	8.7	7.0	0	0	-2.	0	J	2.9%
G	1	ZERO ORDER HARMONIC OCT. AT DEFOCUSING LOC. (E4)	24	0.382	2.62	6.7	2.2	4.2	0	0	0	J	2.9%



$C_0 = \text{Cost of 100000 units} = 8 \text{ million dollars}$

$c_3 = 11$ $\theta_8 = 70.6^{\circ}$ $\alpha = 11$

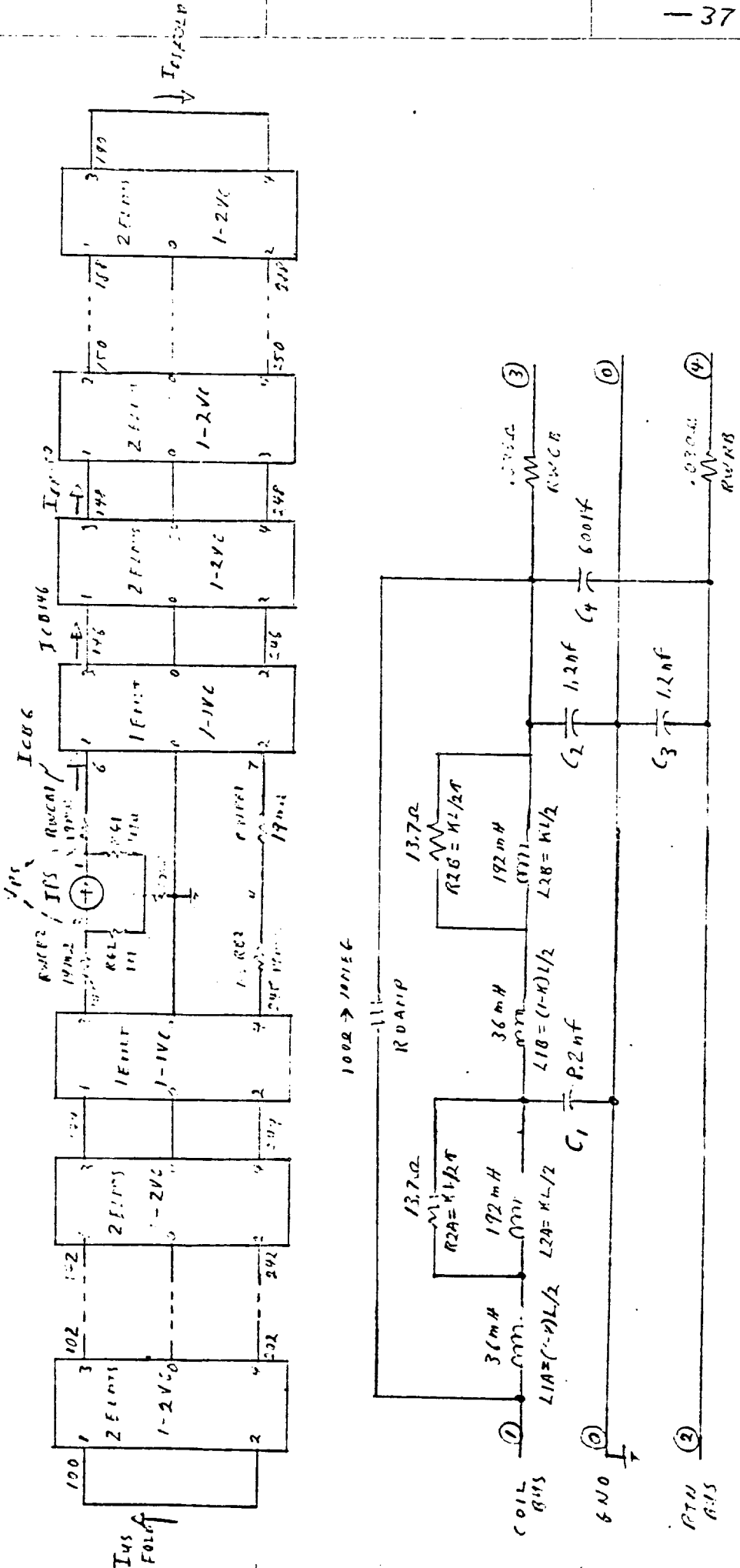
۳۶-
مکانیزم ایجاد کنترل مداری در گردشگری این امر را می‌داند

11. *Am. Mus. Nat.* 11: 116.

卷之三

卷之三

卷之三



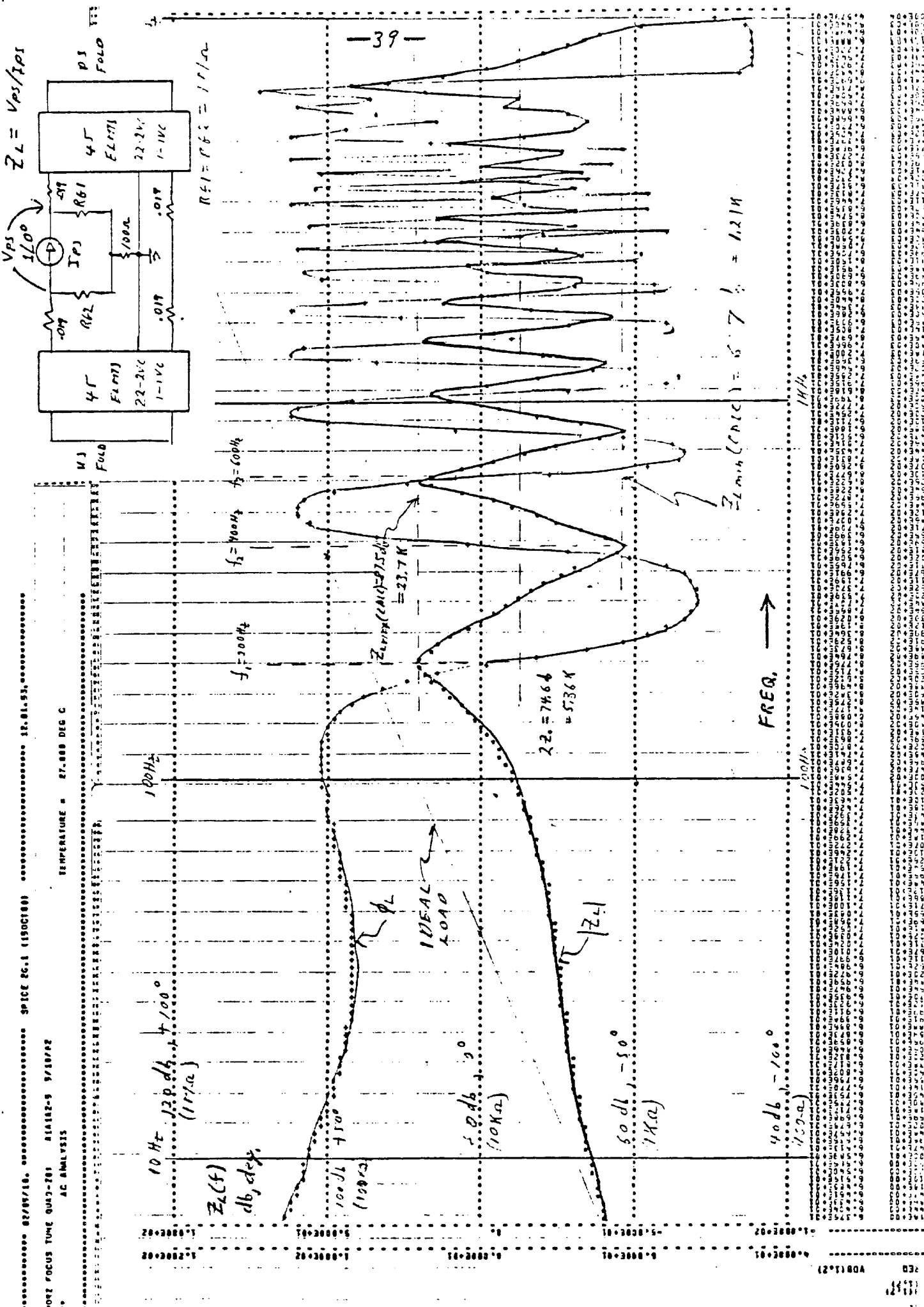
SPLICING MODEL OF LINE 1 - 1 VC (L VALUE CR12) "CUTTA"
 $2VC \sim \text{FACT VALUE } 15 X 2$ ($f_1, L_1 = 4, r_{20H} = 2^{dymH}$)

FIG. (2) Typ. Spec. model of TAN₂ and circuit

FILE NUMBER: 100-100000000000000000

CHT	C. S.	BUS	RDW	CELL	ANALYSIS
A - TUNE QVAD	1 - COUNTER 2 - VSWR 3 - SWR	A - GAINING 4 - SWR 5 - FOCUS 6 - RDW	1 - GAIN = 10dB = 20/2 2 - SWR = 2.2 3 - RDW = 10dB 4 - SWR = 2.2	2 - AC 3 - THRU (TRAN)	
B - Extracell H2O & QVAD	2 - VOLTS				
C - 2 EFG HARM. SVC & QVAD	3 - STRUT 4 - LINE FOR.	C - CONSTANT 2.2 - 4V 5 - GAIN = 10dB 6 - RDW = 10dB		C - 2.2, 10dB C - 2.2, 10dB	
D - STAB MPP	6 - Volt. Stab.				
E - 3rd Order, Octave	7 - STAB	J - VARIO 2.2 - 10 8 - INCL (RIGHT/W)		H - 2.2, 10dB C - 2.2, 10dB	
F - 2 EFG's ORDER, HARM, OCT	8 - OCTAVE				
G - 2 EFG's ORDER, HARM, OCT	9 - OCTAVE	9 - 2.2, 10dB 10 - 2.2, 10dB			
		11 - 2.2, 10dB 12 - 2.2, 10dB			
		N - 2.2, 10dB 13 - 2.2, 10dB			
		14 - 2.2, 10dB 15 - 2.2, 10dB			
		M - 10 FREQ. FILTER			
		L - 4 FILTER			

FIG. (4): TUNE QUAO - ZL VS. Q w/ ROAD OPEN



F16,(5) : TUNF Q(1,10-22 vs 11-21) = 0.051 (R61-R62 = 10K)

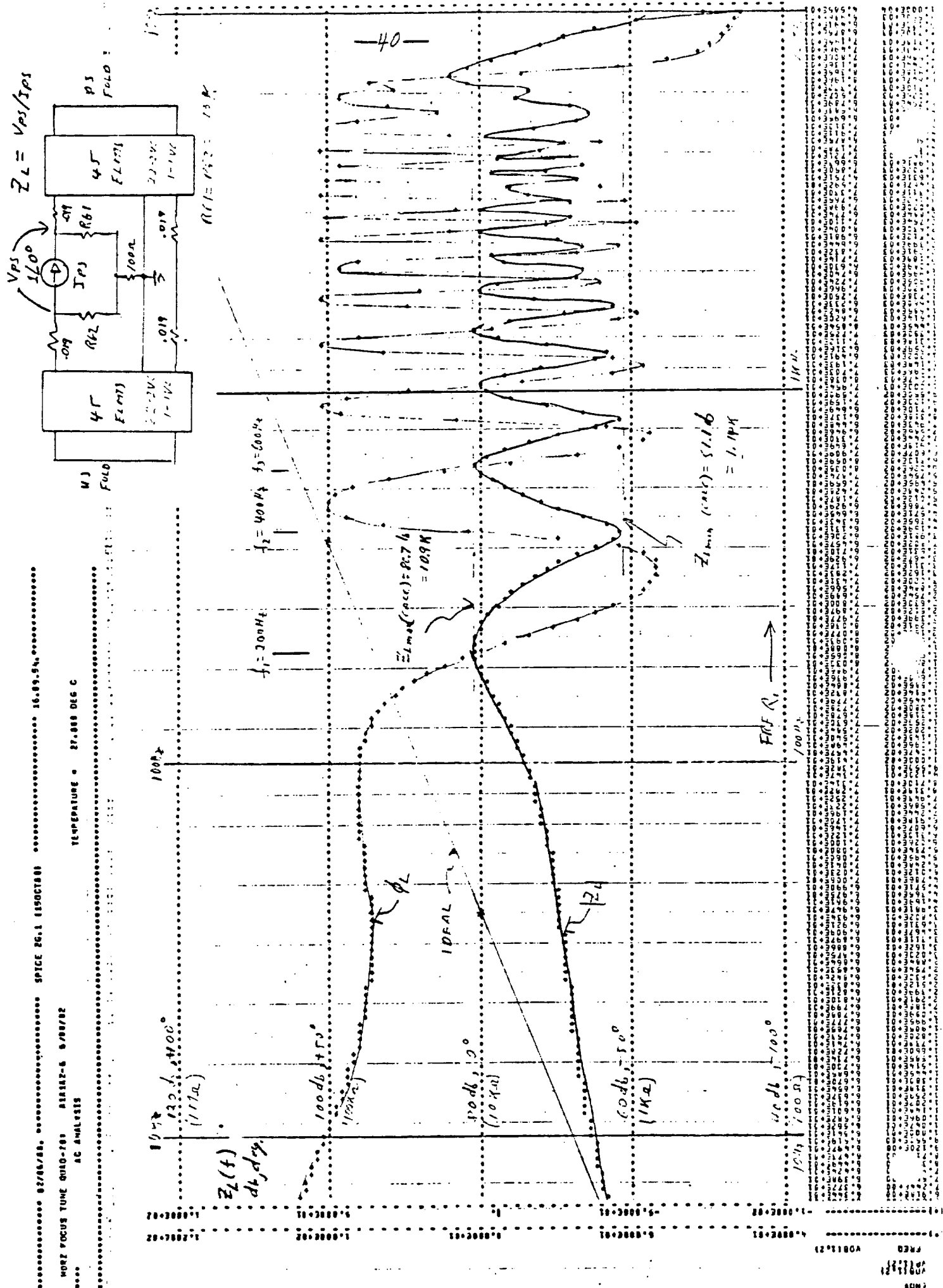


FIG. (6) : TUNE QUADE-2L VS F1 & W/ROAD = 1KΩ

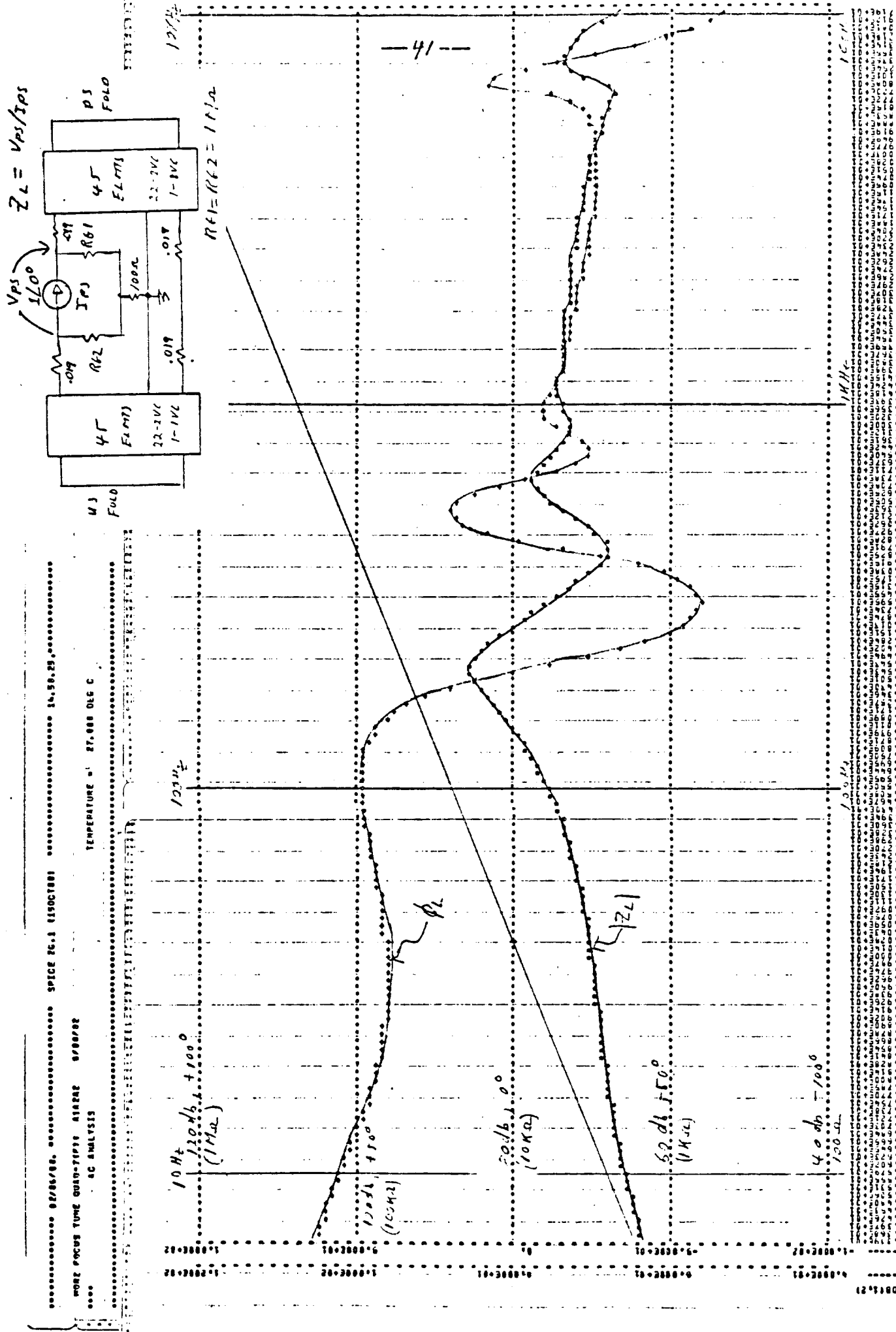


FIG. (7): TUNE QUAO- \bar{Z}_L VS FNER w/ $\rho_{DM} = 500 \text{ g/cm}^3$

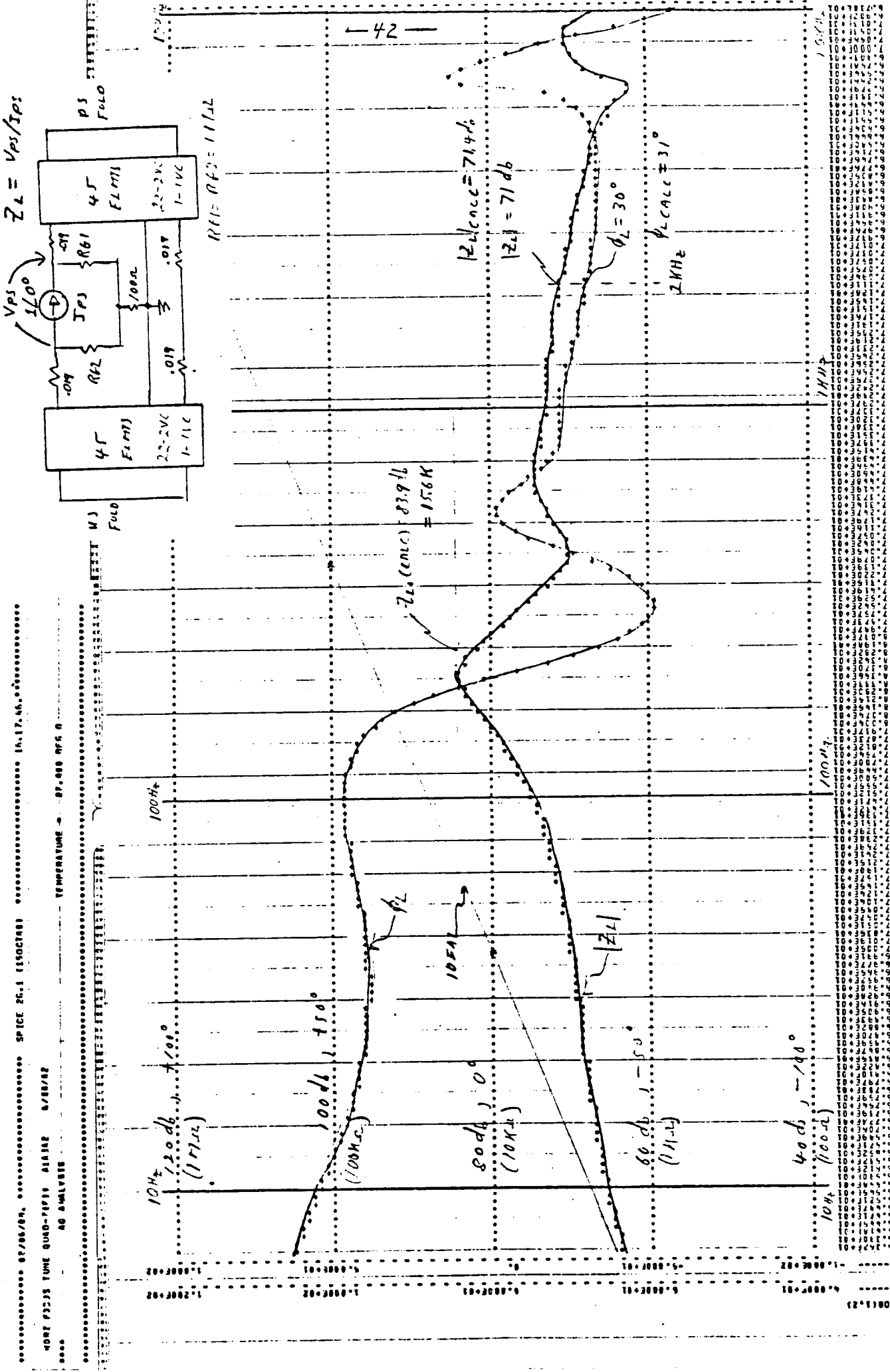
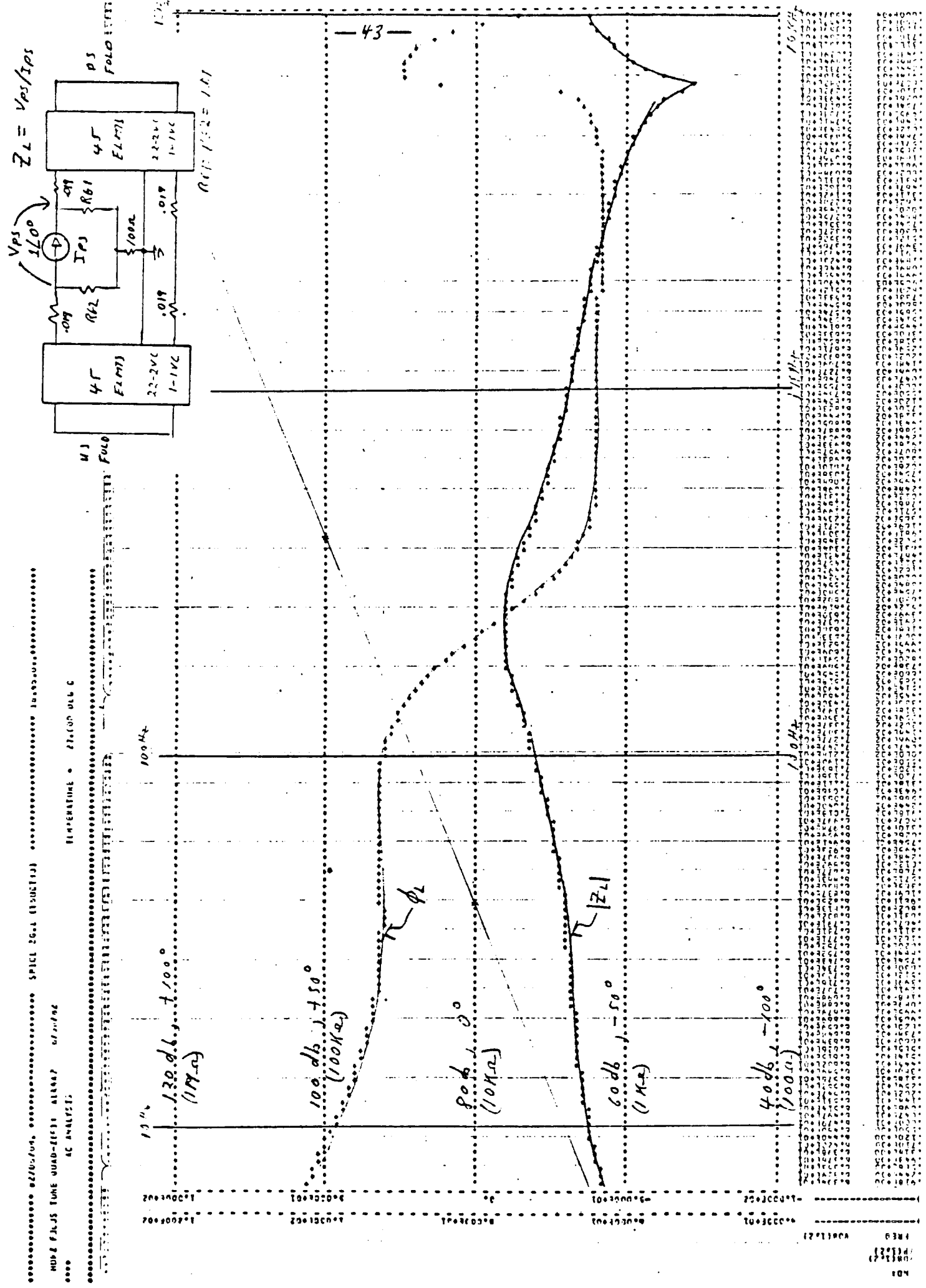
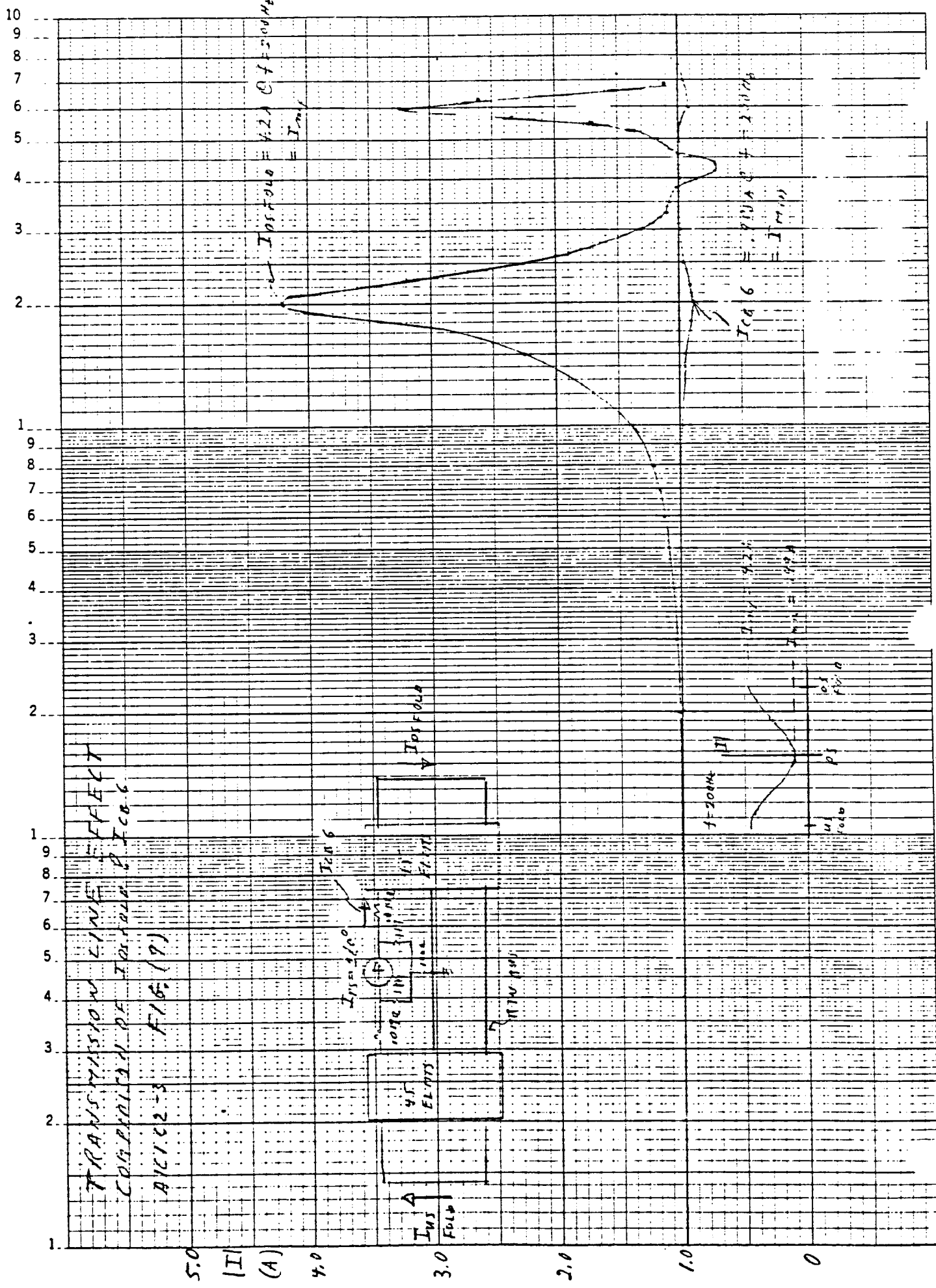


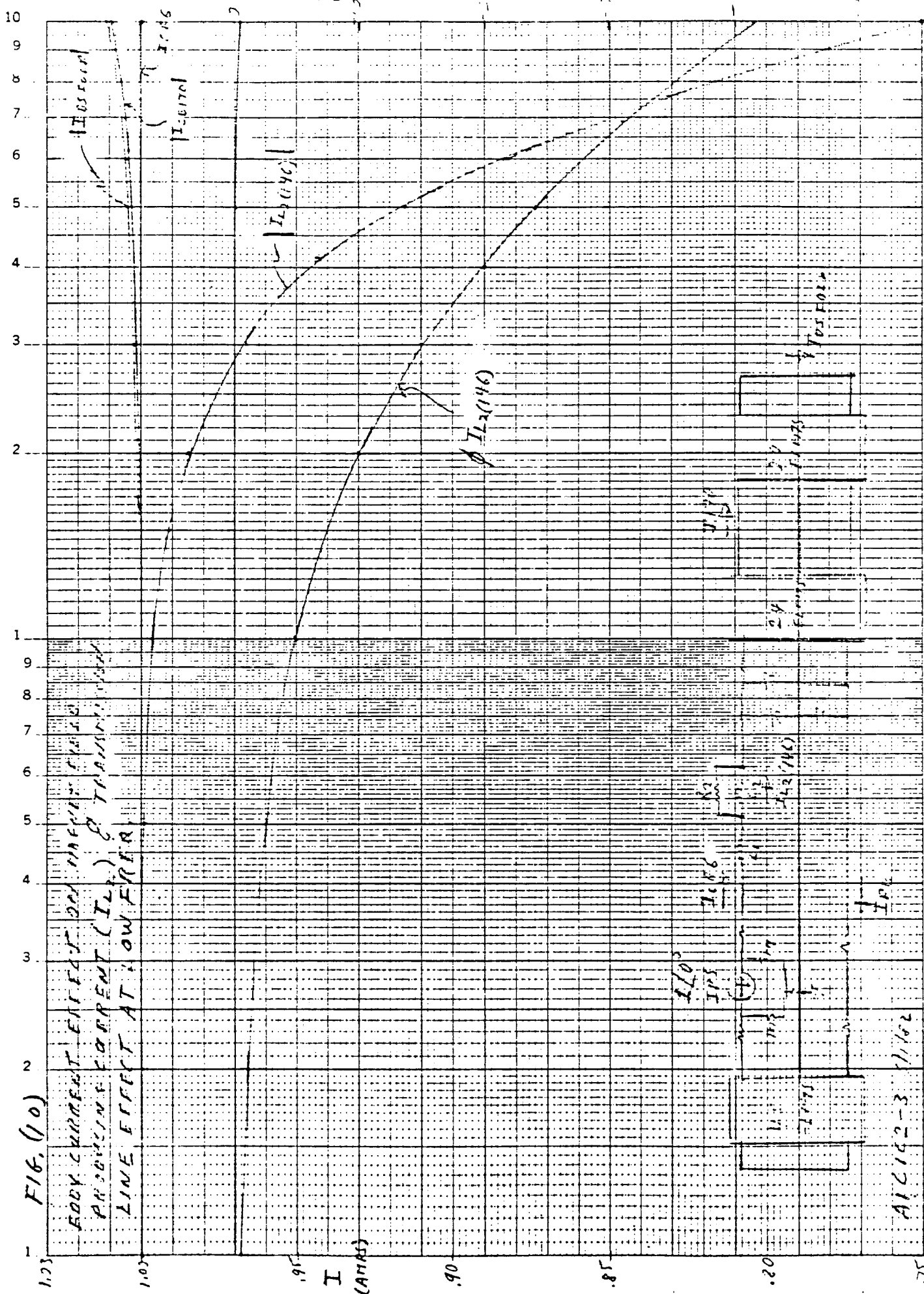
Fig. (8) : TUNE Q410-2L VS F-Q. w/ ROAD = 100cc





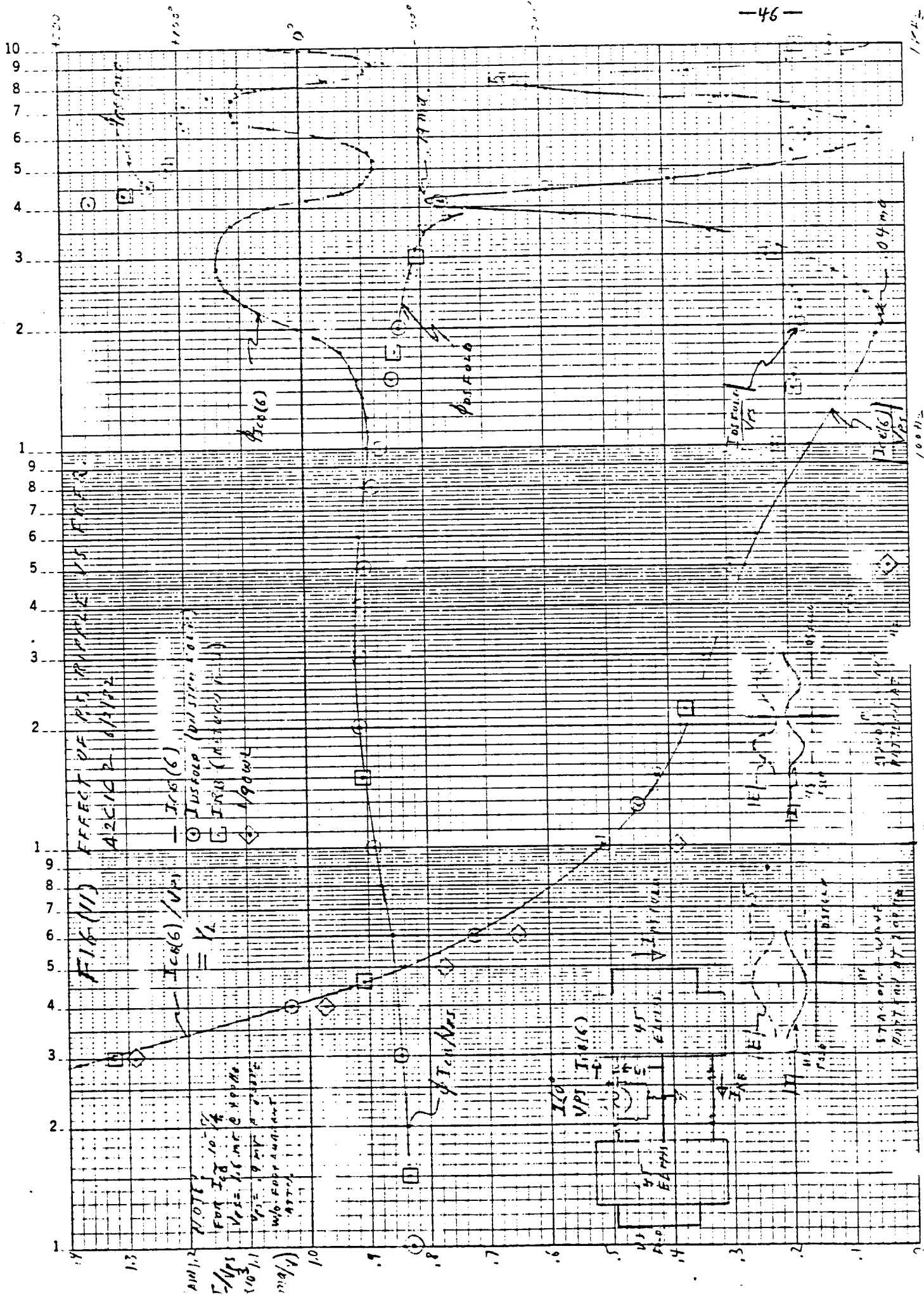
- FIG. 16.

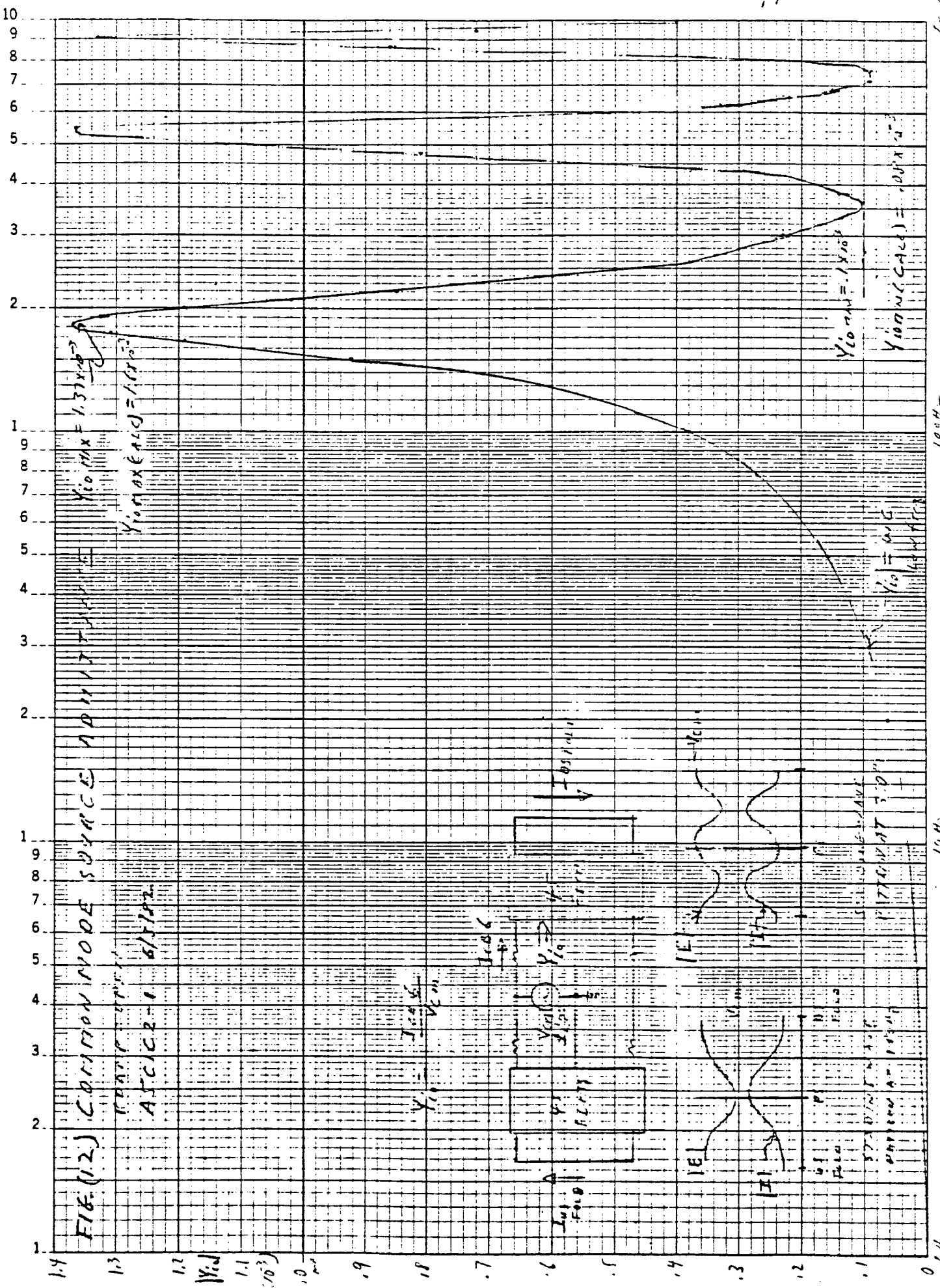
GOOD CURRENT EFFECT AND HIGH
PROBLEMS OF CURRENT (I_2) AND TRANSFORMER
LINE, EFFECT AT ONE PER CENT



$$A/C_{12} = 3 \times 10^2$$

15





F16.1(3): Common mode gain (T_{2214}/V_{cm}) vs FREQ

卷之三

145121-4703849
145121-4703849

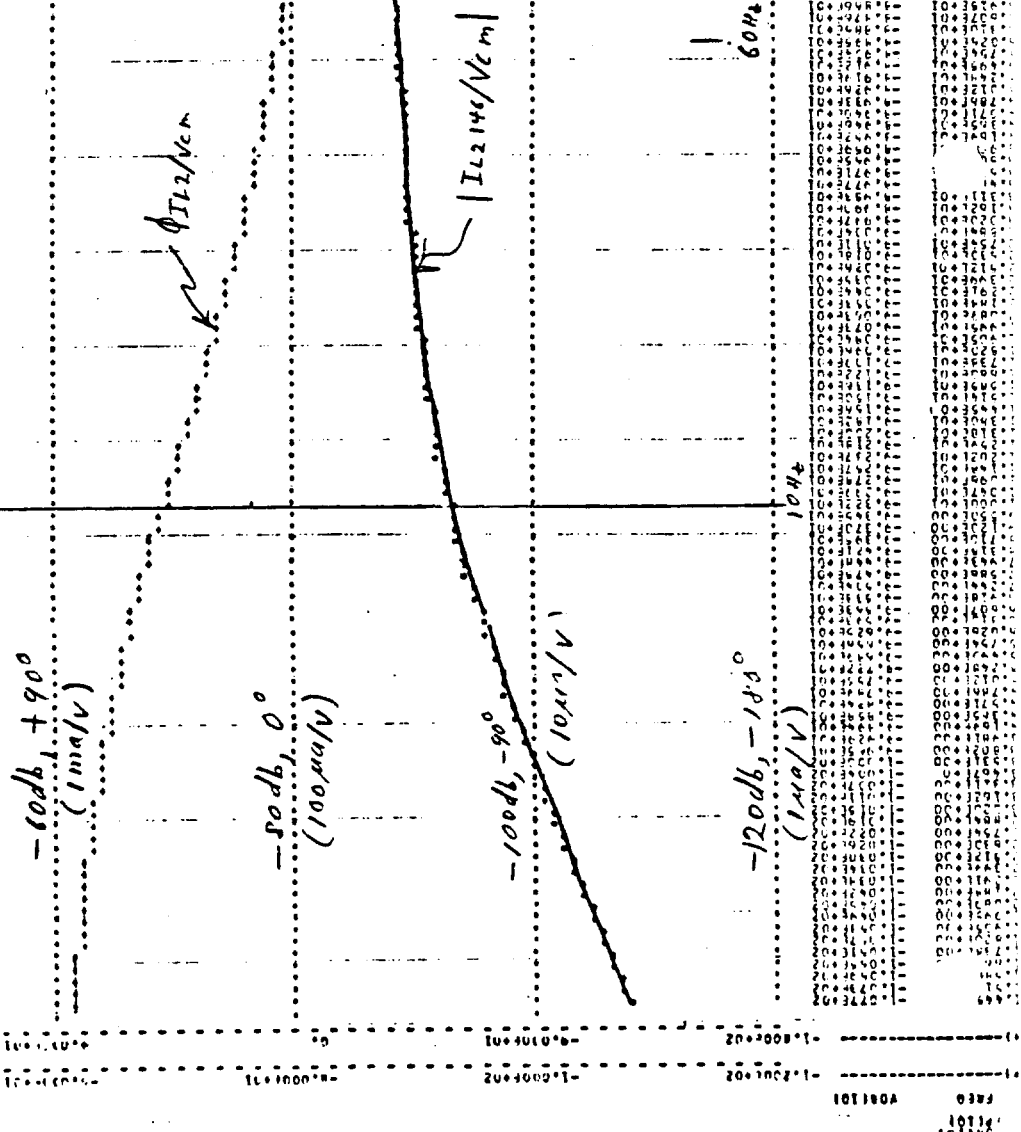
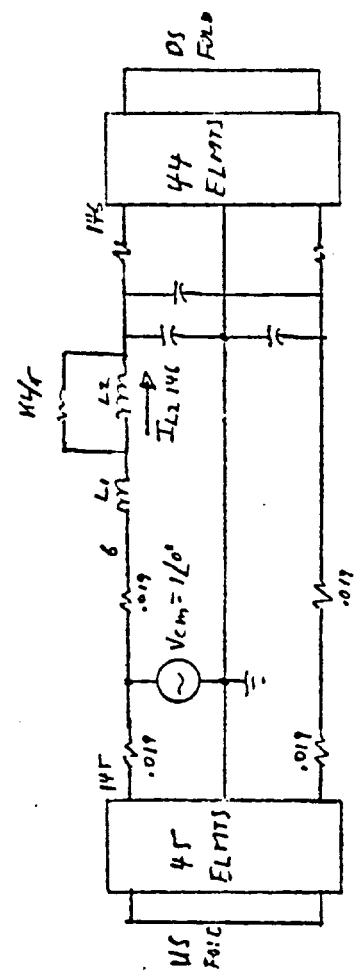
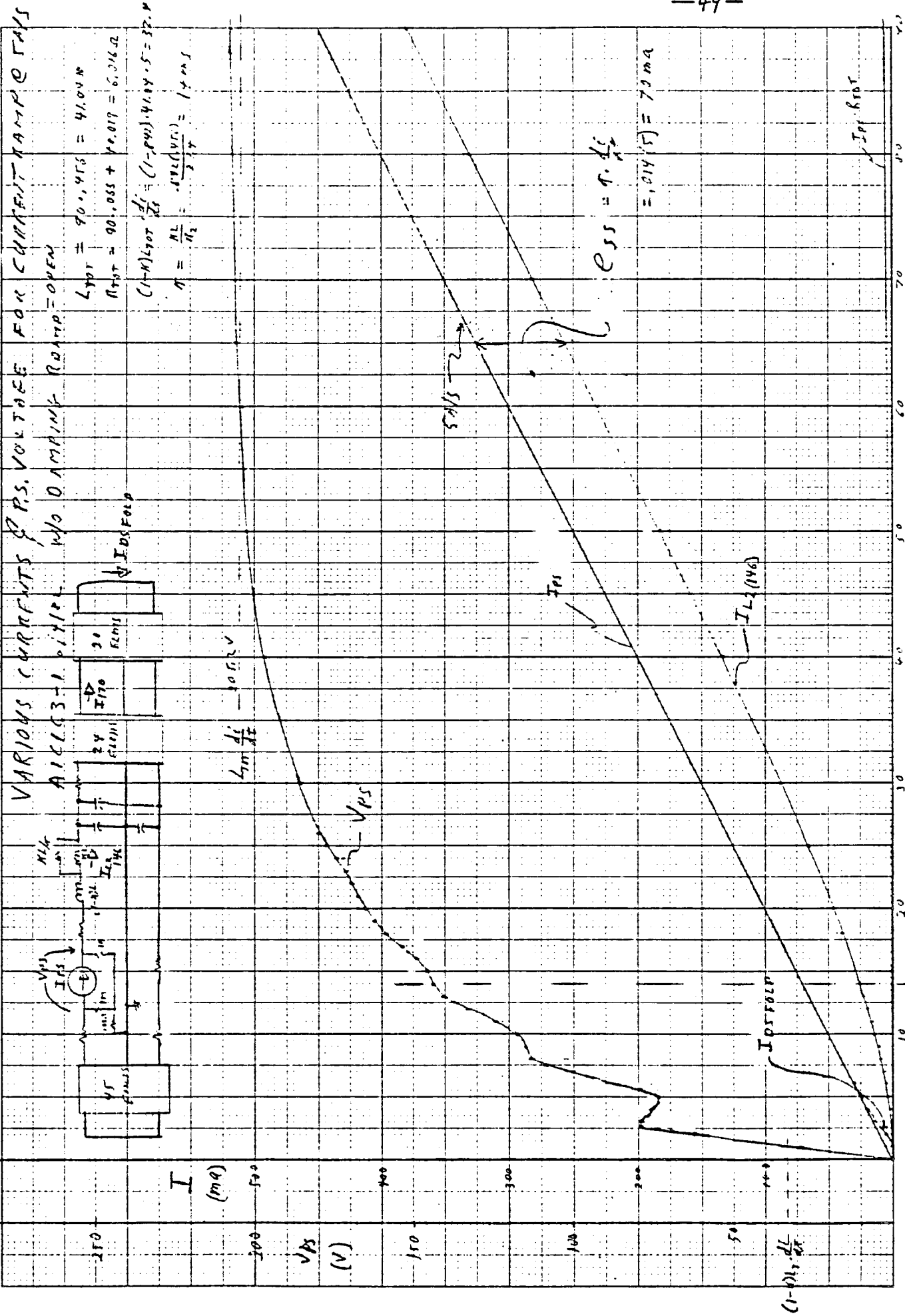
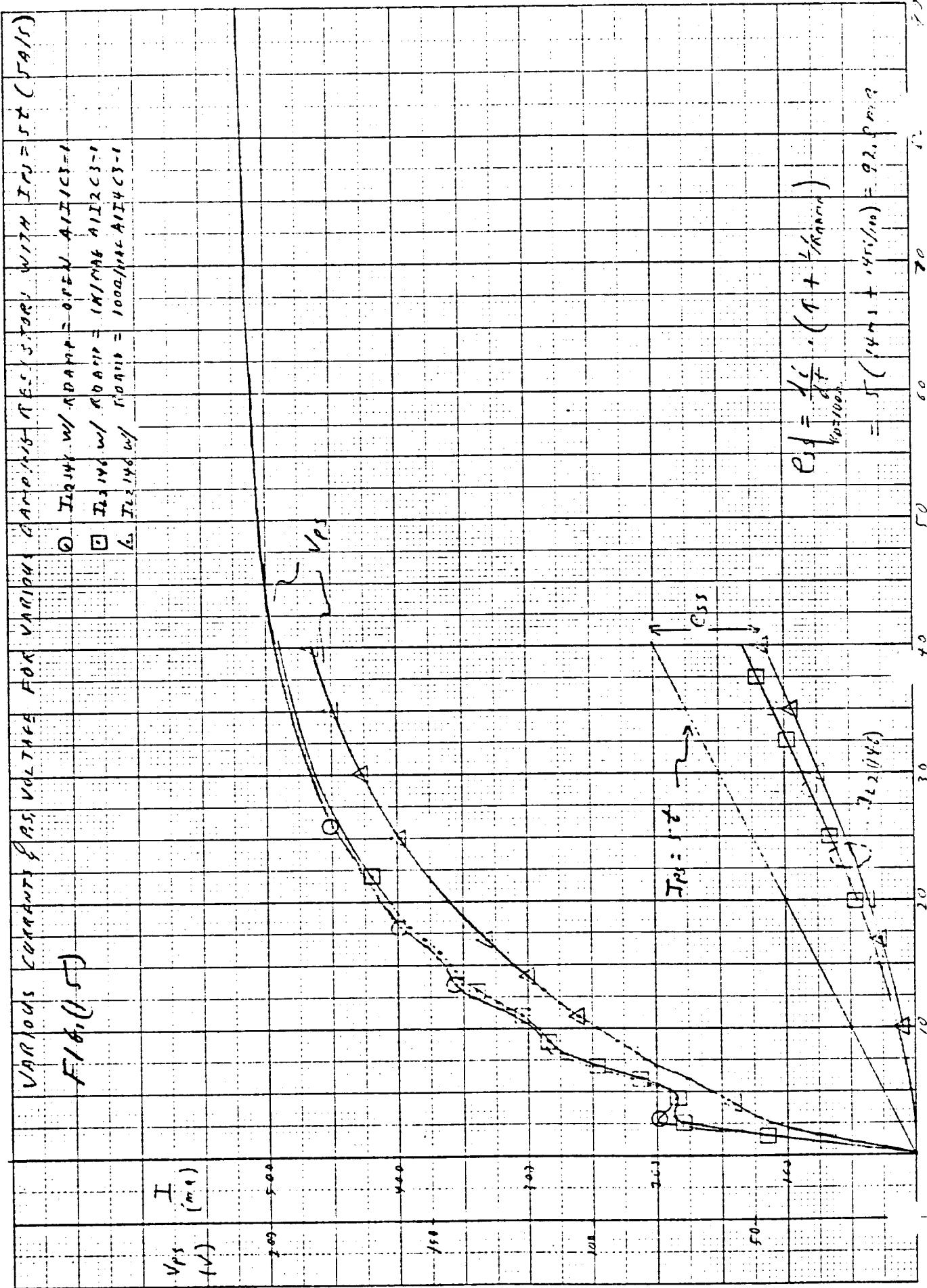
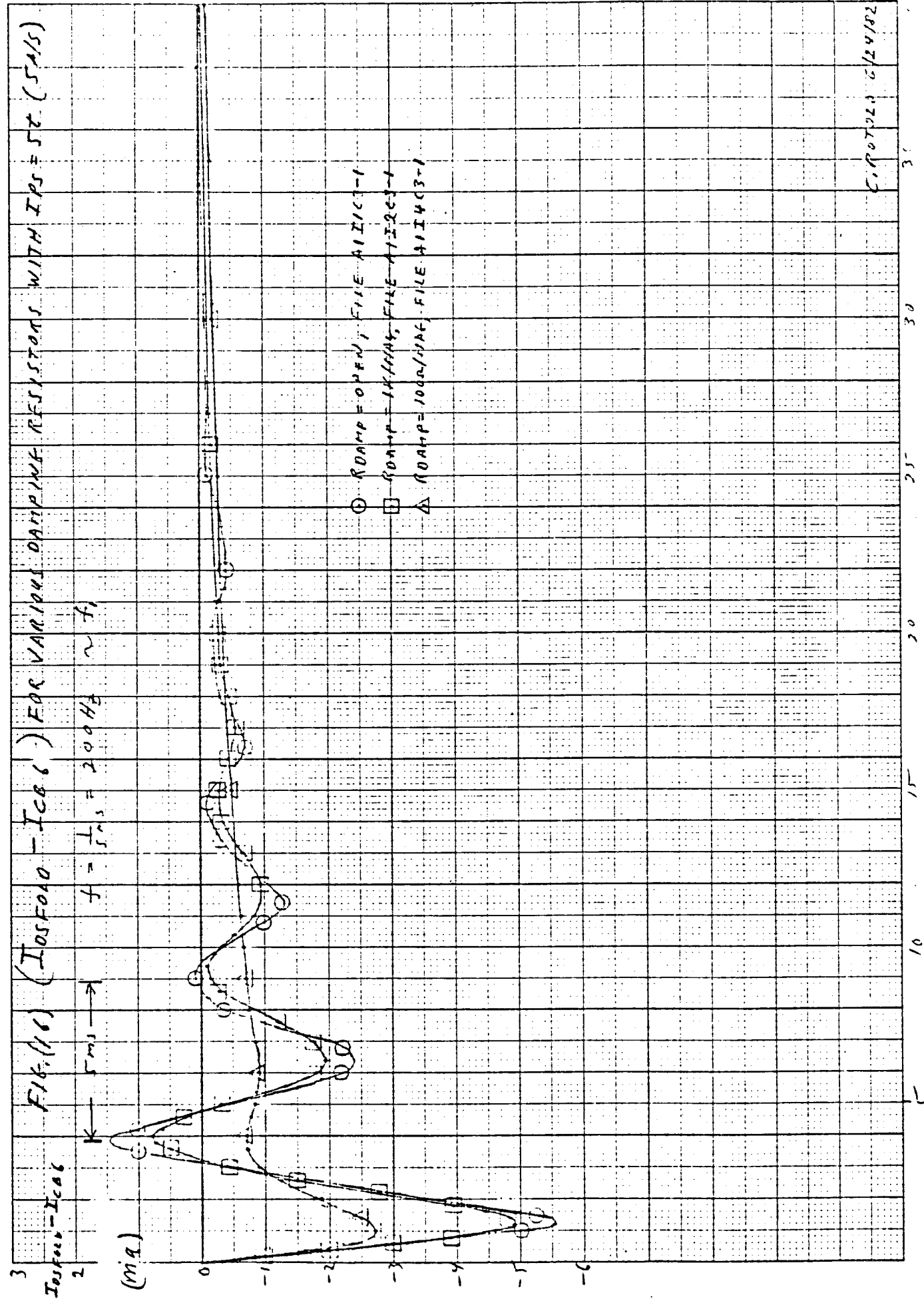


Fig. (14)







F16.(Y7) DIFFERENCE BETWEEN EXCITATION ENERGY FOR VARIOUS OXYGENIC ABSORPTION WRIGHT THIN A & (5A/5 CLASS)

ΔT
(m.e.)

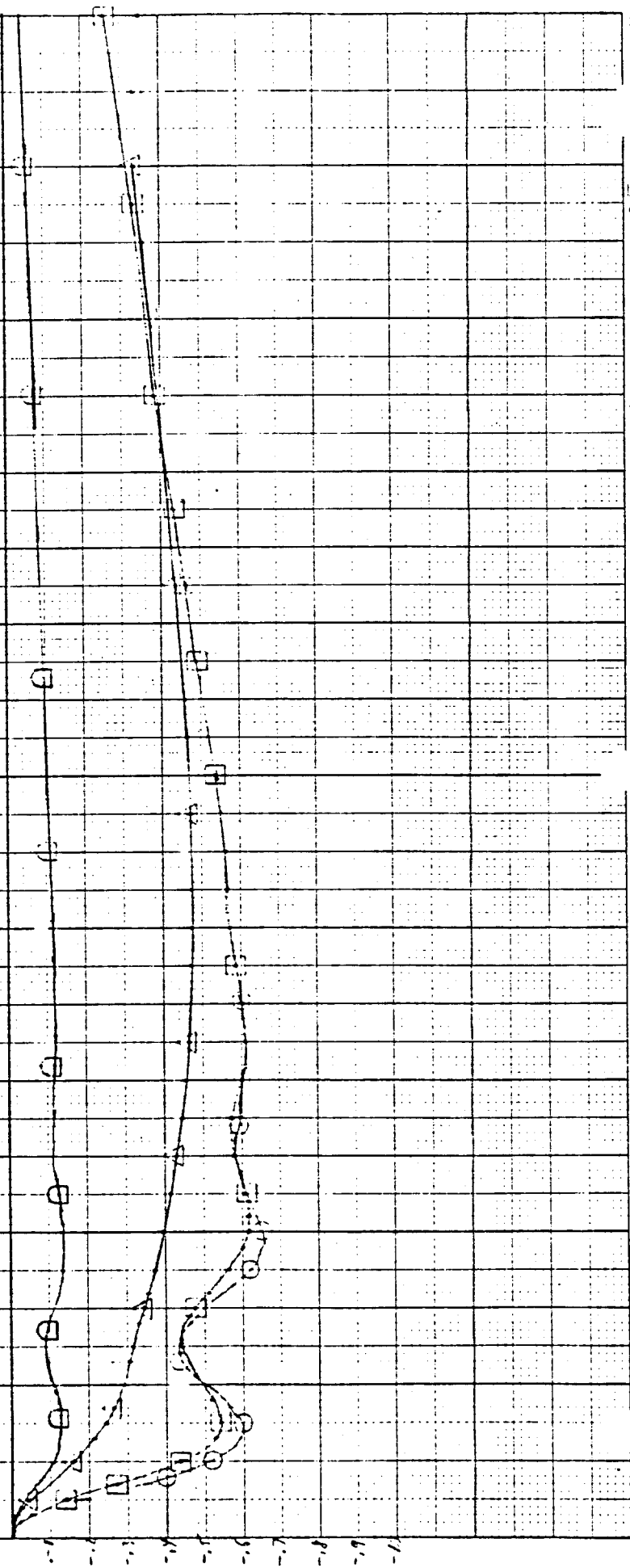
$$\textcircled{1} (T_{2190} - T_{2140}) \text{ with } R_{2170} = 0.176, A_{12/C3-1}, T_{205} = 52 \text{ (5A/5)}$$

$$\square (T_{2190} - T_{2140}) \text{ " } A_{11/11A6}, A_{11T2C3-1}, "$$

$$\triangle (T_{2190} - T_{2140}) \text{ " } A_{12/11A6}, A_{11T2C3-1}, "$$

$$\textcircled{2} (T_{2190} - T_{2140}) \text{ " } 0.176, Q_{205} = 52 \text{ (1A/5)}$$

$$\square (T_{2190} - T_{2140}) \text{ " }$$

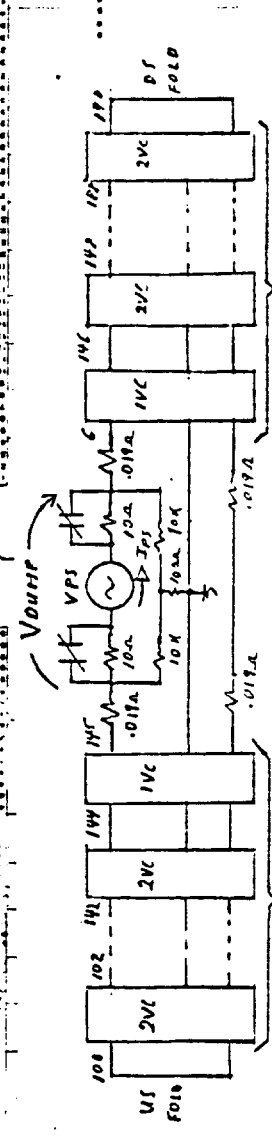


F16(18): $V_{A,NO}$, I_{PS} (OVERALL) VS TIME $\omega/R_0 Amp = 10K$

MATLAB FORTUNE QUAG-DURE, ANALYSIS-1 0/25/02 SPICE 26.1 (130C100) 10.29.2001

TEMPERATURE = 27,000 0E+0

TRANIENT ANALYSIS



-53-

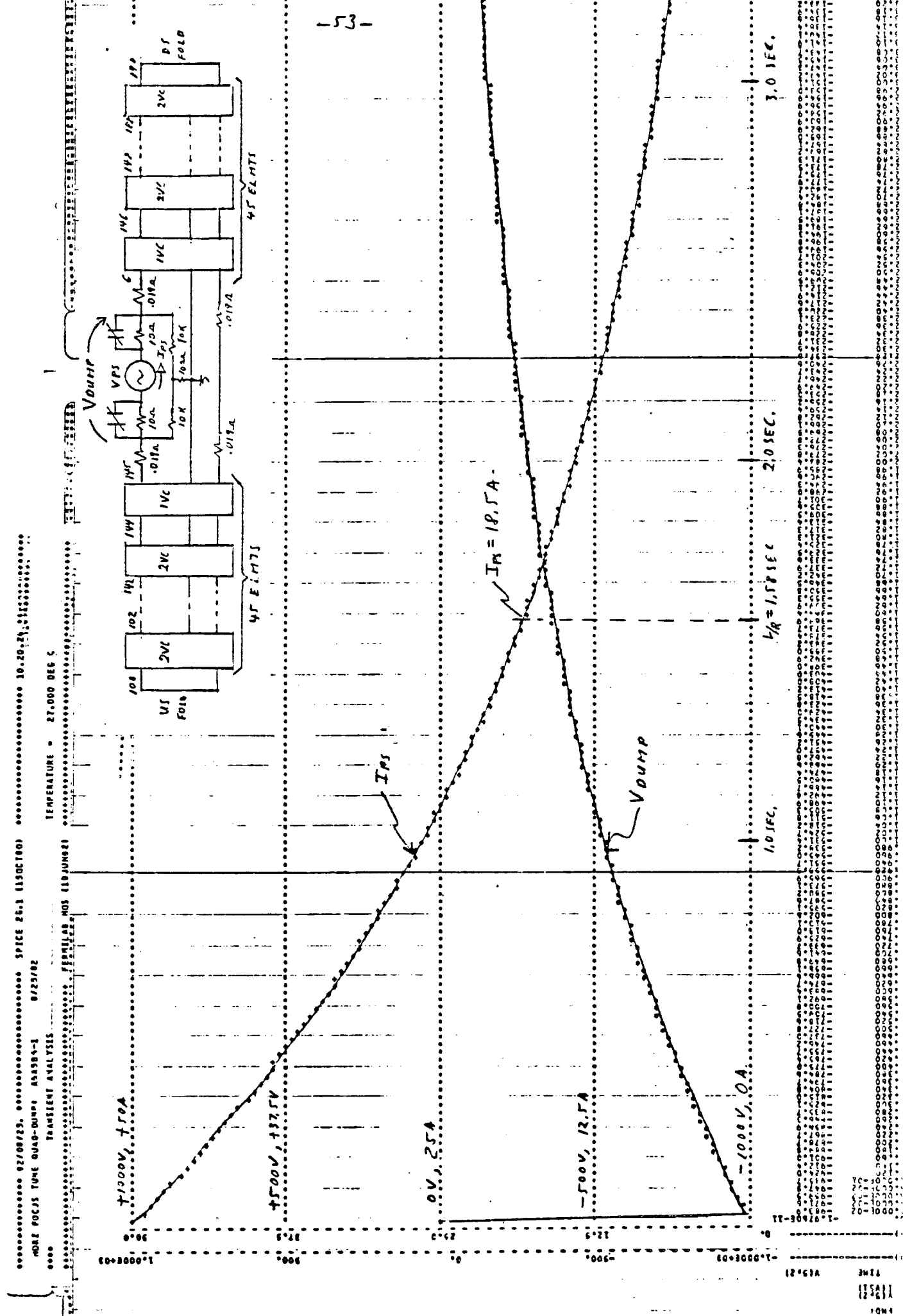


Fig. (19): Young, Ios vs T / T_E w/ Roam = 100

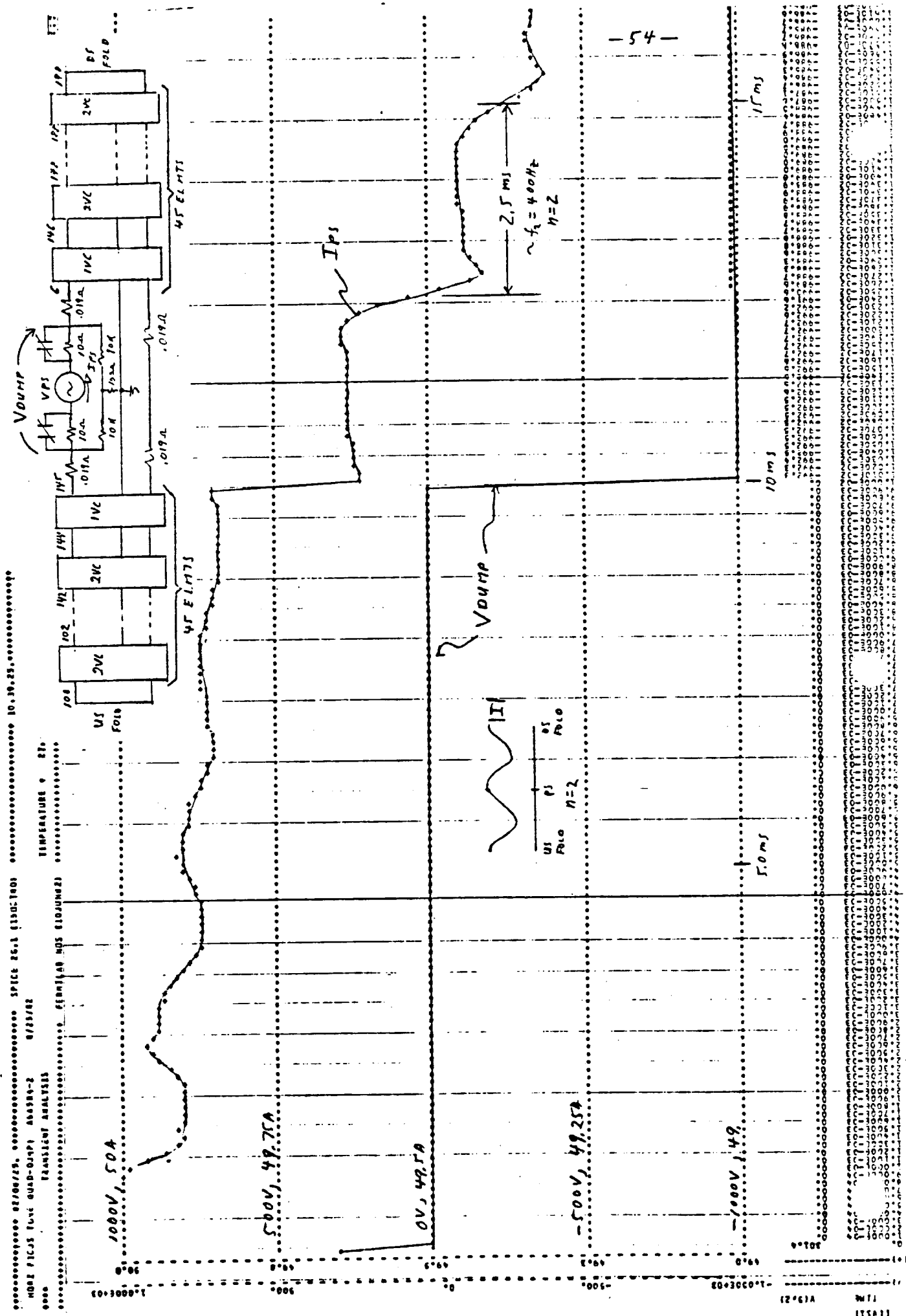
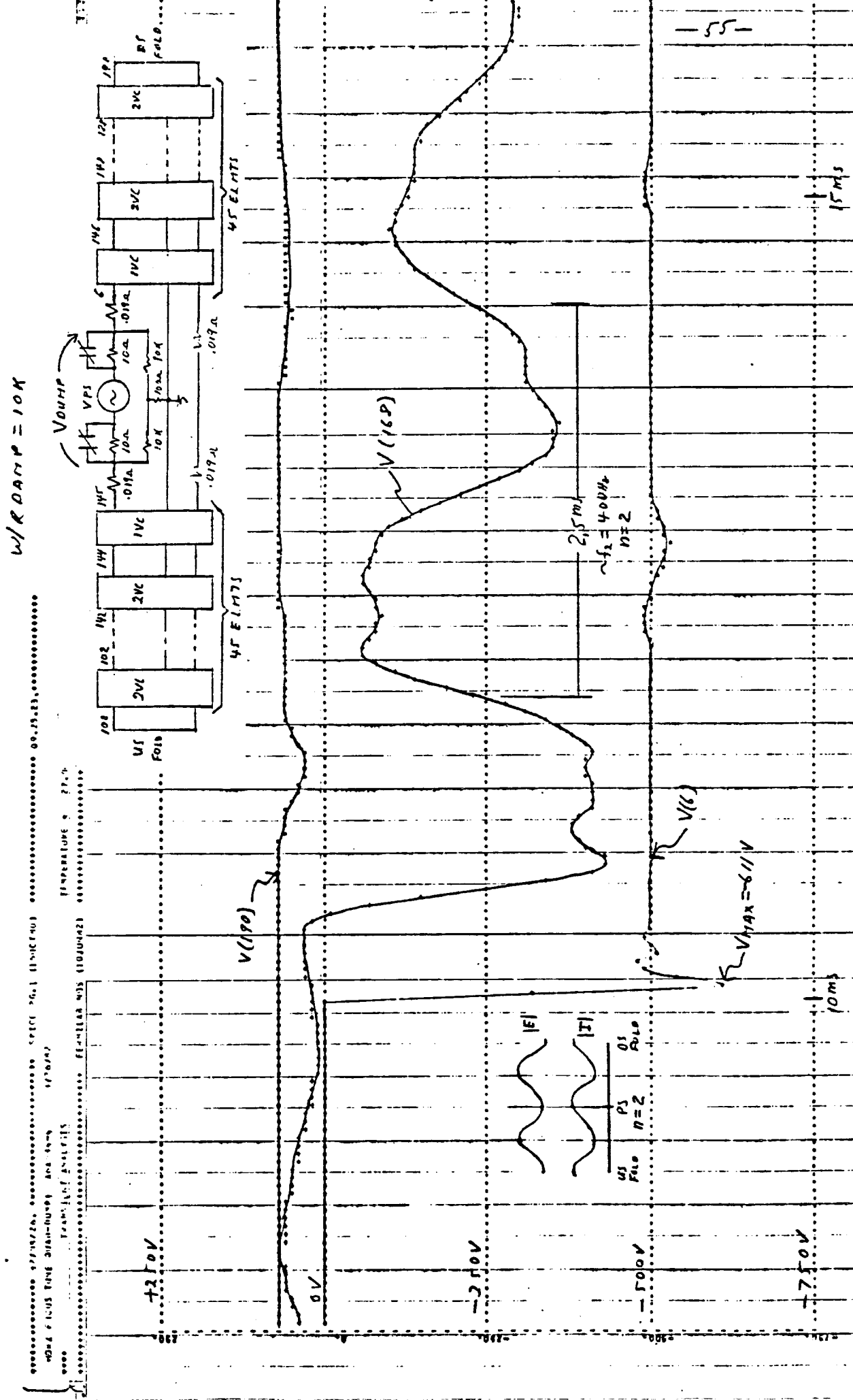
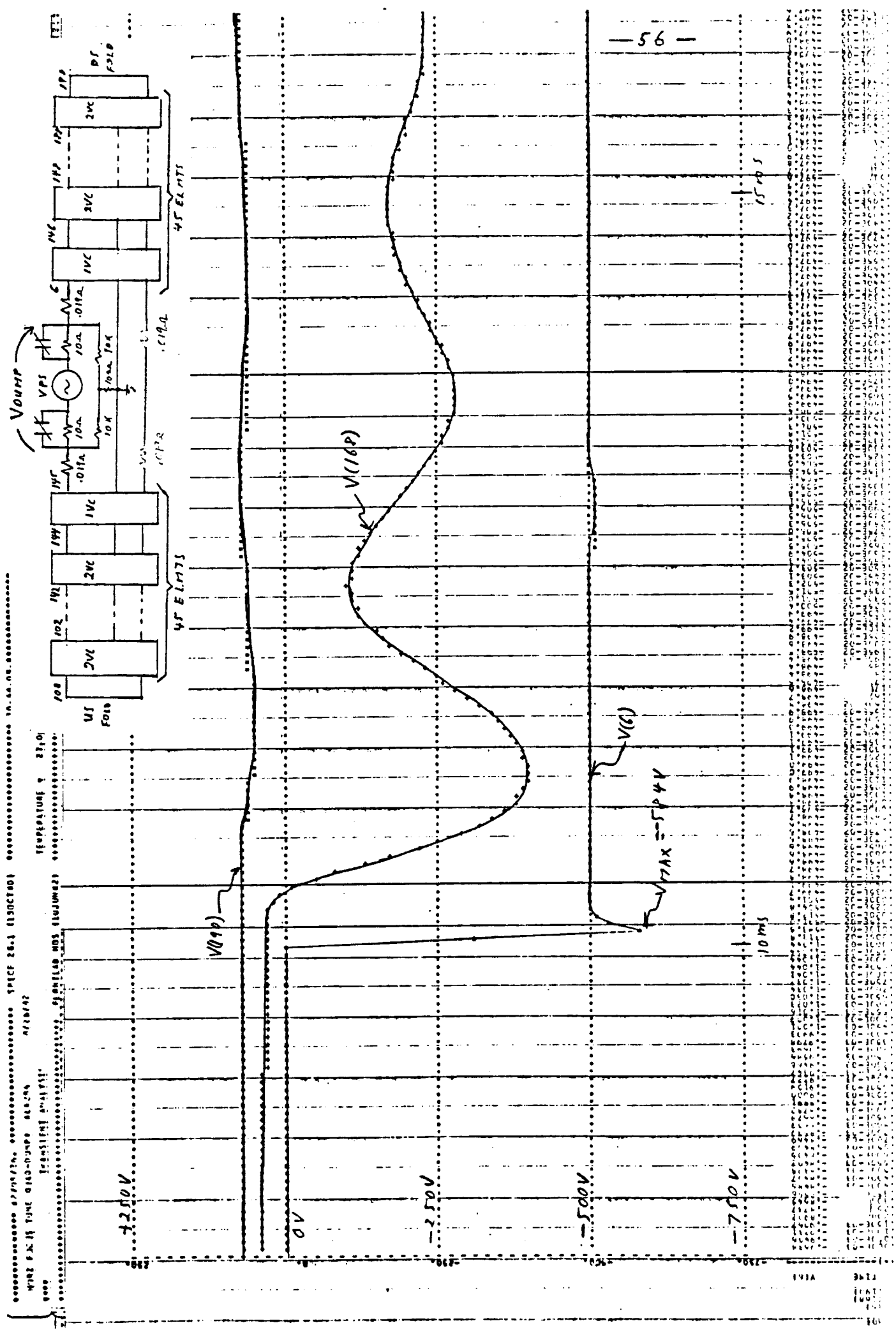


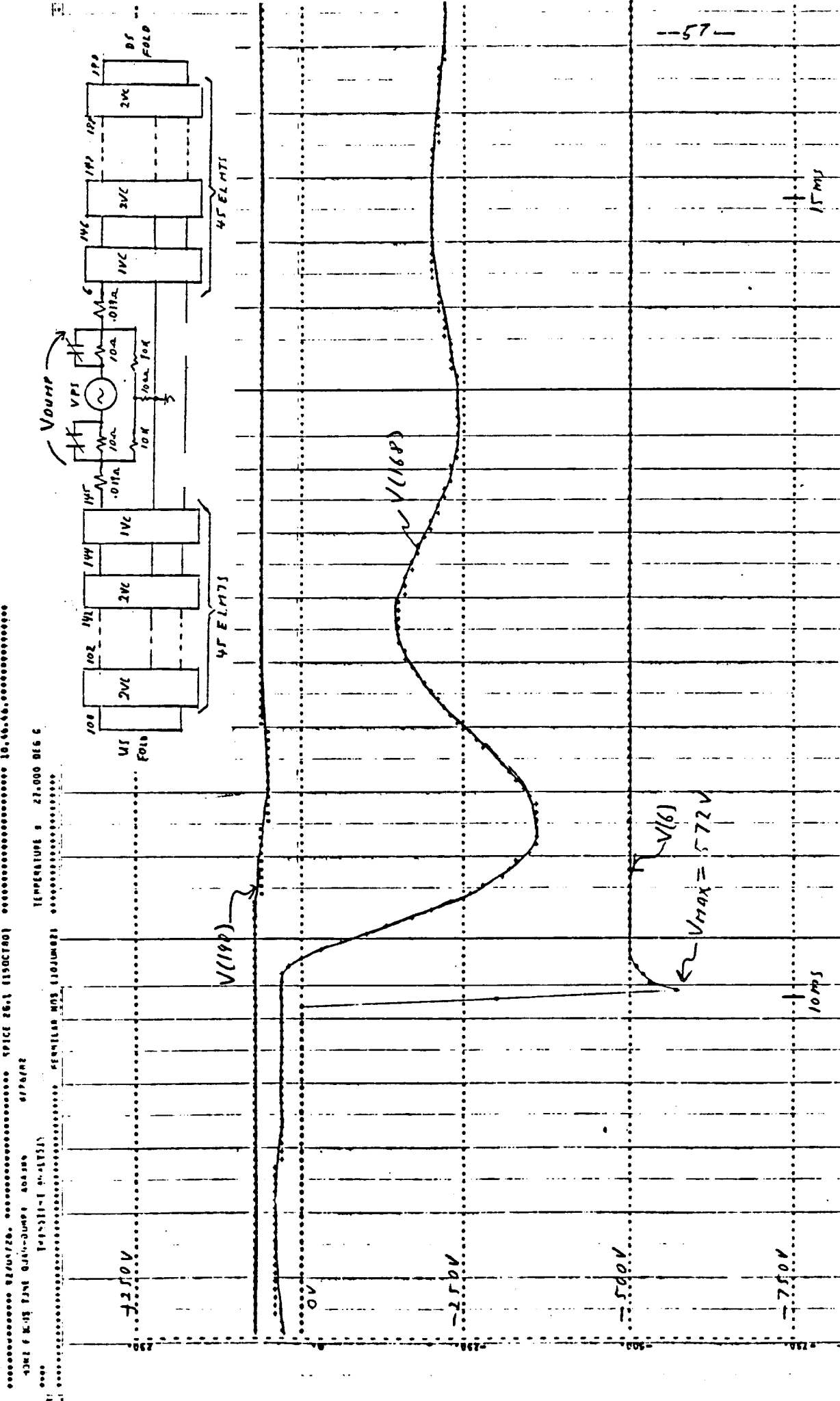
FIG. (20): VOLTAGE TO GROUND AT NOES 6, 168, & 190 (DOWNSTREAM)



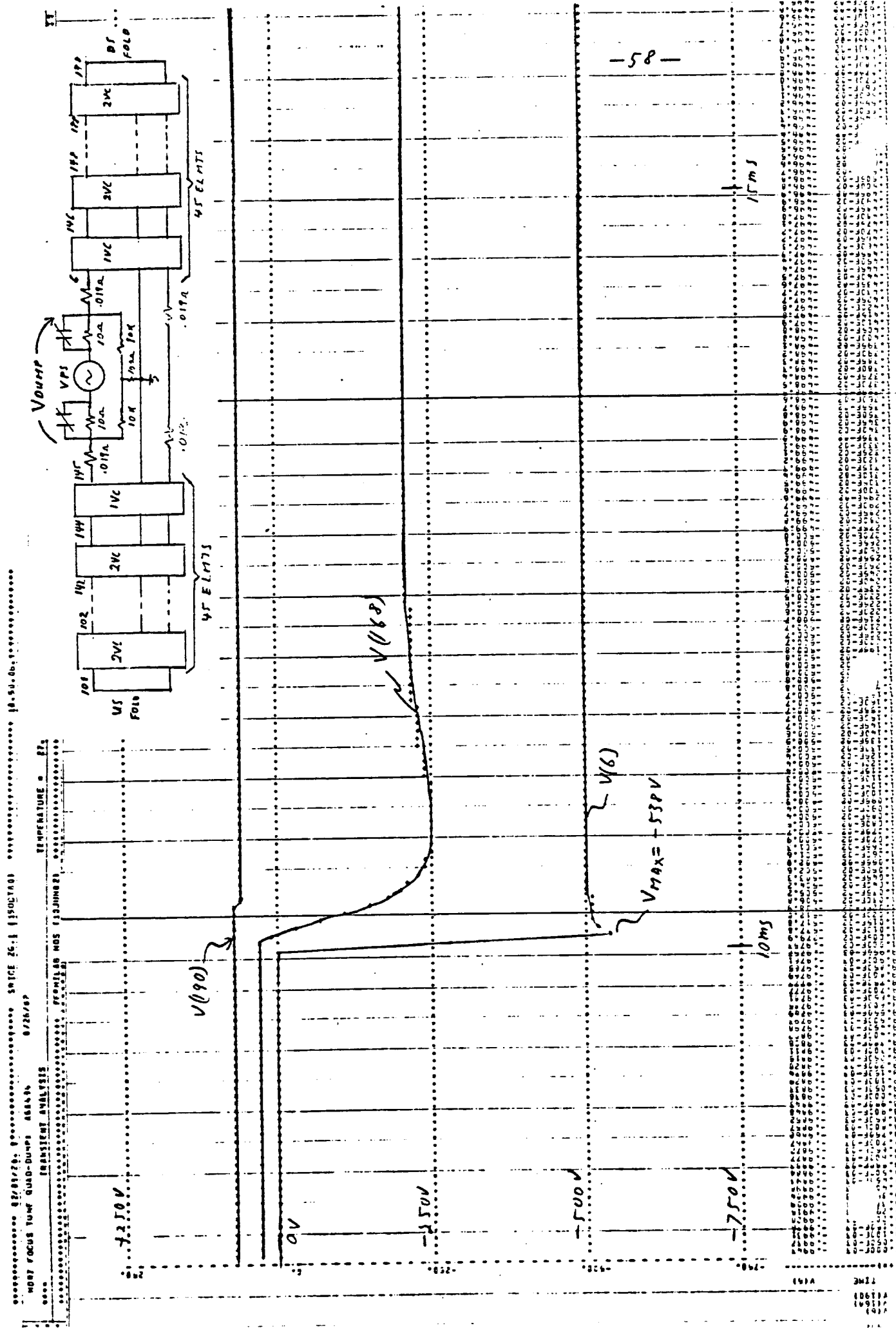
F16. (21) VOLTAGE TO GROUND AT NODES 6, 10P, & 190 w/ R_{ONNO} = 1M



F16. (22): VOLTAGE TO GROUND AT NOOES 6, 168, F190 WITH ROA110 = 500Ω



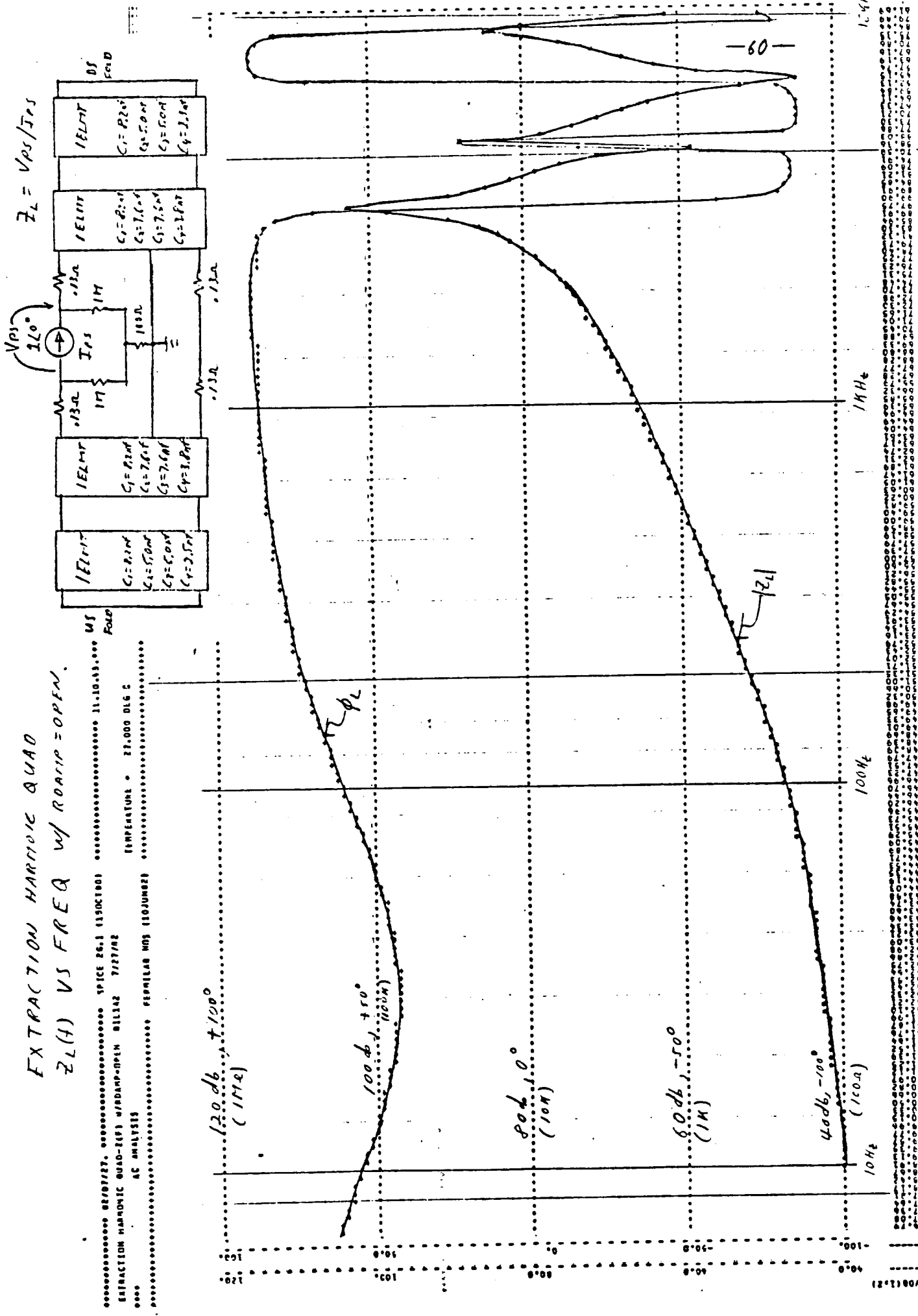
F16. (23): VOLTAGE TO GROUND AT NODES 6, 168, 6190 AND RAMP = 100Ω



APPENDIX A

Appendix A contains pertinent graphs of all the Higher Order Correction Element circuits, except the Tune Quad. Presented are the impedance seen by the power supply $Z_L(f)$ with soft ground resistors of 1 Meg ohm for various damping resistors. In addition, various voltages to ground along the bus are given to simulate conditions during a dump for which the power supply was simulated as a voltage source having a 1,000 V step at $t = 0$.

$Z_L(f)$ VS FREQ w/ RODRIP = OPEN



EXTRACTION HARMONIC QVAD

$Z_L(t)$ VS FREQ W/ LOAD = 1K

Extraction harmonic load=1K w/ load=1K
AC analysis
Spice 3.1 (structure 7727702)
Temperature = 27.000 deg C
FAB

120 dB_r + 100°
(100Hz)

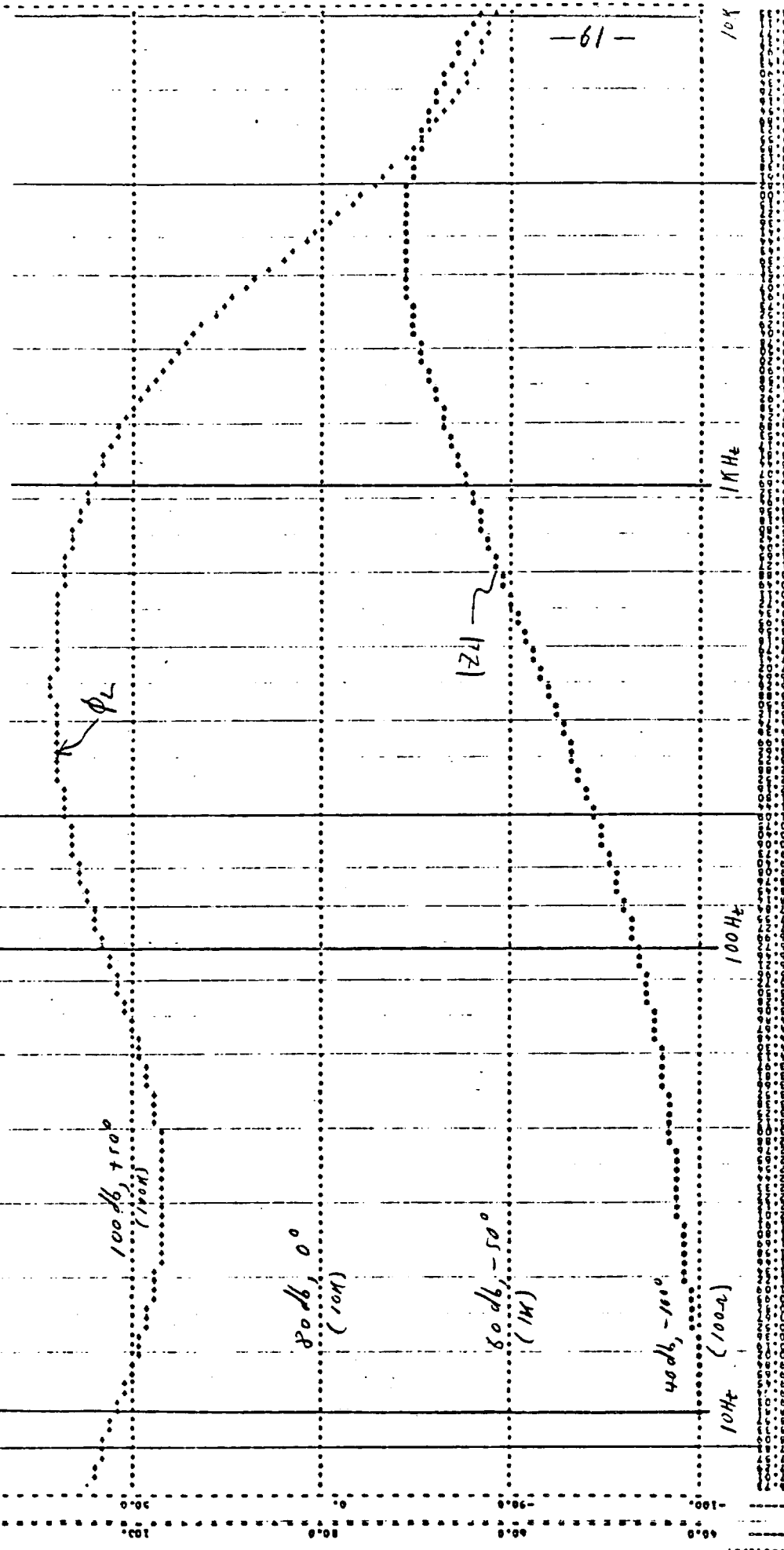
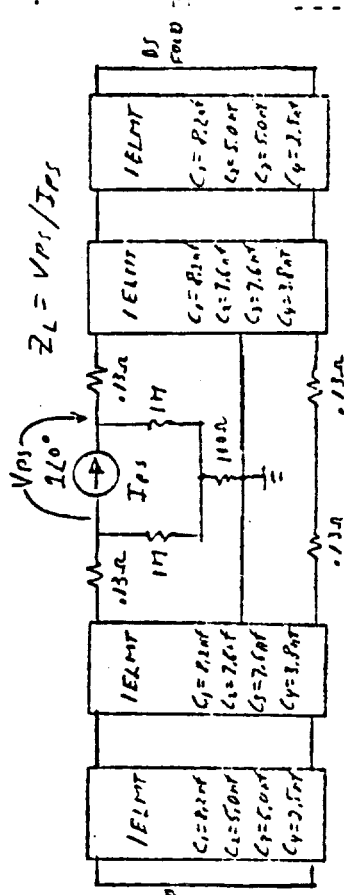
100 dB_r + 100°
(100Hz)

80 dB_r 0°
(100Hz)

60 dB_r -50°
(100Hz)

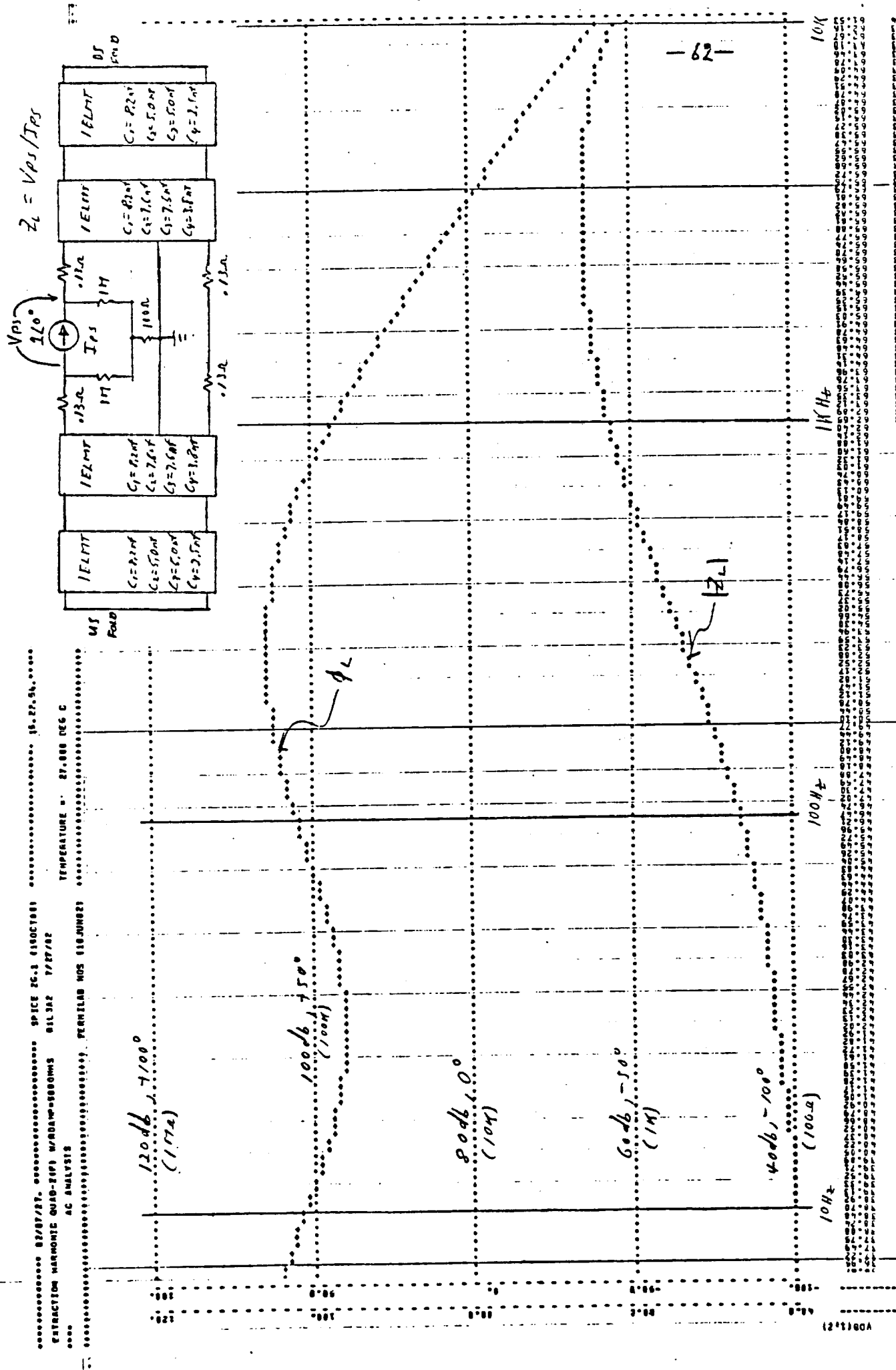
40 dB_r -100°
(100Hz)

10H_r 100°
(100Hz)

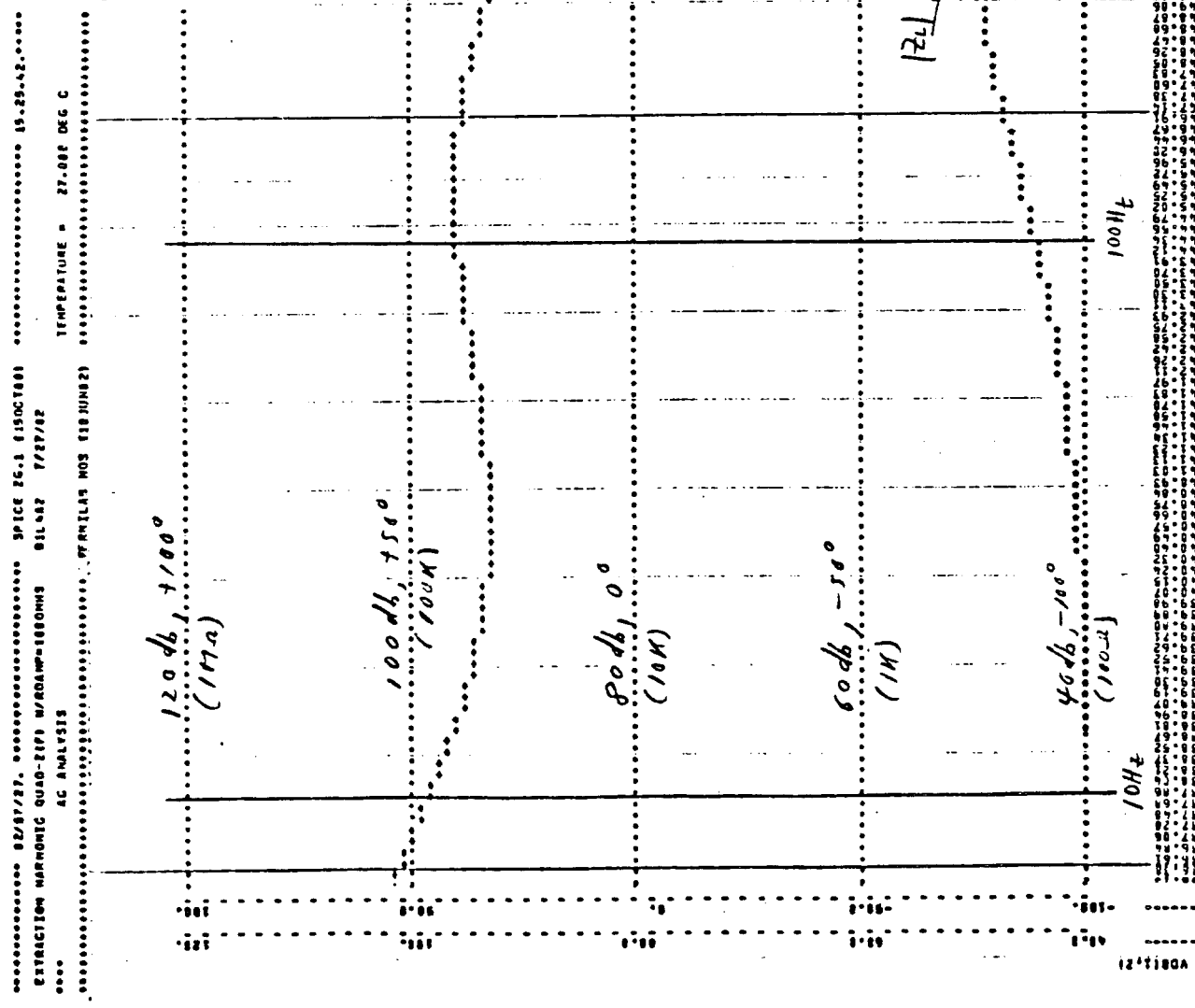


EXTRACTION HARMONIC QUNO

$Z_L(f)$ VS $FREQ$ w/ $R_{LOAD} = 500\Omega$



EXTRACTION OF AN IONIC Q.
 $\Sigma_L(t)$ VS FNE Q. w/ R_D11P = 100A



The diagram illustrates a transmission line model with the following components and parameters:

- Series Voltage Source:** V_{psi}
- Shunt Load:** $Z_L = V_{psi} / I_{psi}$
- Series Admittance:** Y_0
- Transmission Line Segments:** The line is divided into four segments, each with its own parameters and reflection coefficient calculations.

Segment 1 (Bottom):

- Series admittance: $Y_{1,ext}$
- Shunt load: $C_1 = 2.5 \mu F$
- Series admittance: $Y_1 = 2.5 \mu A$
- Shunt load: $C_2 = 2.5 \mu F$
- Series admittance: $Y_2 = 2.5 \mu A$
- Shunt load: $C_3 = 2.5 \mu F$
- Series admittance: $Y_3 = 2.5 \mu A$
- Shunt load: $C_4 = 2.5 \mu F$
- Series admittance: $Y_4 = 2.5 \mu A$

Segment 2 (Second from Bottom):

- Series admittance: $Y_{2,ext}$
- Shunt load: $C_1 = 2.5 \mu F$
- Series admittance: $Y_1 = 2.5 \mu A$
- Shunt load: $C_2 = 2.5 \mu F$
- Series admittance: $Y_2 = 2.5 \mu A$
- Shunt load: $C_3 = 2.5 \mu F$
- Series admittance: $Y_3 = 2.5 \mu A$
- Shunt load: $C_4 = 2.5 \mu F$
- Series admittance: $Y_4 = 2.5 \mu A$

Segment 3 (Third from Bottom):

- Series admittance: $Y_{3,ext}$
- Shunt load: $C_1 = 2.5 \mu F$
- Series admittance: $Y_1 = 2.5 \mu A$
- Shunt load: $C_2 = 2.5 \mu F$
- Series admittance: $Y_2 = 2.5 \mu A$
- Shunt load: $C_3 = 2.5 \mu F$
- Series admittance: $Y_3 = 2.5 \mu A$
- Shunt load: $C_4 = 2.5 \mu F$
- Series admittance: $Y_4 = 2.5 \mu A$

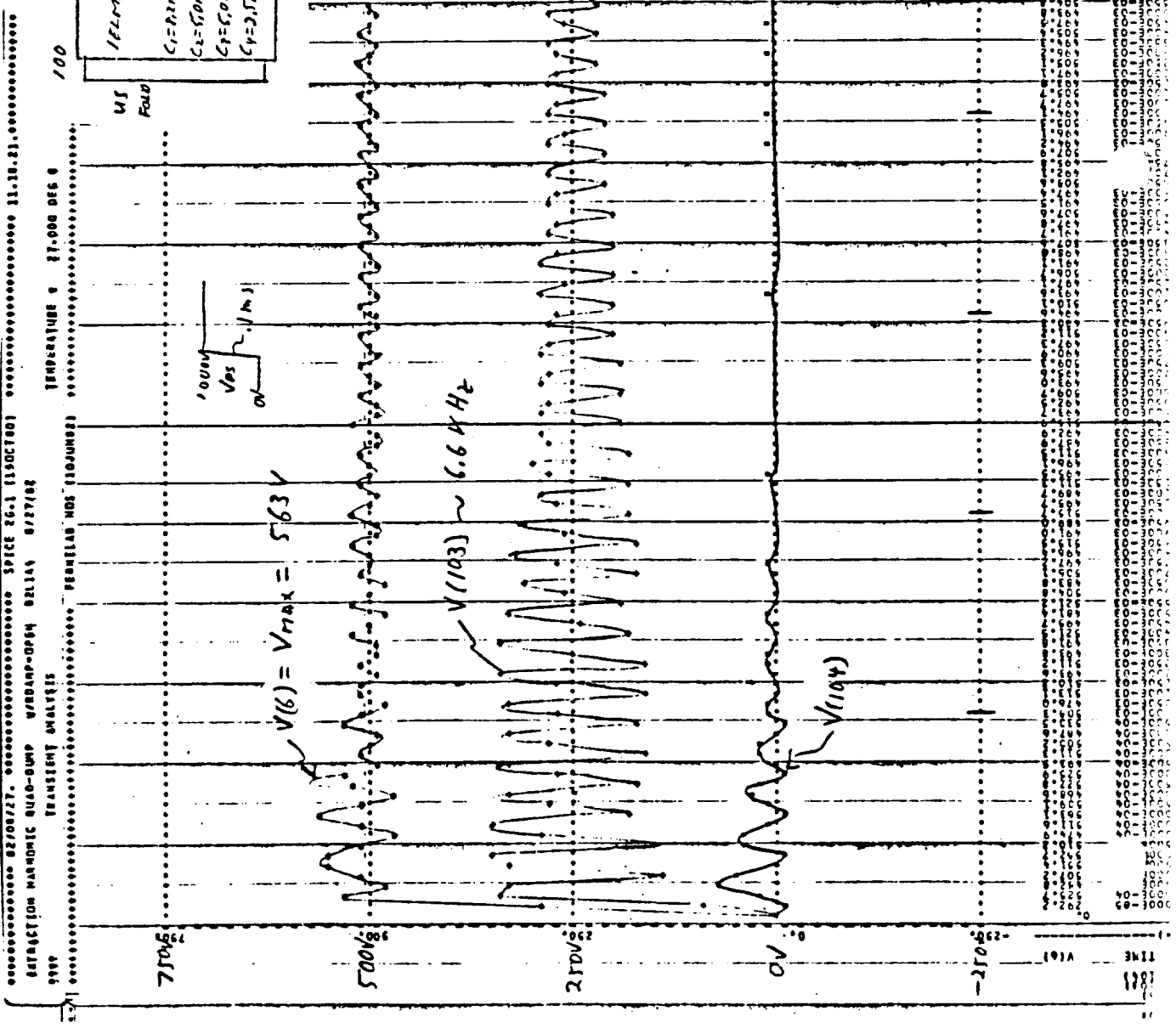
Segment 4 (Top):

- Series admittance: $Y_{4,ext}$
- Shunt load: $C_1 = 2.5 \mu F$
- Series admittance: $Y_1 = 2.5 \mu A$
- Shunt load: $C_2 = 2.5 \mu F$
- Series admittance: $Y_2 = 2.5 \mu A$
- Shunt load: $C_3 = 2.5 \mu F$
- Series admittance: $Y_3 = 2.5 \mu A$
- Shunt load: $C_4 = 2.5 \mu F$
- Series admittance: $Y_4 = 2.5 \mu A$

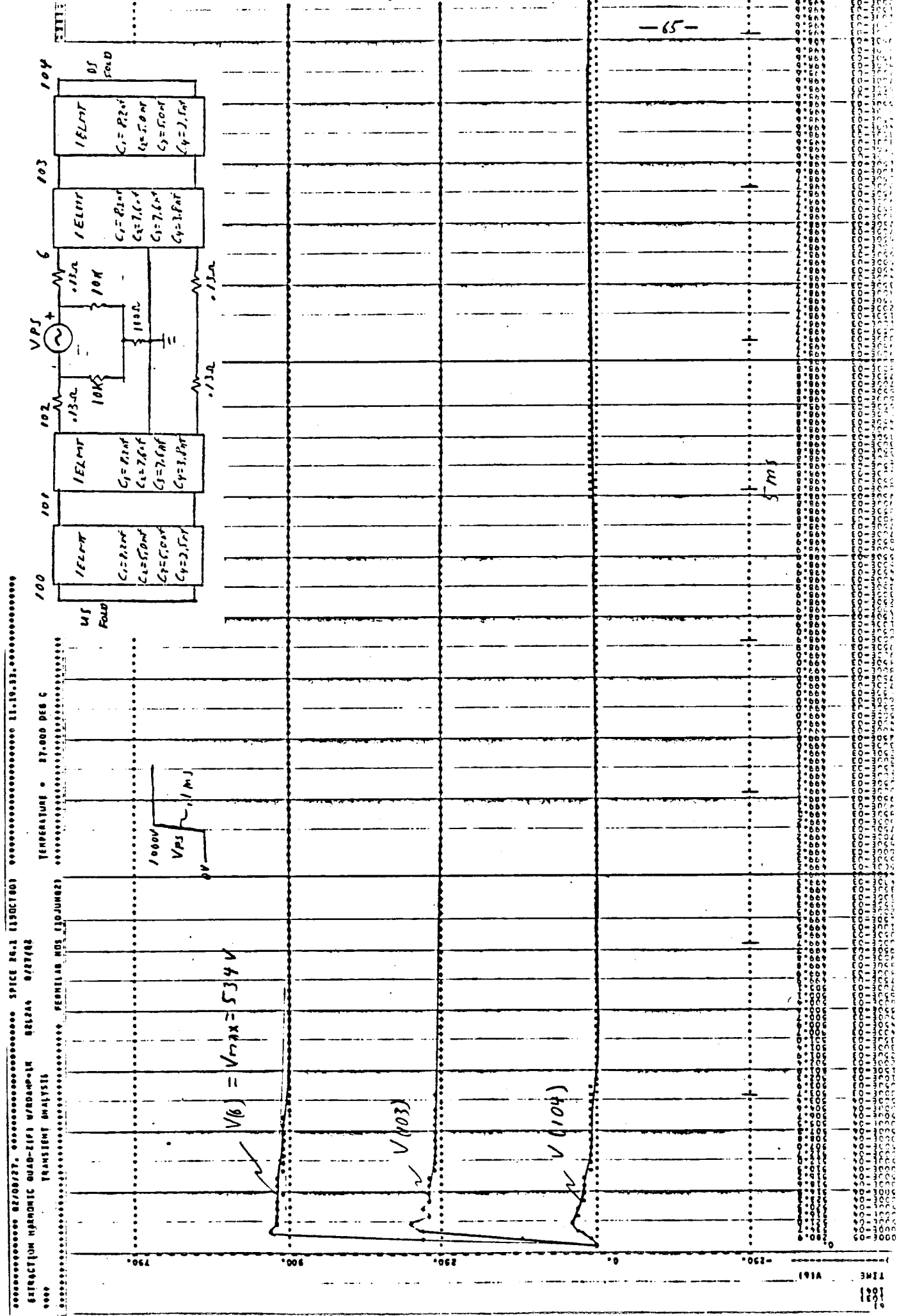
-63-

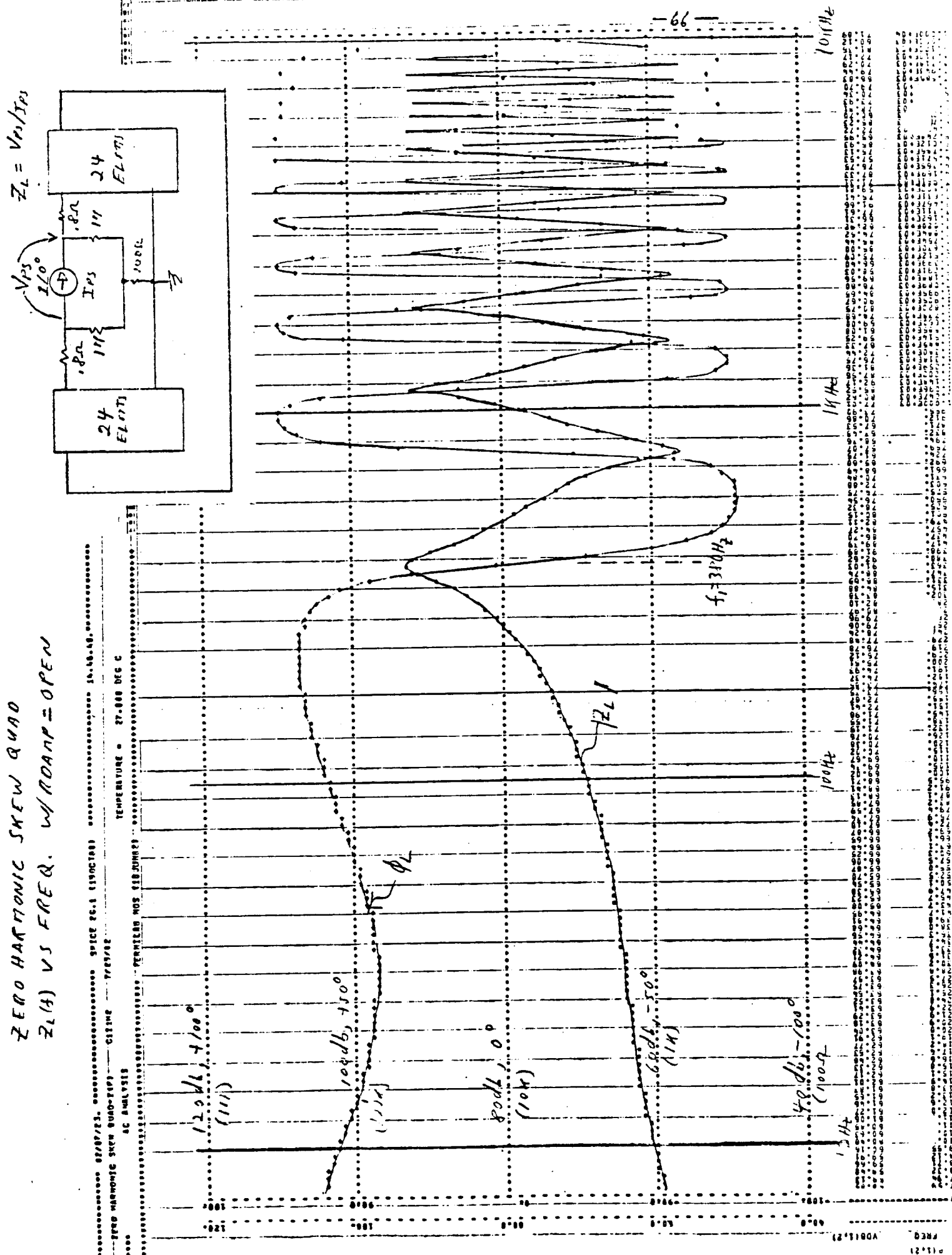
107

EXTRACTION HARMONIC & QAD: D4MP w/ R00mp = OPEN

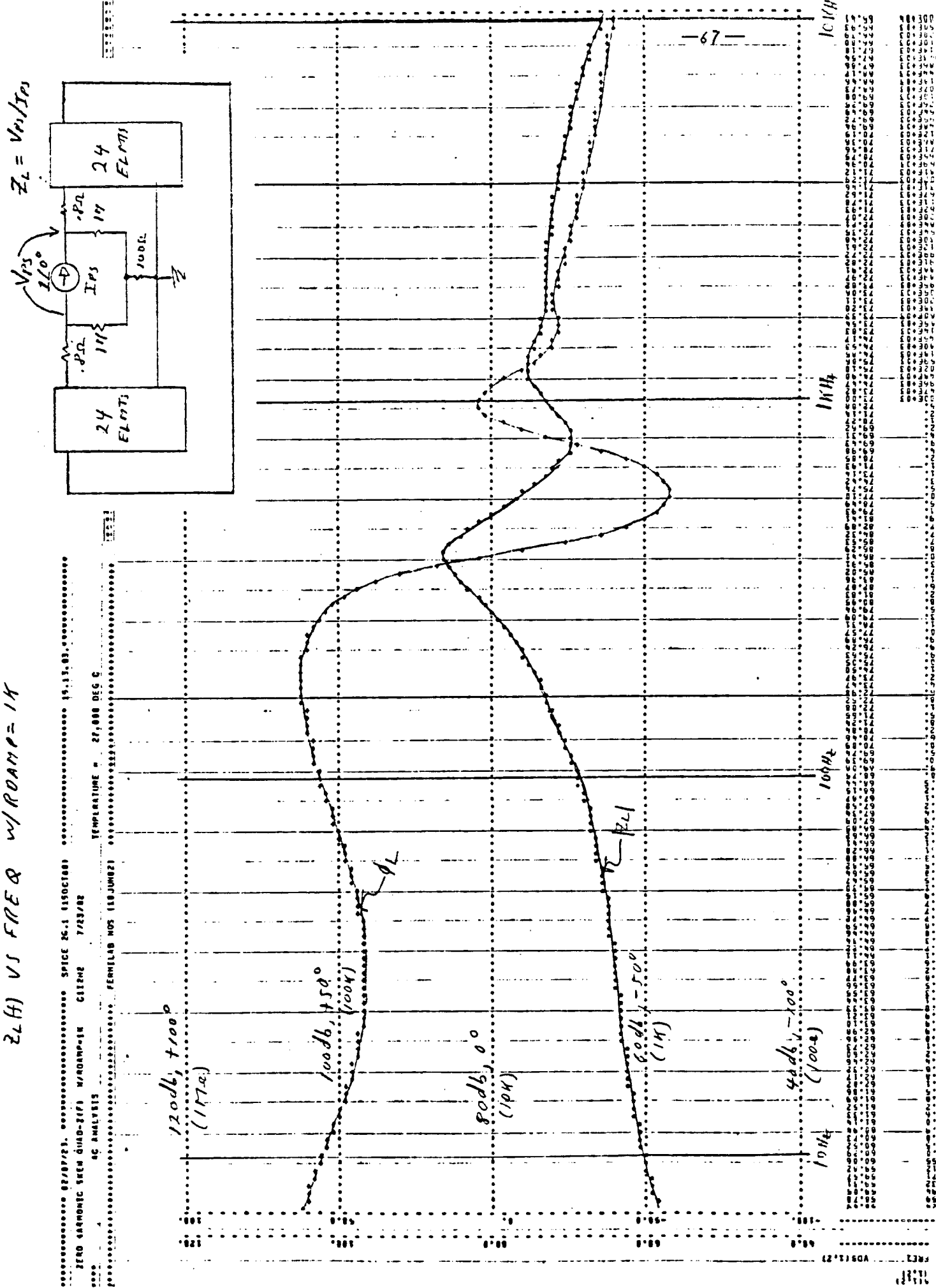


EXTRACTION HARMONIC QUAD: D47P W/R DARTP = 11

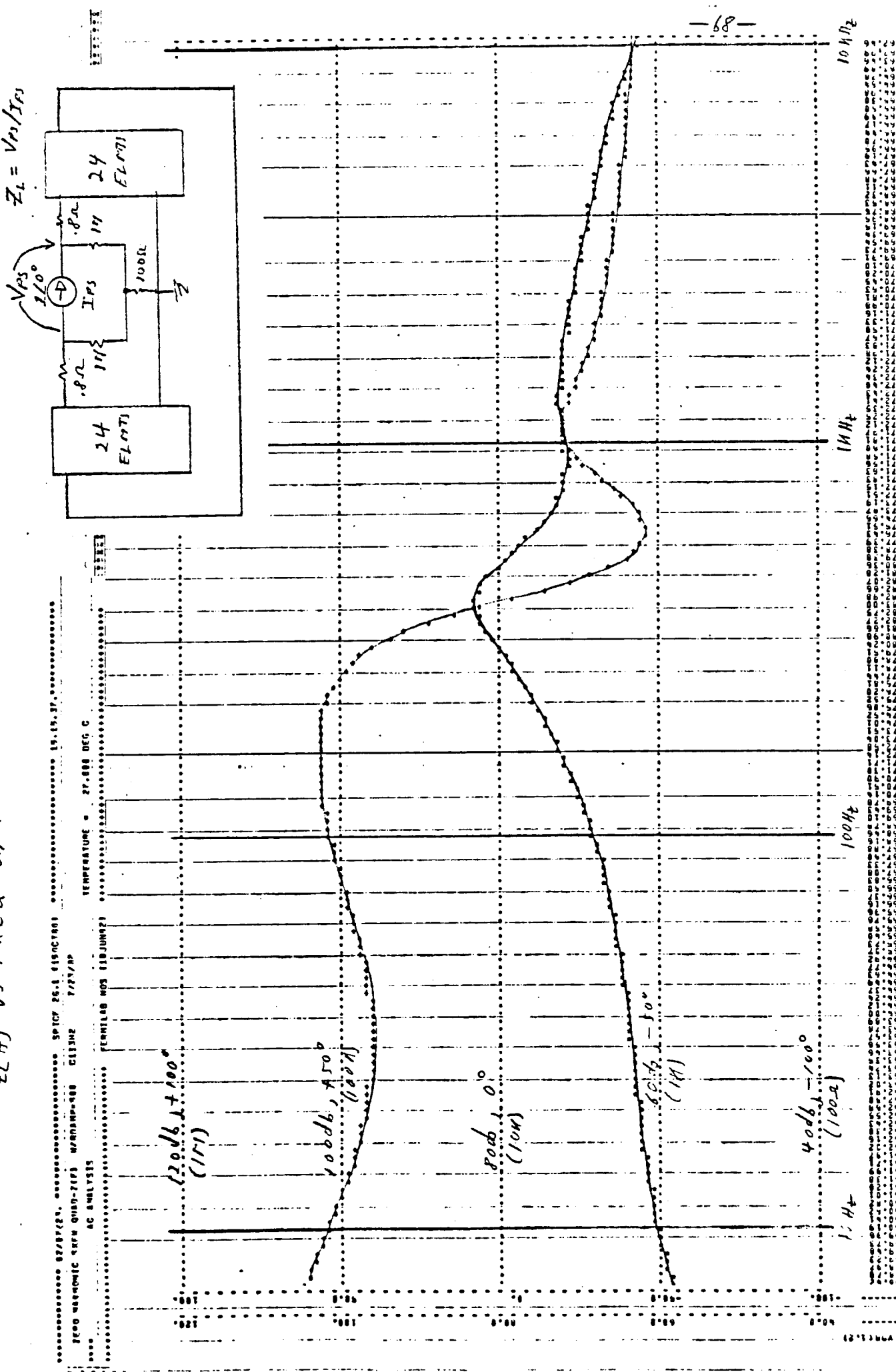




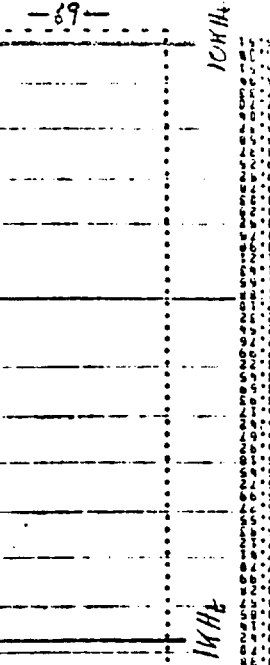
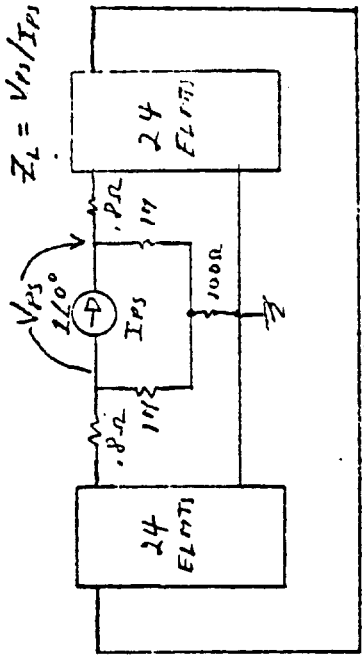
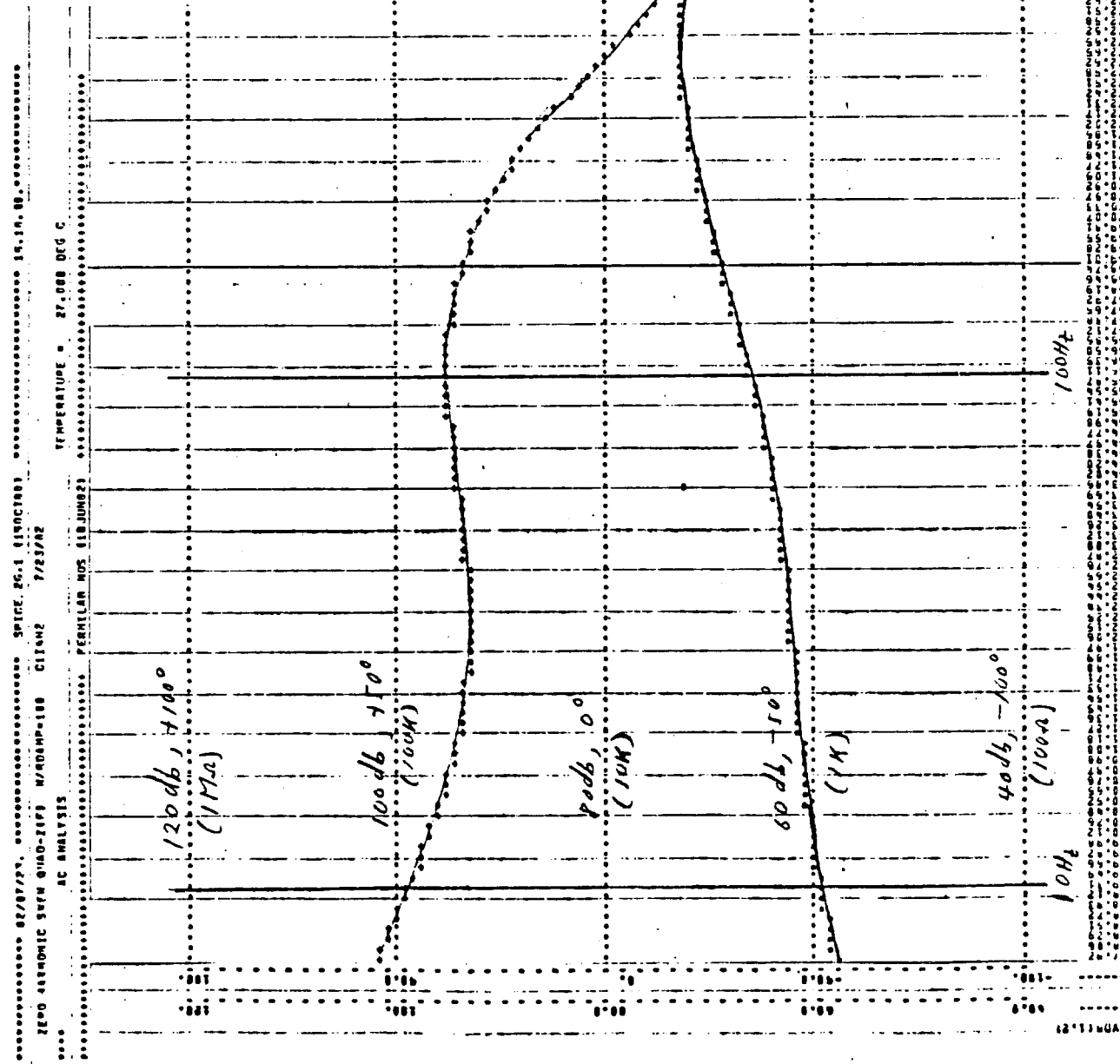
ZERO HARMONIC SWING QUAD
Z_L(Hz) VS FREQUENCY & W/ROAMP = 1A



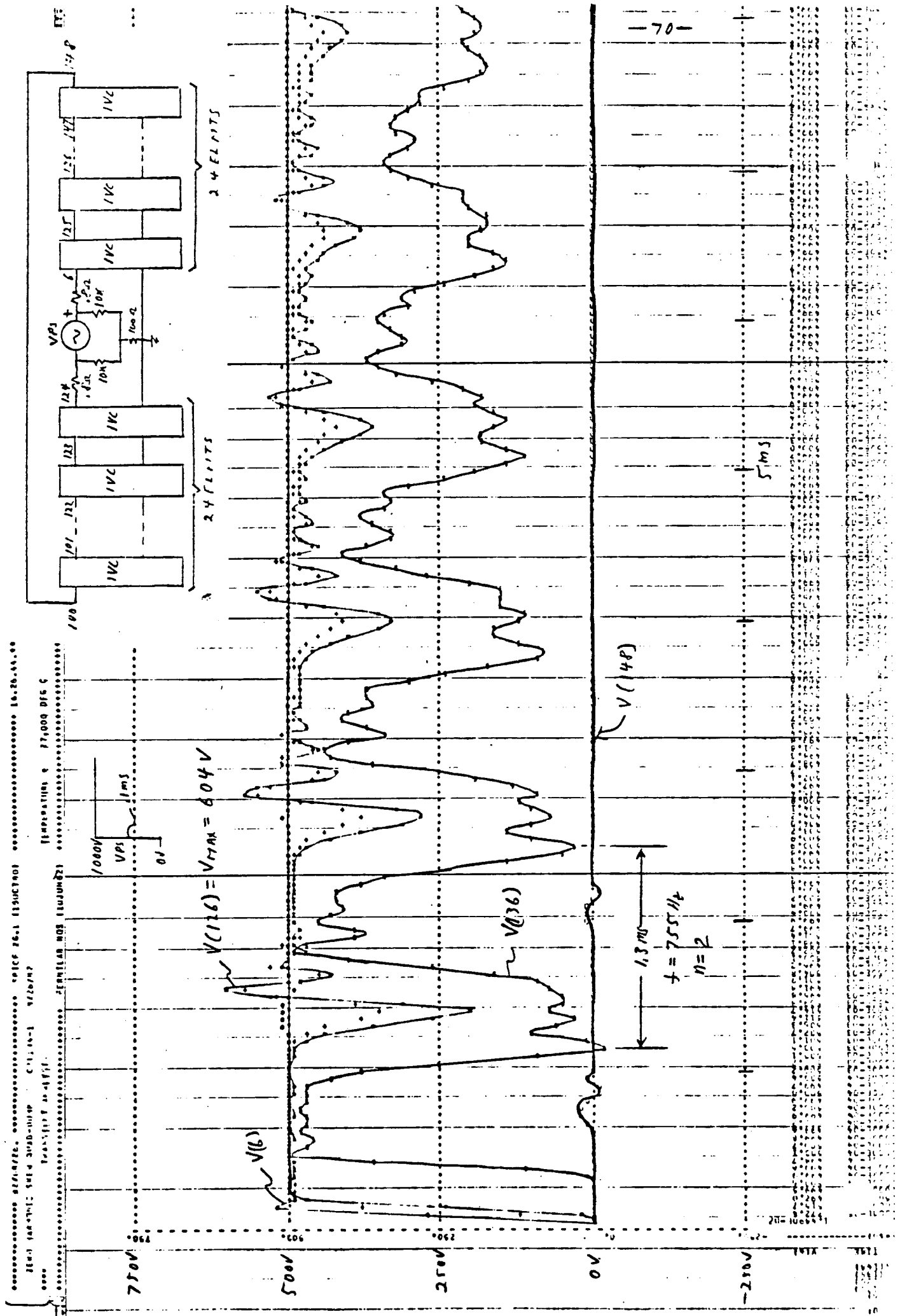
ZERO HARMONIC SWING QUAD
 Z_L vs FREQUENCY $\omega = 500 \text{ rad/sec}$



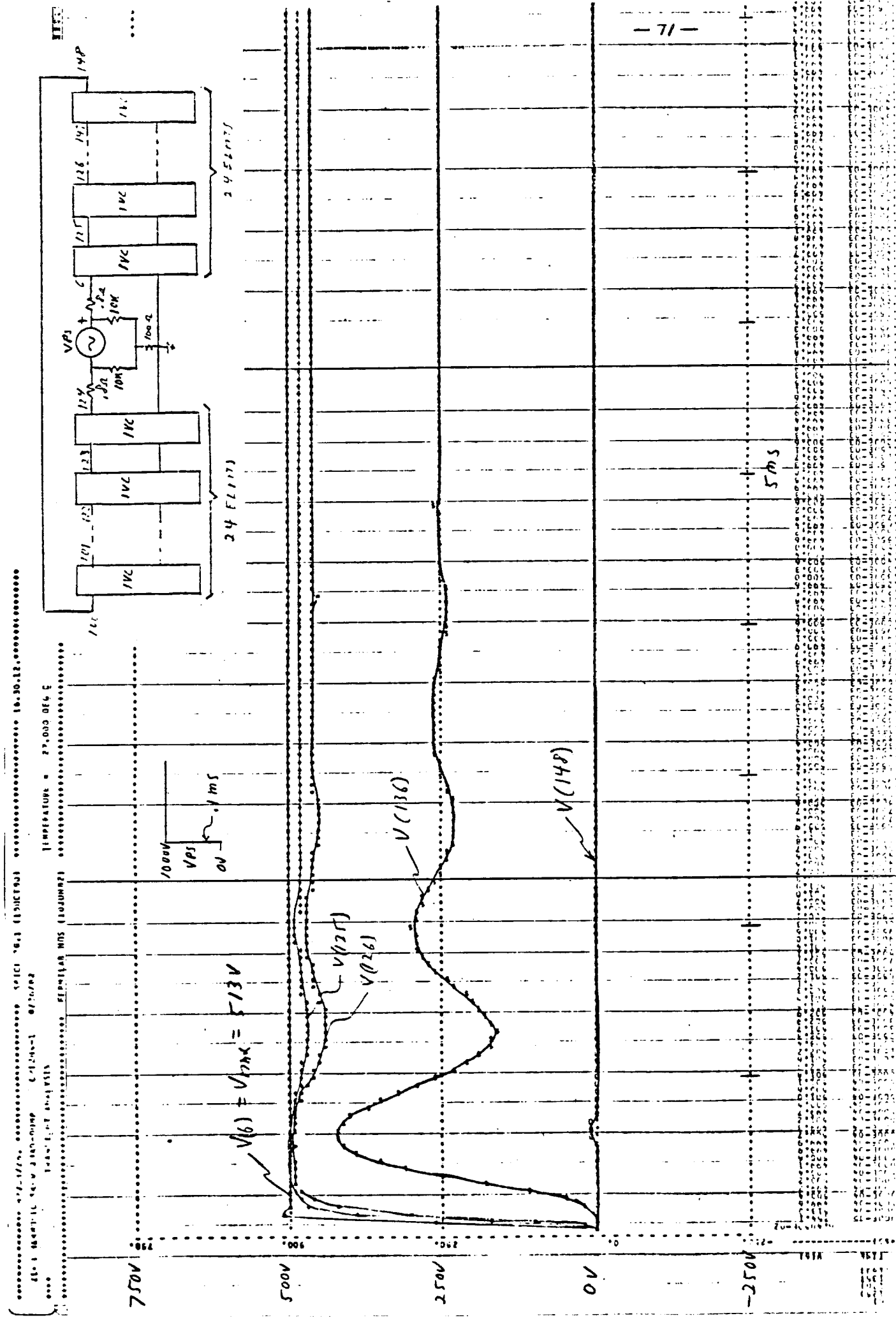
ZERO HARMONIC STHW & WAO
Z_{L(f)} VS FREQ. w/ ROAMP = 1000



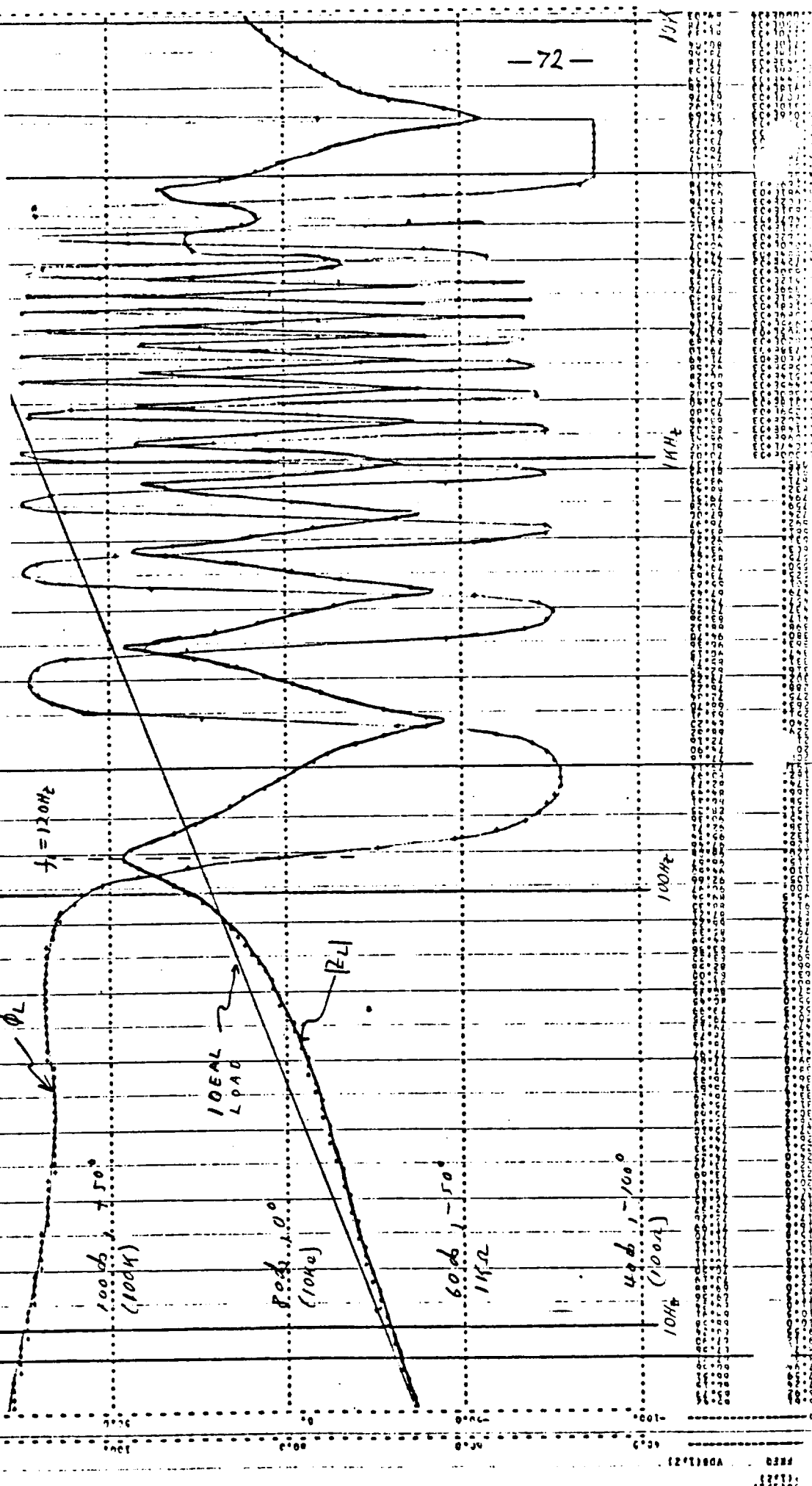
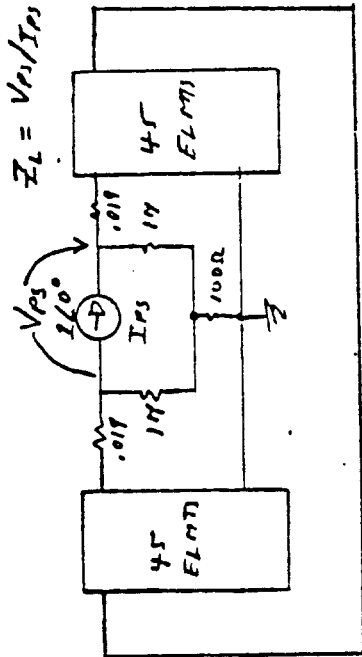
ZERO HARMONIC SHOTWAVE QUAD: DUMP w/RDAMP = OPEN



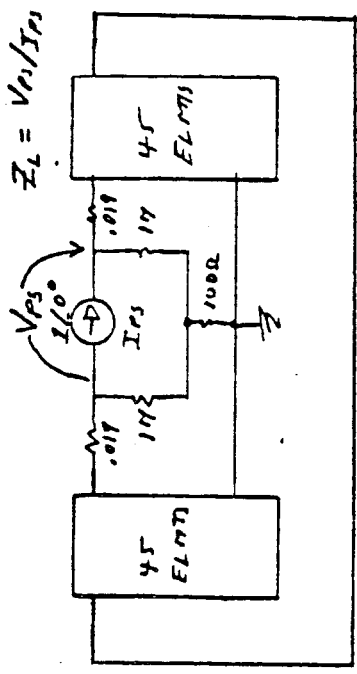
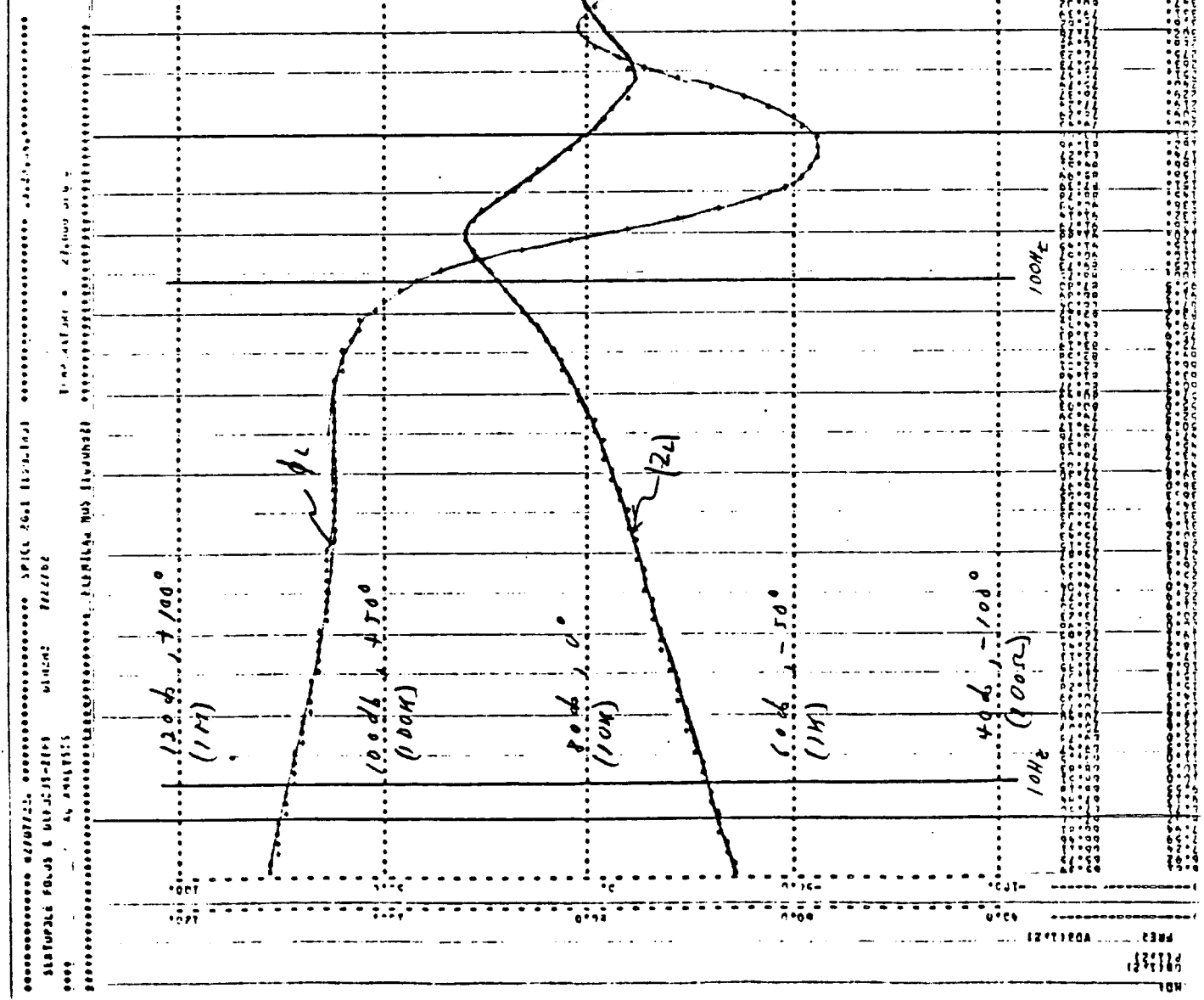
ZERO HARMONIC SKew QGAD: DUNE w/ R0 AND = 14



SEXTUPOLE - Z_L VS FREQ w/ NOAMP = OPEN



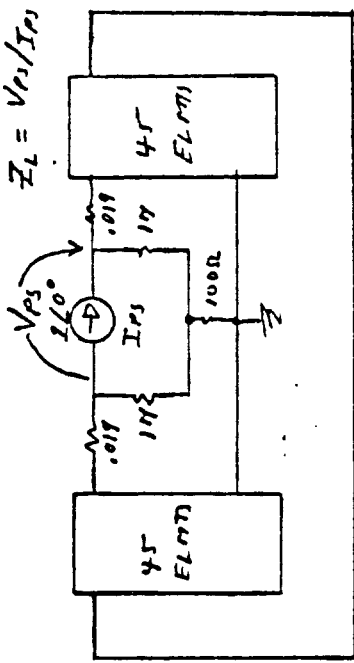
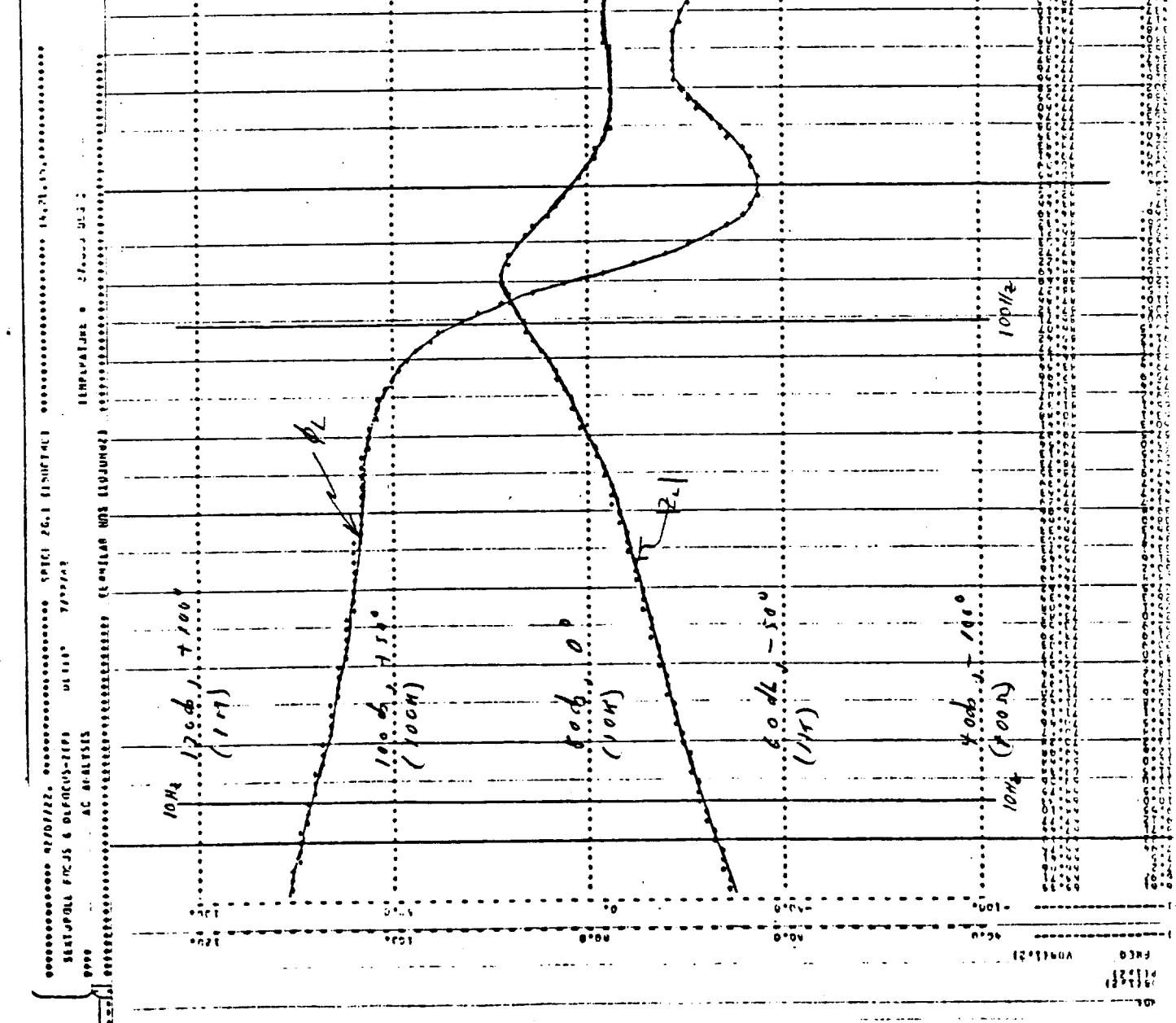
SEXTAPOLE - Z_L



- 73 -

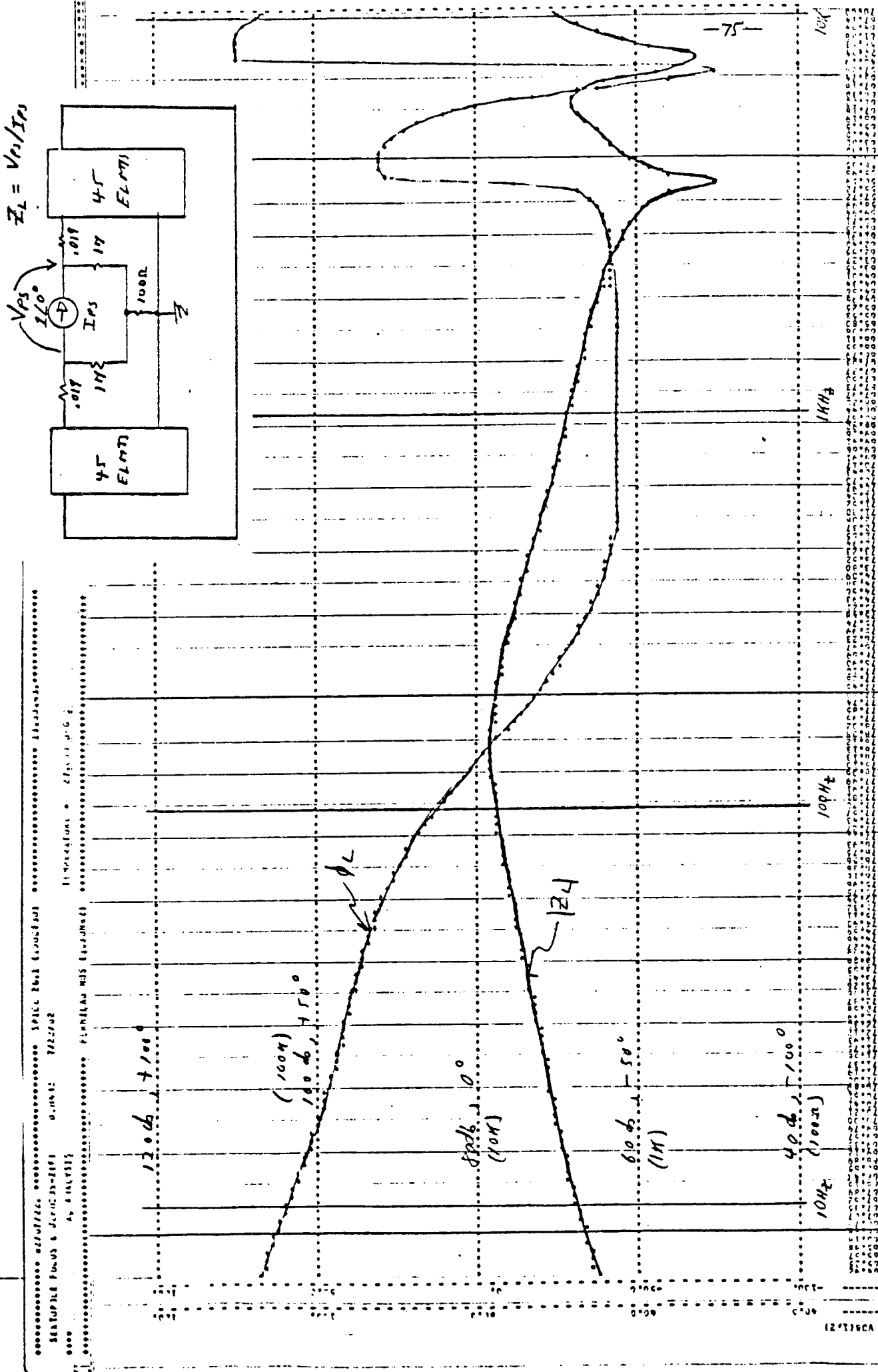
104

SEXTUPOLIE Z_L VS FREQ w/ RAMP = 500Ω



-74-

SEXTUPOLE - Z_L V. FREQ w/RAMP = 100Ω



SEXTAPOLE AT FOCUSING AND DEFOCUSING LOCATIONS WITH RAMP = OPEN

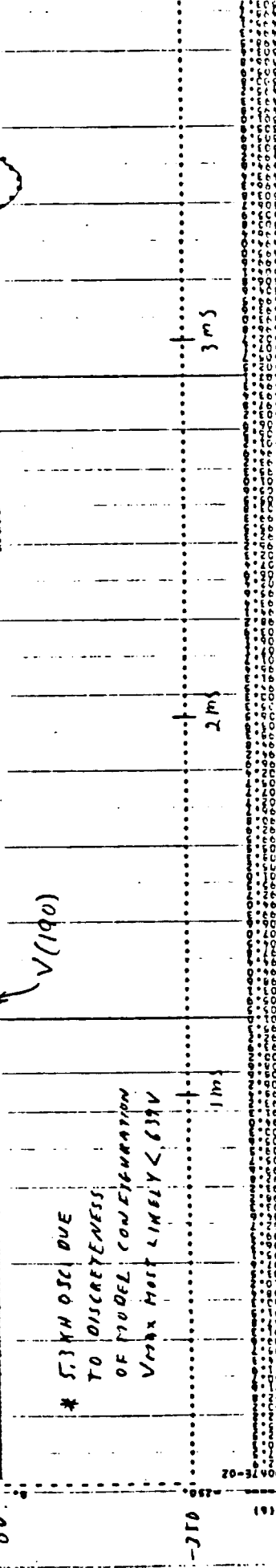
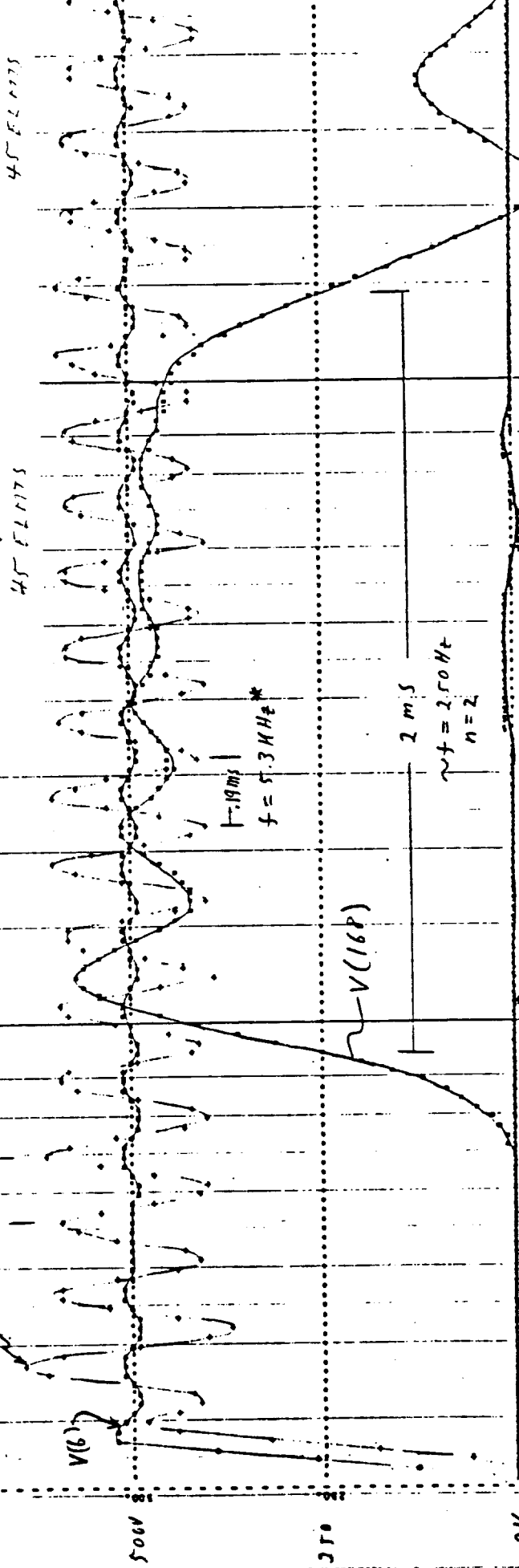
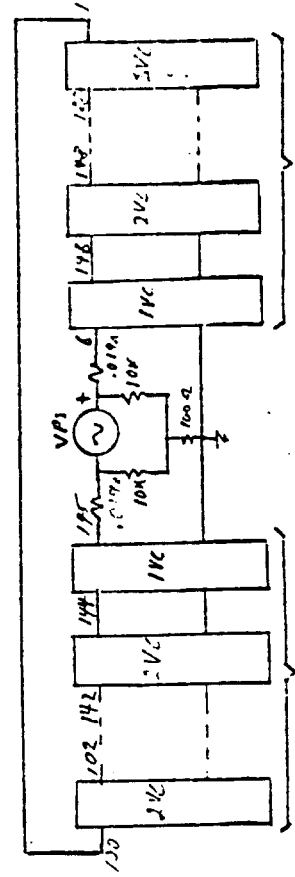
STARTUP STATUS & OPERATING SPICE 201 (150740)

TRANSIENT ANALYSIS

DISCRETE GROUP

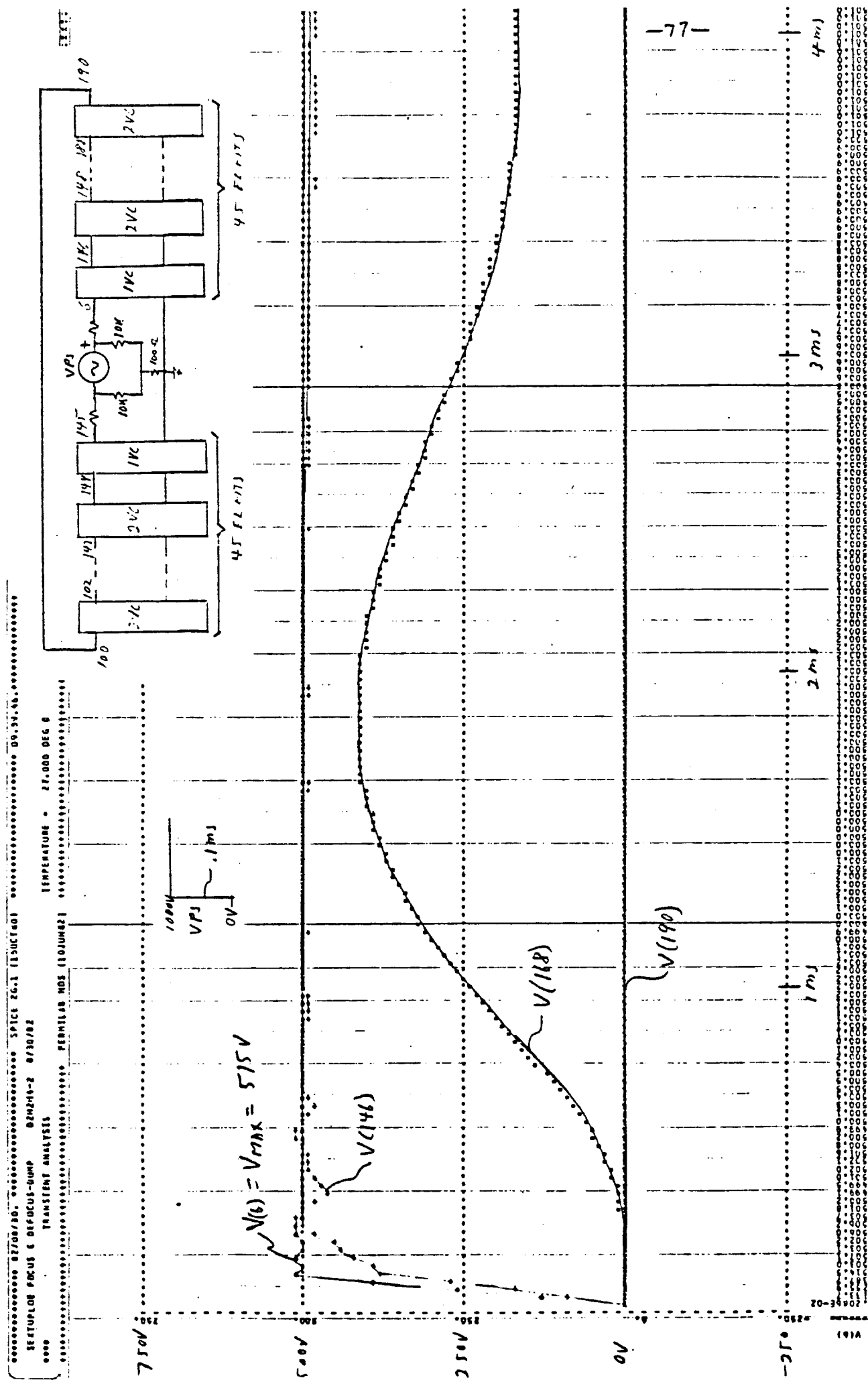
INITIAL CONDITIONS

OPERATING MODE



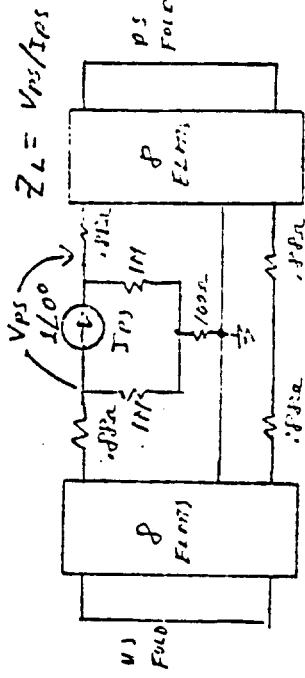
* SMOOTH DUE
TO DISCRETENESS
OF MODEL CONSTRUCTION
WITH LINEAR < 639V

SETUPOLE AT FOCUSING AND DEFOCUSING LOC.: D=1000 m/ ROD=14



39 TH HARMONIC OCTOPOLE

$Z_L (H)$ VS FREQ w/ ROTATO = OPEN



$Z_L = V_{ps}/I_{ps}$

Spice Ver. 1.19.00
with analytic
models

1000

120 $d_1 + 100$
(1MHz)

100 $d_1 + 100$
(1MHz)

50 $d_1 + 100$
(1MHz)

60 $d_1 - 50$
(1MHz)

40 $d_1 - 100$
(100Hz)
10Hz

-78-

10K

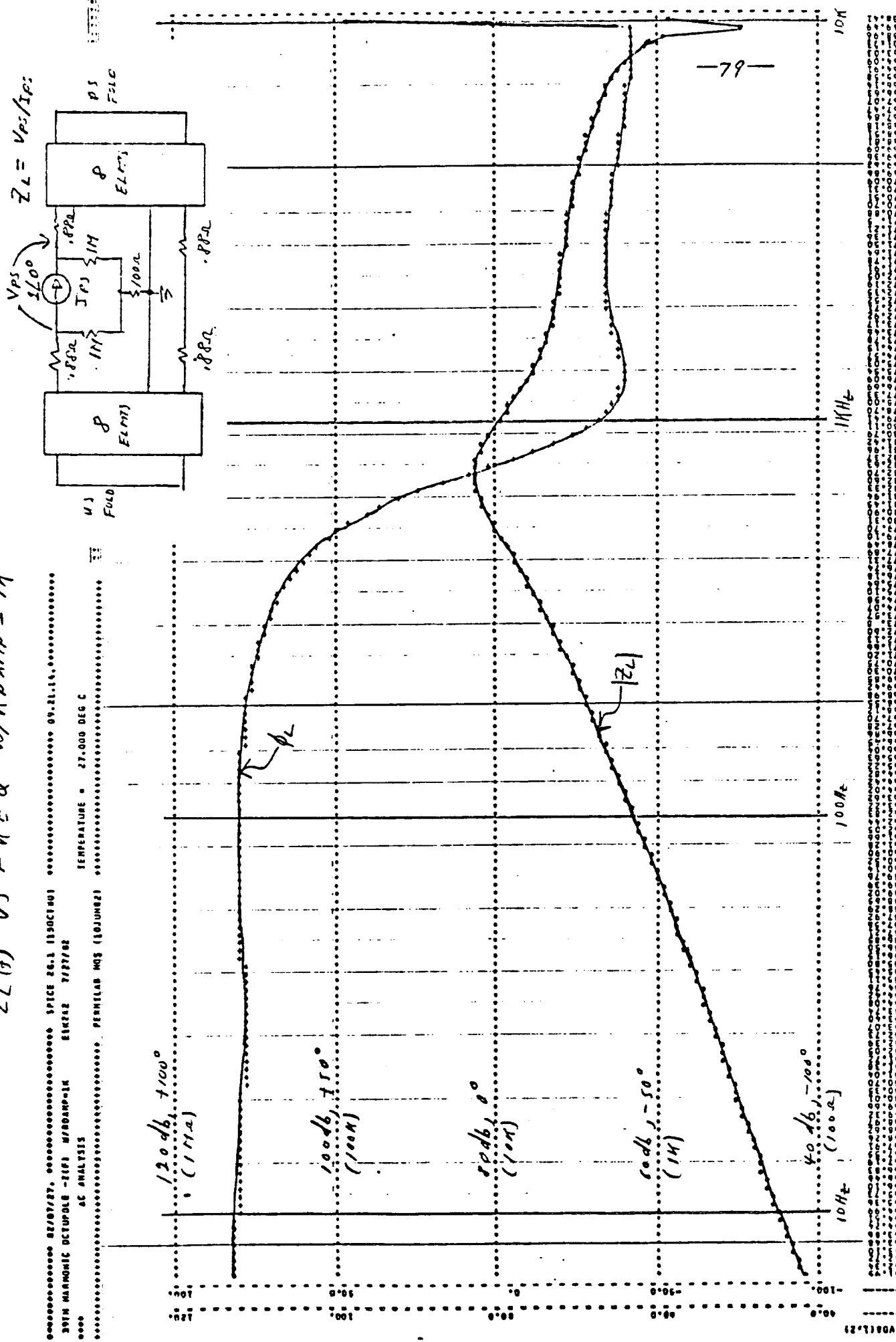
100Hz

10Hz

REB

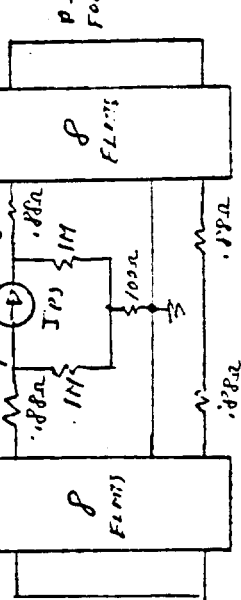
10

39 TH HARMONIC OC. POLE
 $Z_L(t)$ VS θ FREQ w/π RATIO = 14



39 TH HARMONIC OCTA POLE

$$Z_L = V_{PS}/I_{PS}$$



$$Z_L(f) \text{ VS FREQ w/ } R_{DS} \text{ no } = 500 \Omega$$

SPICE 2001 DIRECT
TICKS 1024000
INTERVAL ? 27.000 USEC
FLATLINE NO FLATLINE

Both magnetic shunt -1dB points at 117.4 Hz

All resistors

$$120 \text{ dB, } +100^\circ
(117.4)$$

$$100 \text{ dB, } +50^\circ
(100K)$$

$$60 \text{ dB, } 0^\circ
(1K)$$

$$60 \text{ dB, } -50^\circ
(1K)$$

$$40 \text{ dB, } -100^\circ
(100\Omega)$$

10 Hz

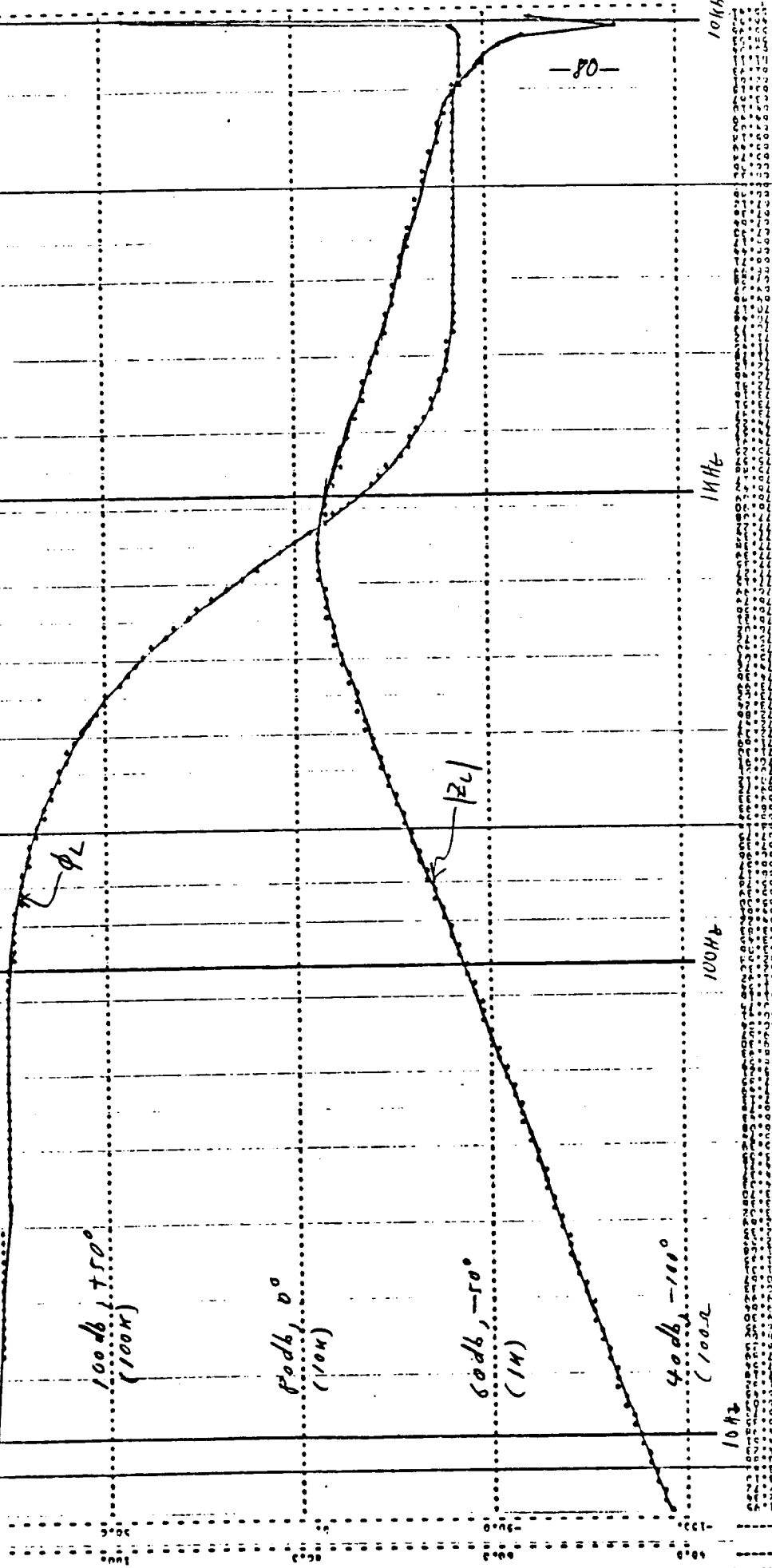
10

100 Hz

1 kHz

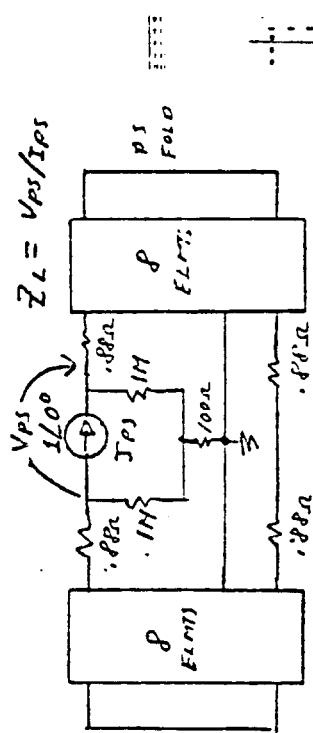
10 kHz

-80-



39TH HARMONIC OCTAVE E

$Z_L(f) \text{ vs } FREQ \text{ w/ } R_{Amp} = 100\Omega$



SPICE 2.0.1 DIRECTED
DATE 8/27/87, 09:00
TIME 12:27:02
TEMPERATURE 27.000 DEG C
AC ANALYSIS
PEMILAB MOS (194002)

120 db, +100°
(100Hz)

100 db, +10°
(100Hz)

80 db, 0°
(100Hz)

60 db, -50°
(100Hz)

40 db, -100°
(100Hz)

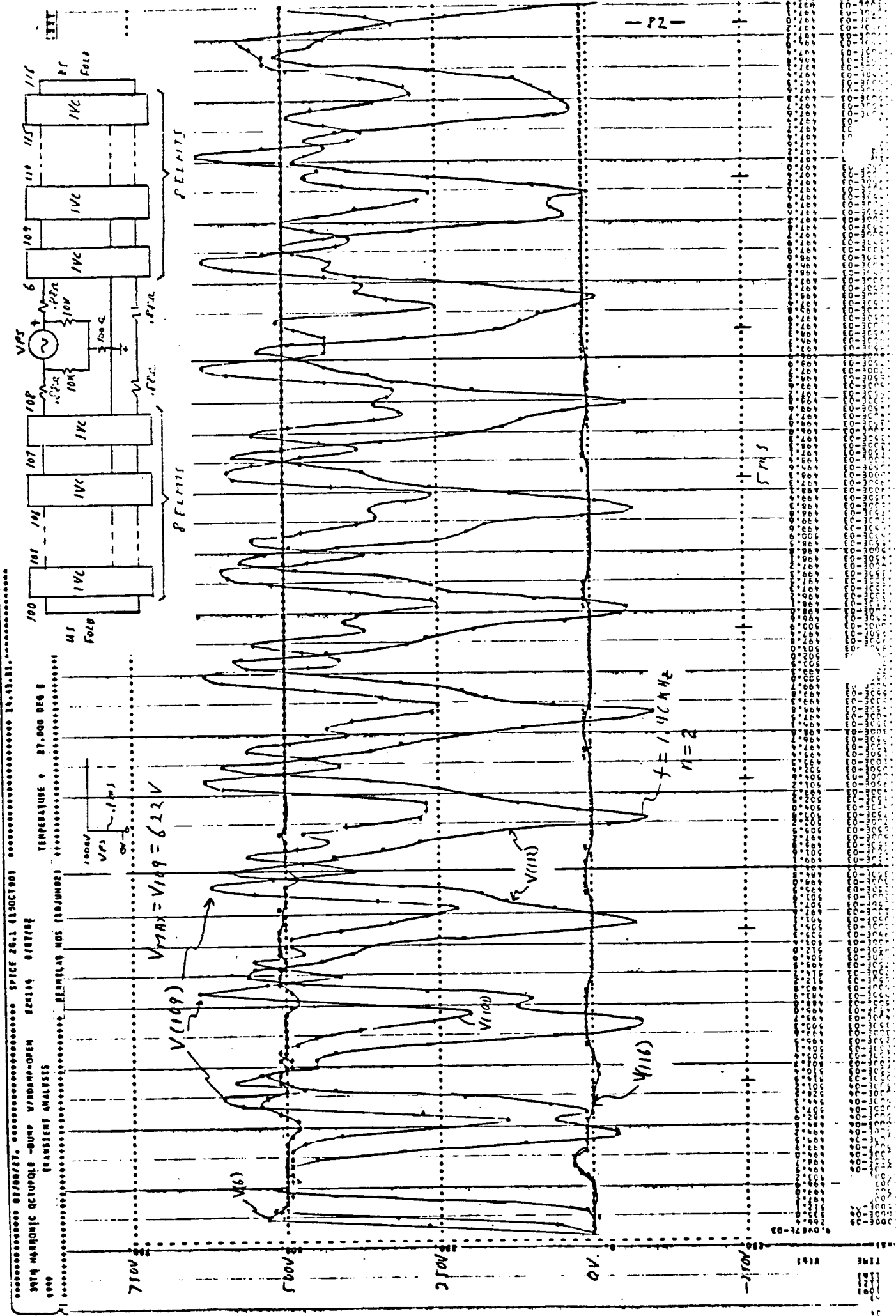
10Hz

1KHz

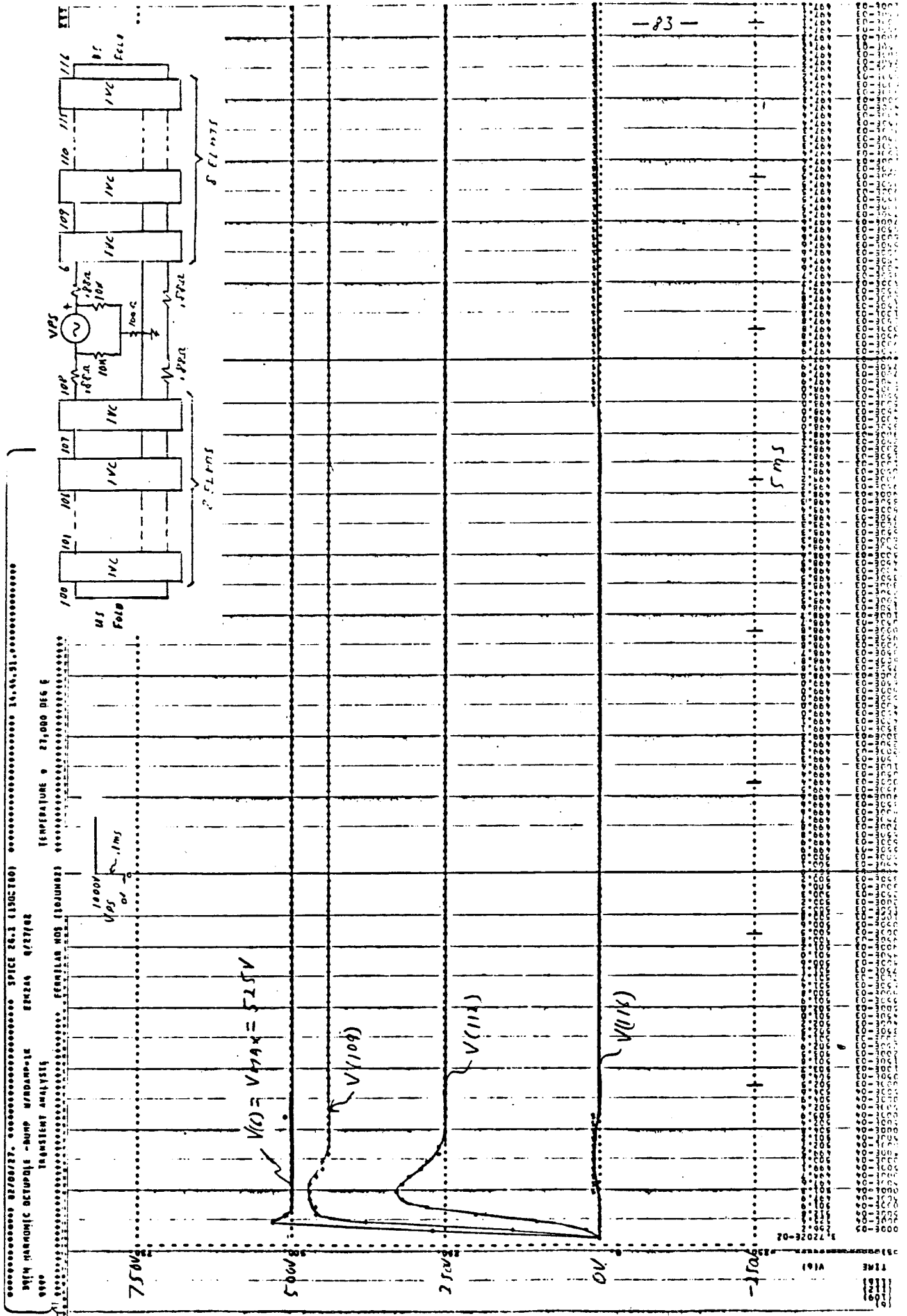
10KHz

-81-

39 TH HARMONIC OCTUPOLE: OUTPUT w/ RAM = OPEN



39 TH HARMONIC OCTOPOLE: DUE TO WIRING = 1/4



ZERO HARMONIC OCTOPOLE AT FOCUSING LOC.

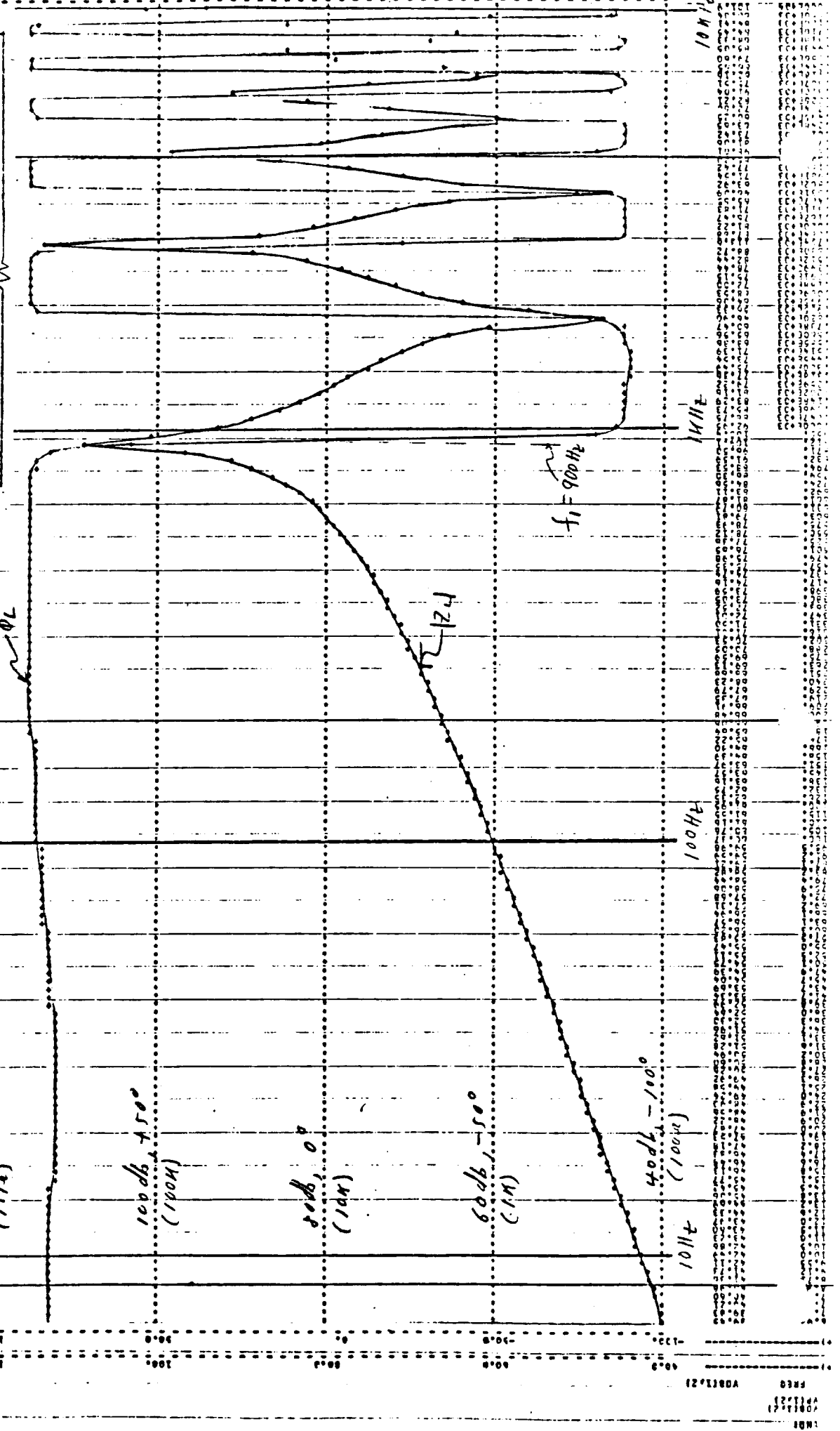
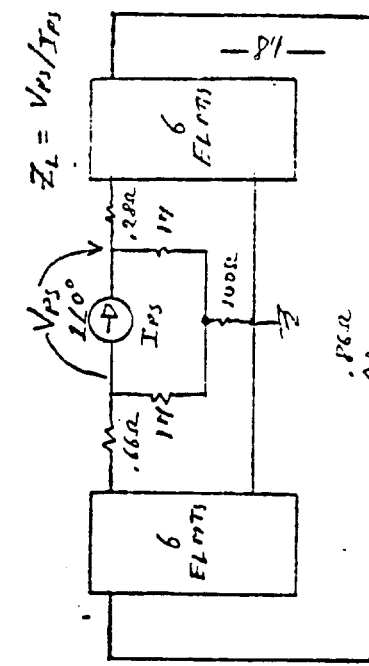
$Z_L(t) \text{ VS FREQ w/ RDA np = 0 OPEN}$

Zero harmonic octopole at focus 17.29.42.0001 Date 7/26/02

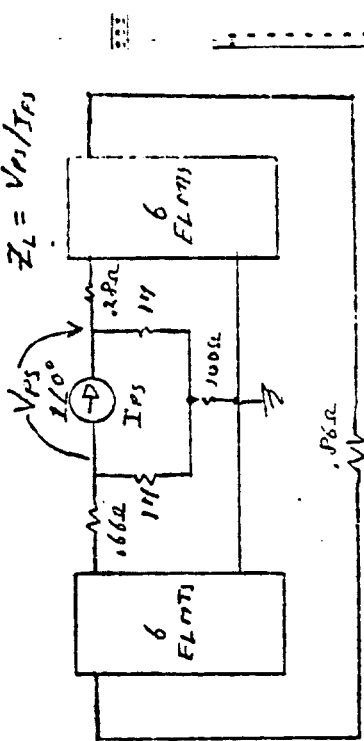
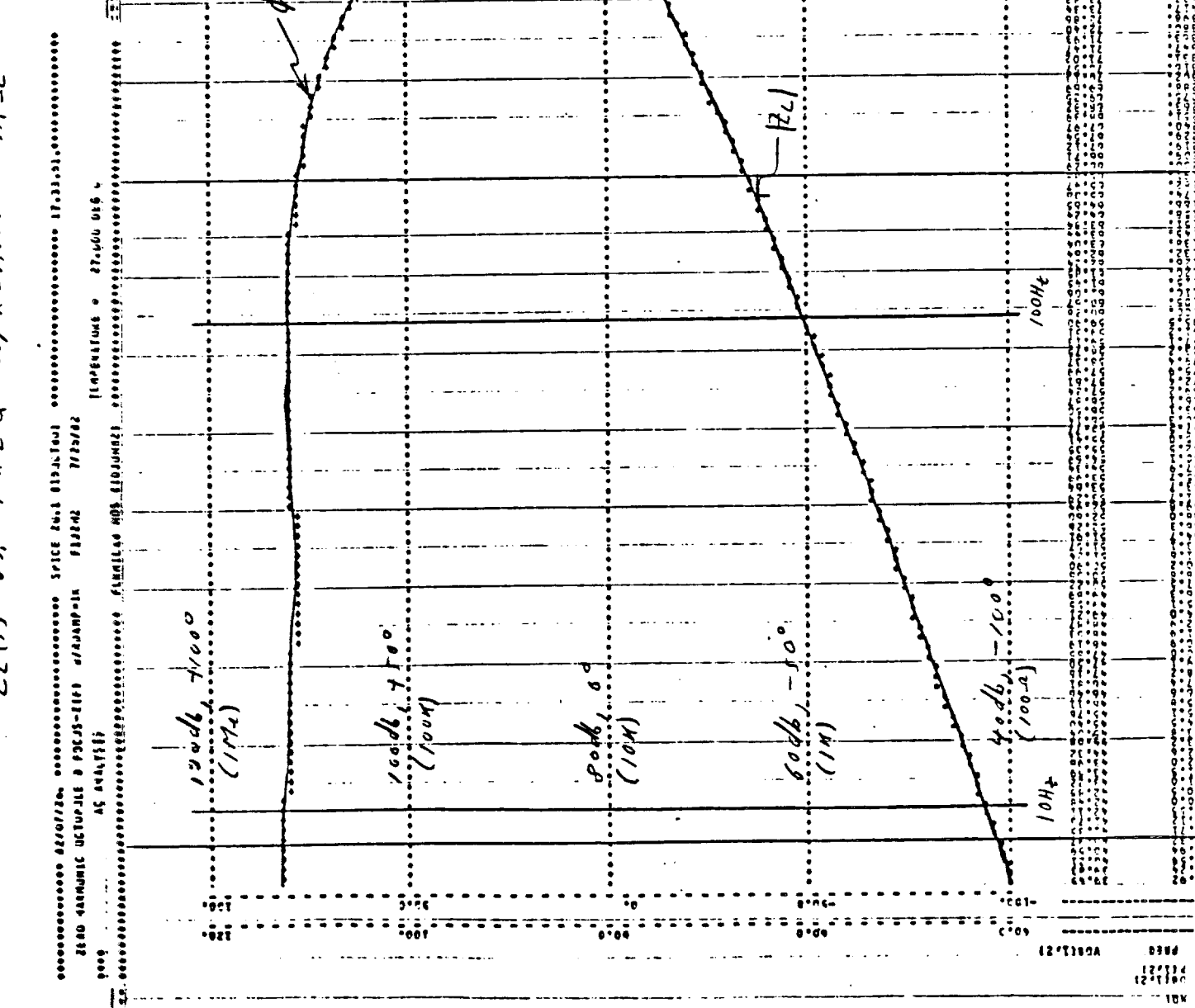
Zero harmonic octopole at focus 17.29.42.0001 Date 7/26/02

AC analysis

Harmonic MOS simulation

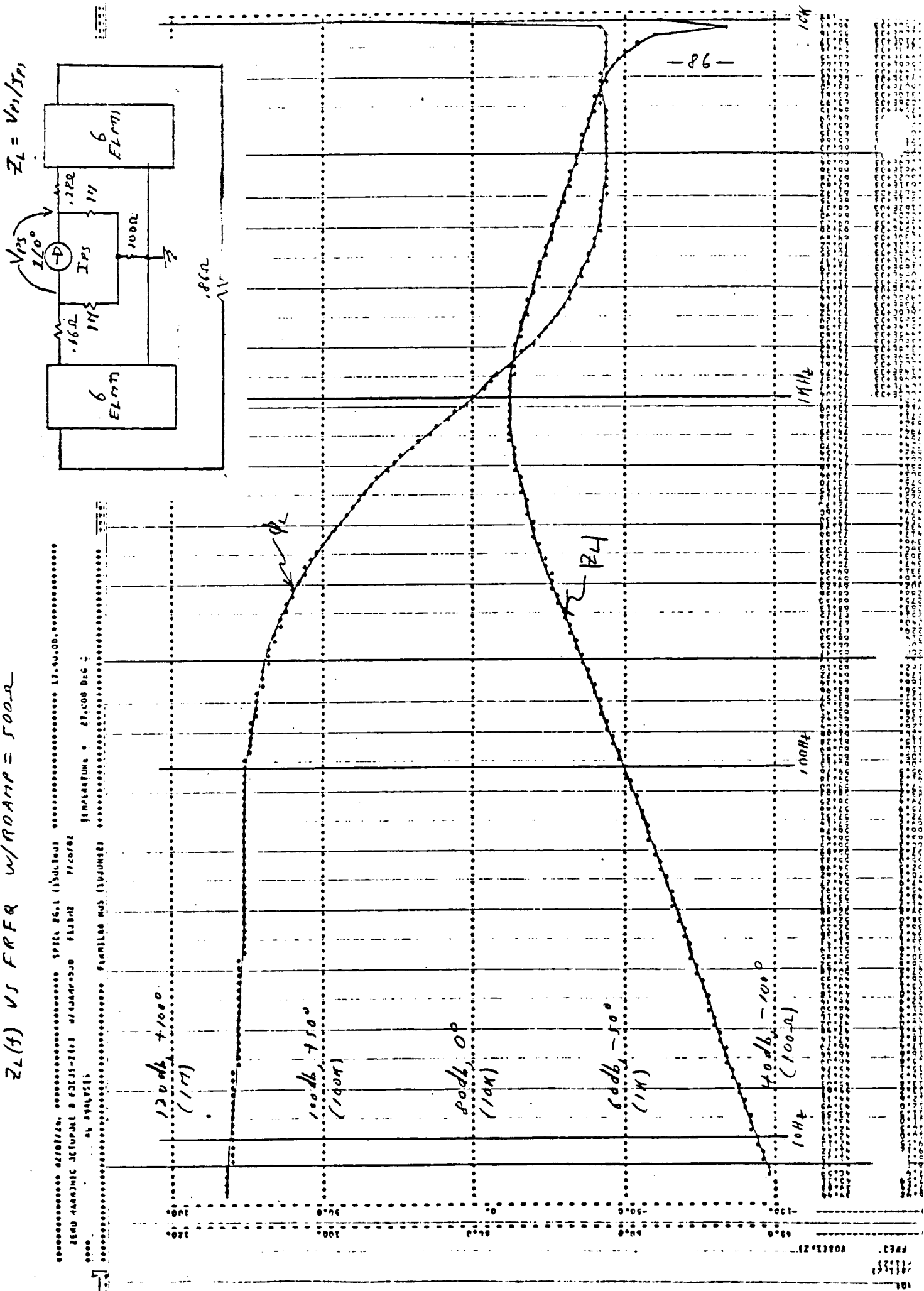


ZERO HARMONIC OCTOPOLE - FOCUSING LOC.
 $Z_L = V_{P1}/I_{R1}$



- 85 -

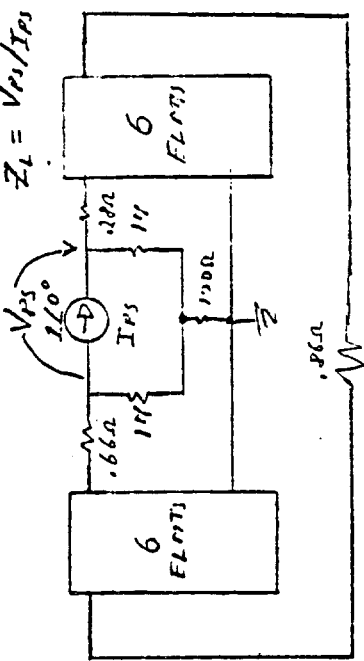
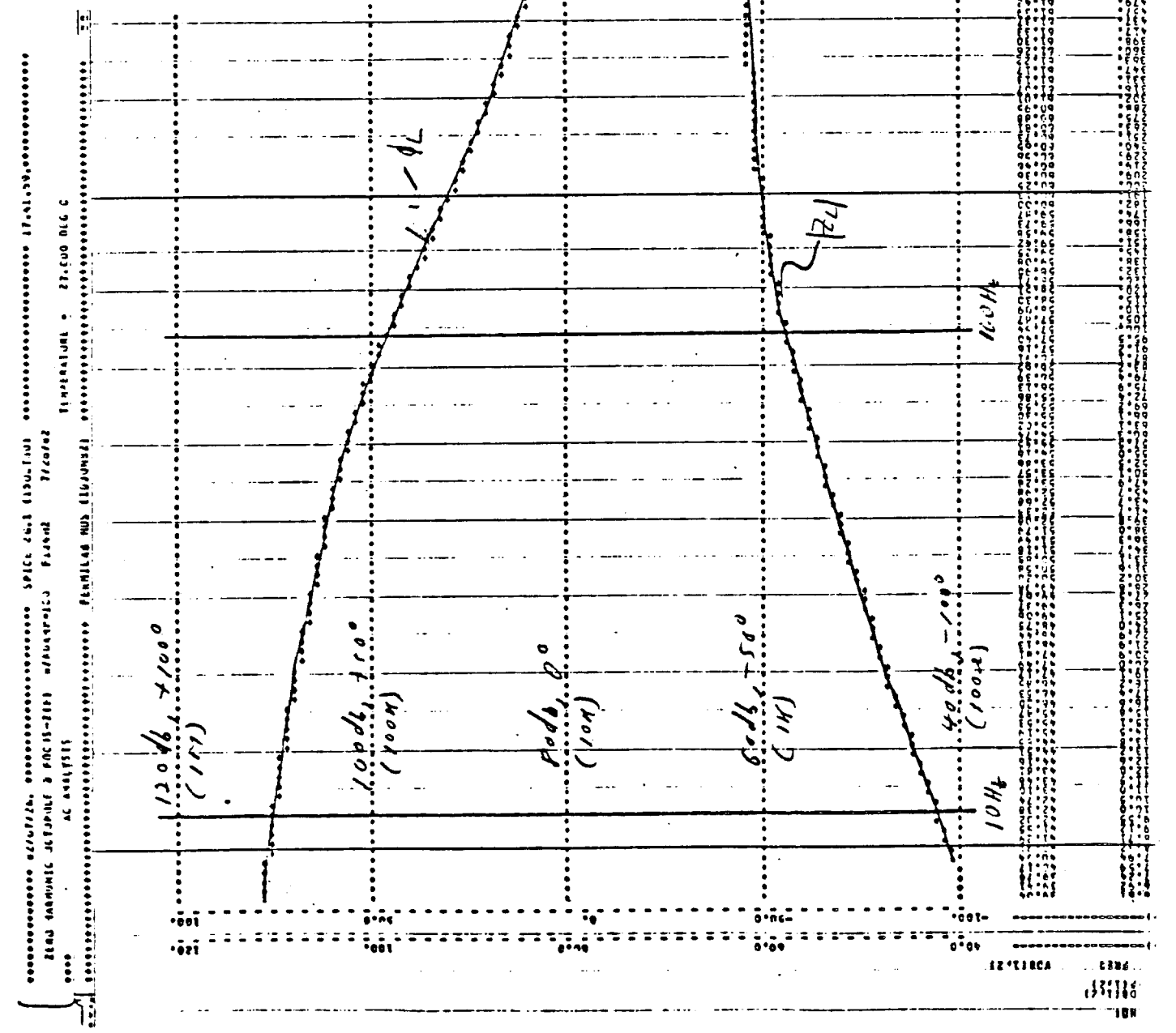
$Z_{L(t)}$ VS FREQ w/ R0 A.M.P = 500Ω



-86-

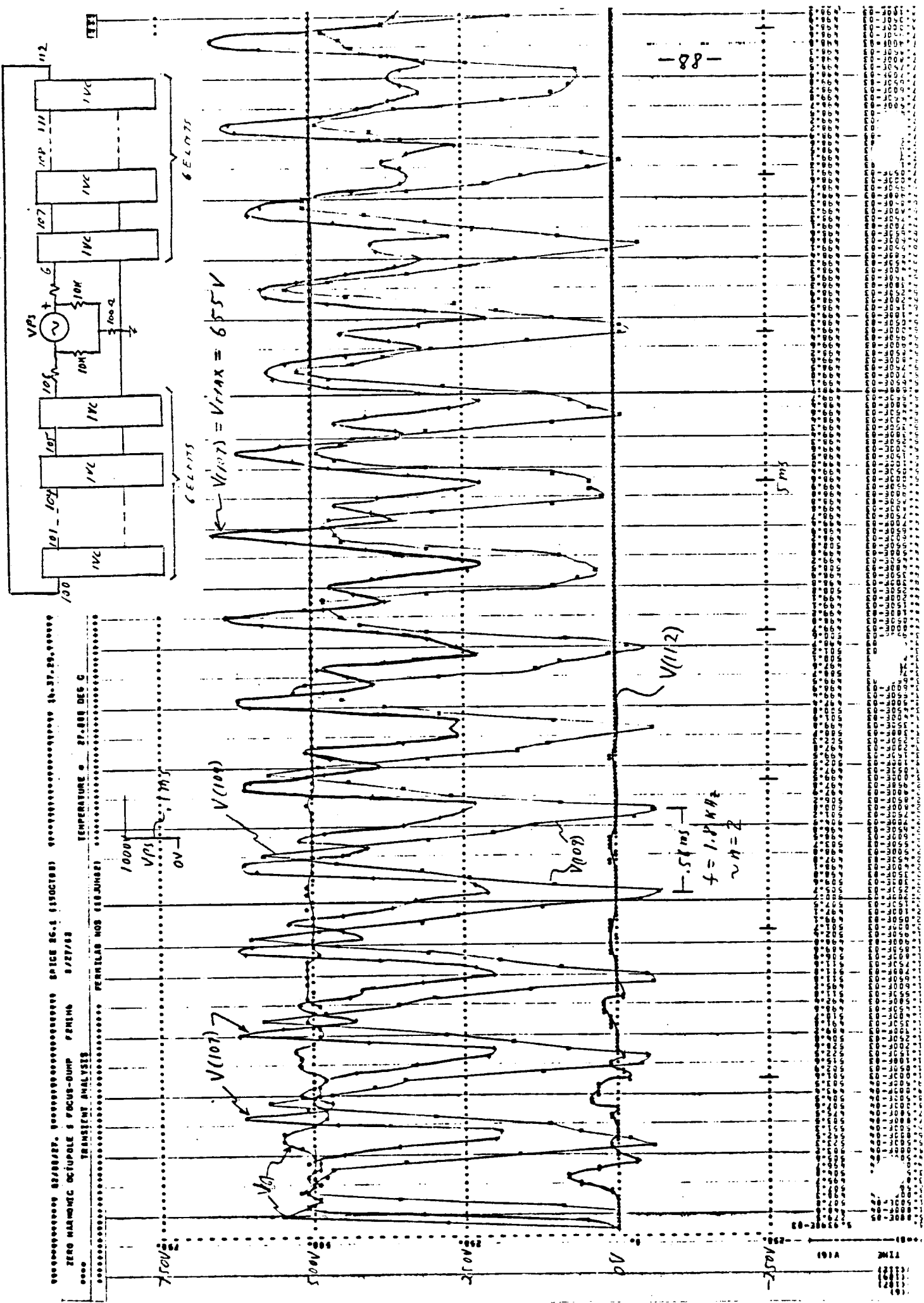
ZERO HARMONIC OCTOPOLE AT, USNT LOC,

$$Z_L(f) \text{ vs } FREQ \text{ w/ } R_{LOAD} = 100\Omega$$

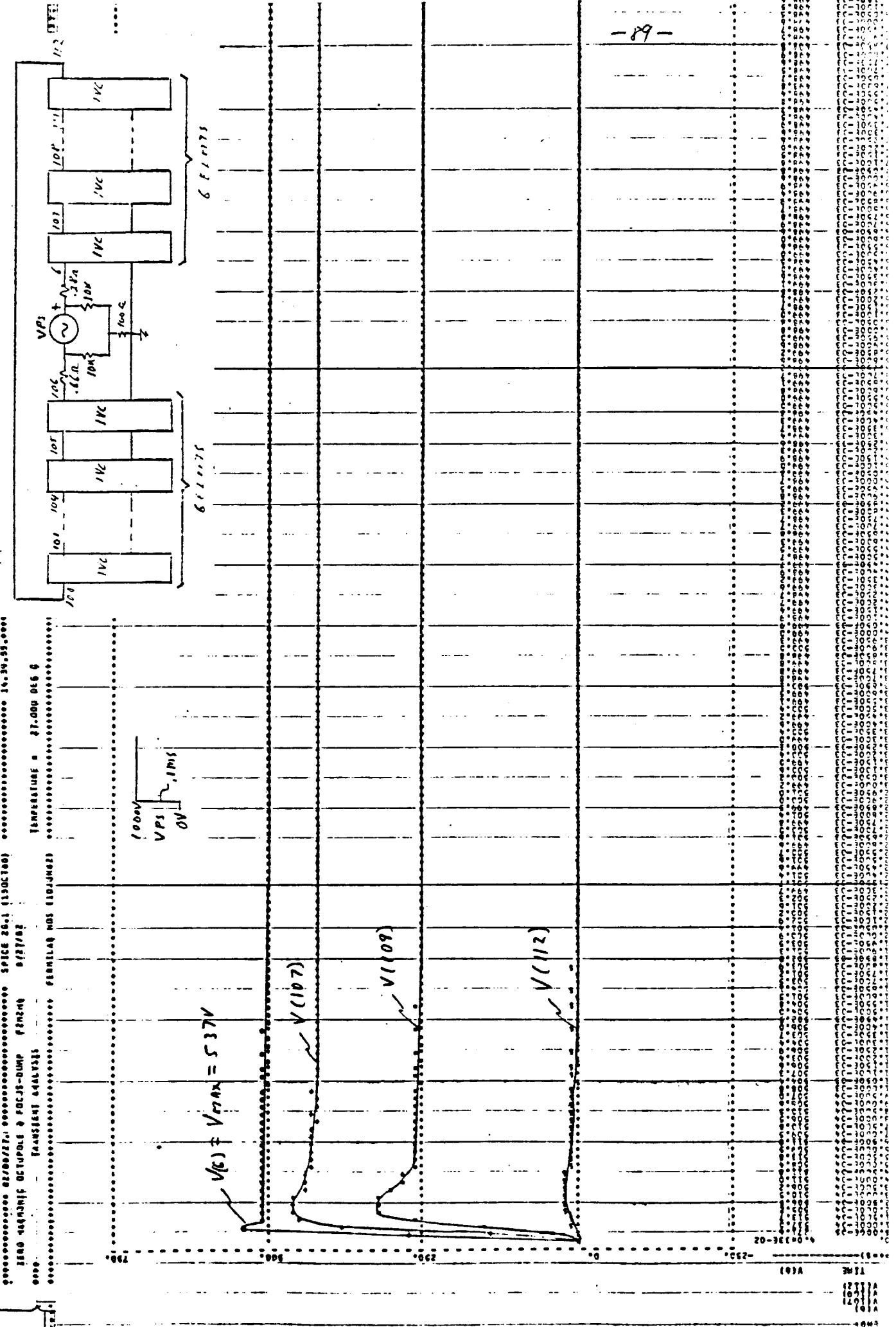


-PT-

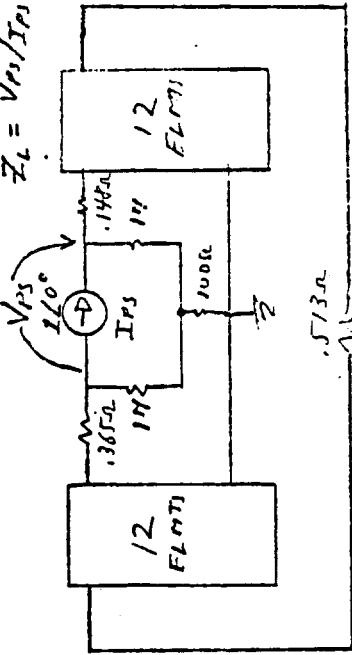
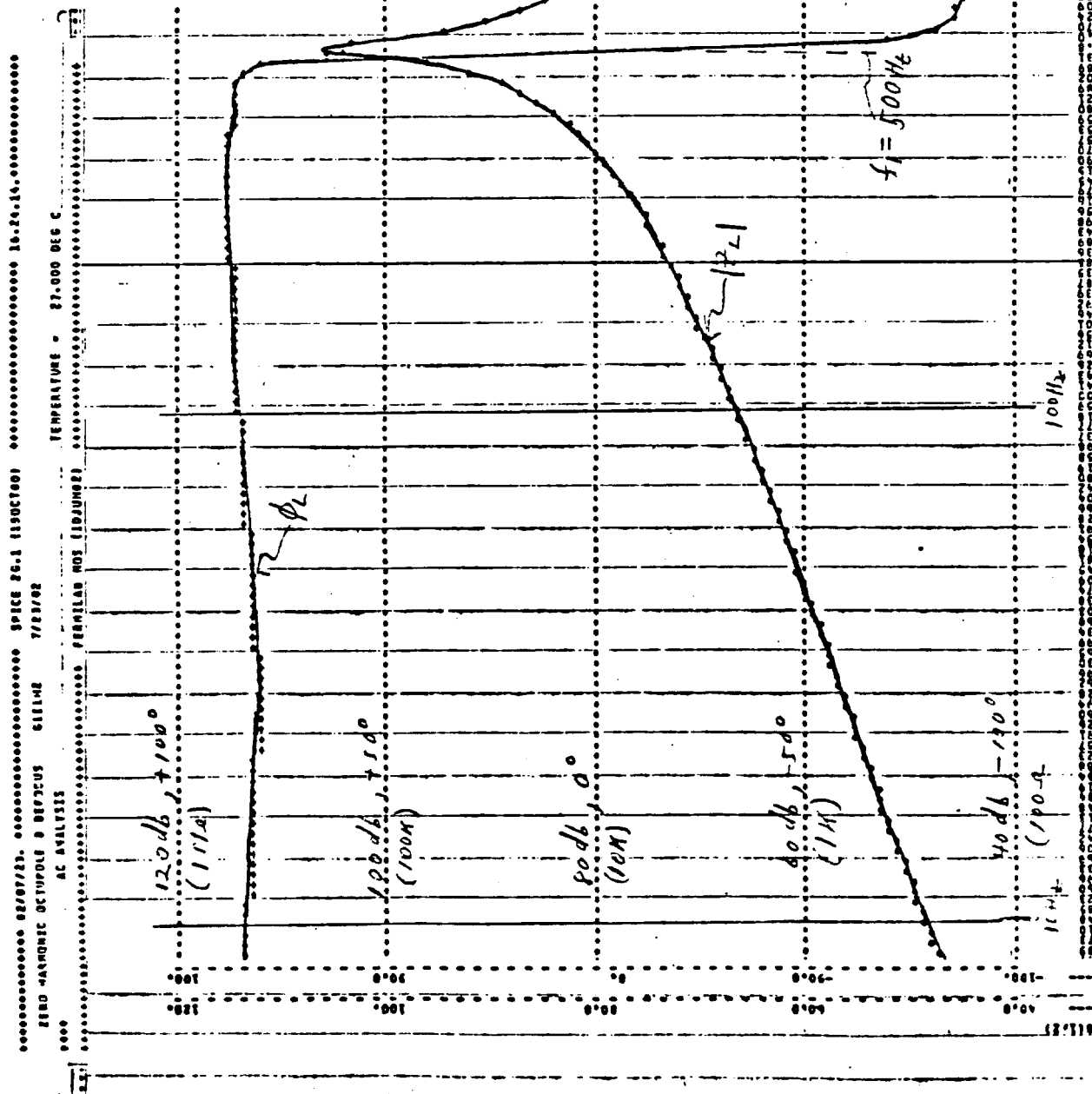
ZERO HARMONIC OCTUPOLE AT FOCUS INTE LOC: OUTP W/ RDA MP=OPEN



ZERO HARMONIC OCTUPOLLE AT FOCUSING LOC.: DUMP W/ R0 = 1.7 = 1/4



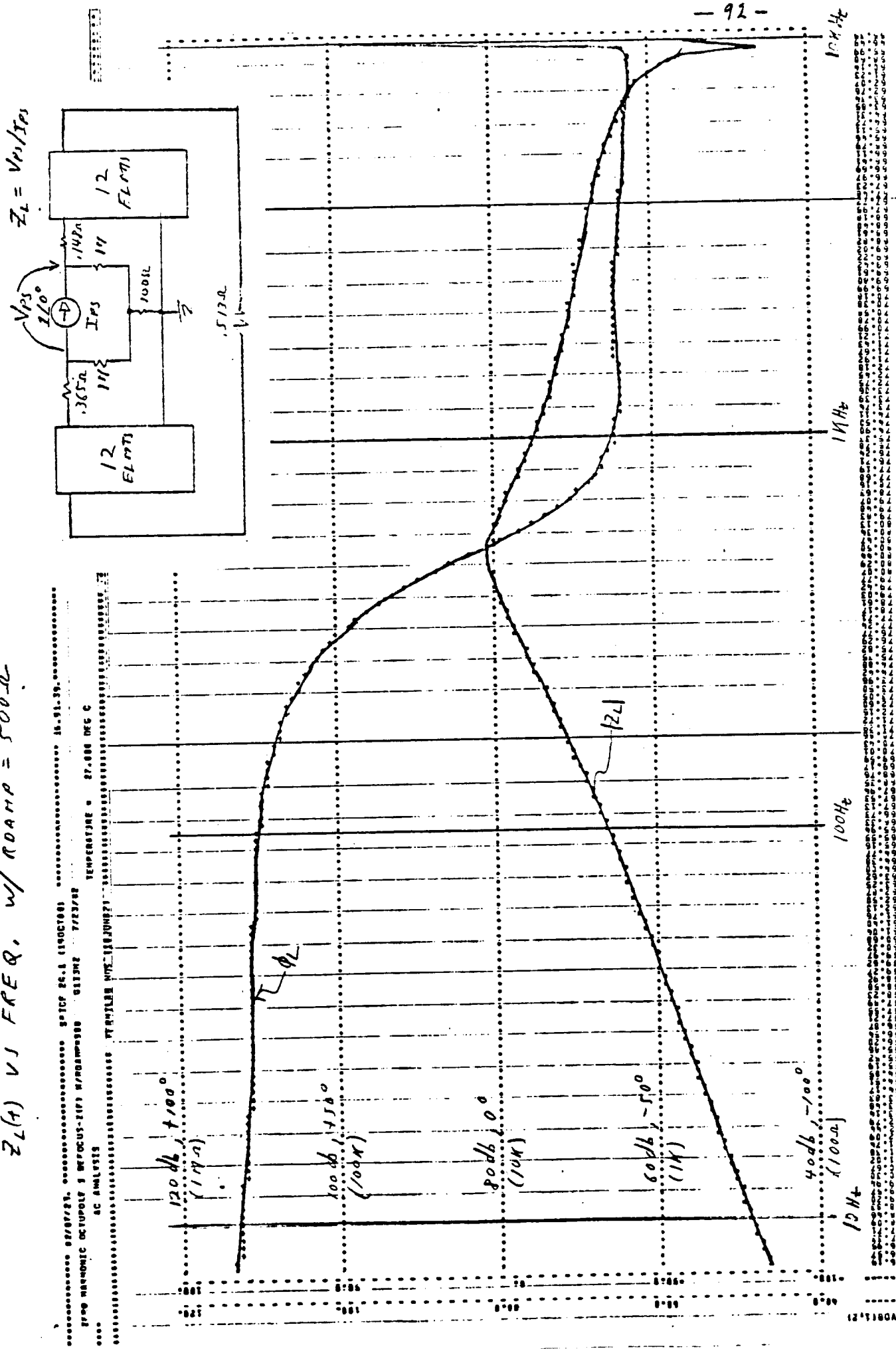
ZERO HARMONIC OCTUPOLE AT DEFOCUSING LOC.
 $Z_L(f)$ VS FREE A, w/ RAMP = OPEN



- 90 -

ZERO HARMONIC OCTUPOLE AT OFFFOCUSING LOC.

$Z_L(t)$ VS FREQ. w/ RDAHA = 500.0



12/18/80A
0362
12/18/80A
0362

ZERO HARMONIC OCTUPOLE AT DEFOCO 16 LOC.

$Z_L(t) \propto V_{FEQ}, \text{ w/ } R_{DAIR} = 100\Omega$

07/07/2000, SPICE 20.0, AC ANALYSIS, SPICE Ver.1 (1996)

PRO HARMONIC OCTUPOLE 1 DIPOLUS-1275 EQUATIONS, CIRCUIT 7723002

AC ANALYSIS

TEMPERATURE = 87.000 DEG C

TRANSISTORS STANAG 2

TRANSISTOR MOS STANAG 2

TRANSISTOR JFET STANAG 2

TRANSISTOR DIODE STANAG 2

TRANSISTOR ZENER STANAG 2

TRANSISTOR BJT STANAG 2

TRANSISTOR FET STANAG 2

TRANSISTOR IGBT STANAG 2

TRANSISTOR MOSFET STANAG 2

TRANSISTOR JFET STANAG 2

TRANSISTOR ZENER STANAG 2

TRANSISTOR BJT STANAG 2

TRANSISTOR FET STANAG 2

TRANSISTOR IGBT STANAG 2

TRANSISTOR MOSFET STANAG 2

TRANSISTOR JFET STANAG 2

TRANSISTOR ZENER STANAG 2

TRANSISTOR BJT STANAG 2

TRANSISTOR FET STANAG 2

TRANSISTOR IGBT STANAG 2

TRANSISTOR MOSFET STANAG 2

TRANSISTOR JFET STANAG 2

TRANSISTOR ZENER STANAG 2

TRANSISTOR BJT STANAG 2

TRANSISTOR FET STANAG 2

TRANSISTOR IGBT STANAG 2

TRANSISTOR MOSFET STANAG 2

TRANSISTOR JFET STANAG 2

TRANSISTOR ZENER STANAG 2

TRANSISTOR BJT STANAG 2

TRANSISTOR FET STANAG 2

TRANSISTOR IGBT STANAG 2

TRANSISTOR MOSFET STANAG 2

TRANSISTOR JFET STANAG 2

TRANSISTOR ZENER STANAG 2

TRANSISTOR BJT STANAG 2

TRANSISTOR FET STANAG 2

TRANSISTOR IGBT STANAG 2

TRANSISTOR MOSFET STANAG 2

TRANSISTOR JFET STANAG 2

TRANSISTOR ZENER STANAG 2

TRANSISTOR BJT STANAG 2

TRANSISTOR FET STANAG 2

TRANSISTOR IGBT STANAG 2

TRANSISTOR MOSFET STANAG 2

TRANSISTOR JFET STANAG 2

TRANSISTOR ZENER STANAG 2

TRANSISTOR BJT STANAG 2

TRANSISTOR FET STANAG 2

TRANSISTOR IGBT STANAG 2

TRANSISTOR MOSFET STANAG 2

TRANSISTOR JFET STANAG 2

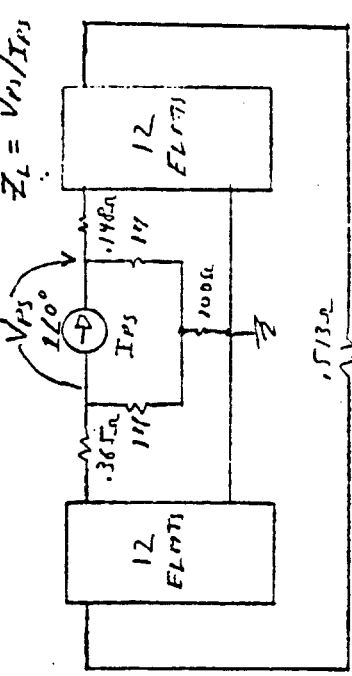
TRANSISTOR ZENER STANAG 2

TRANSISTOR BJT STANAG 2

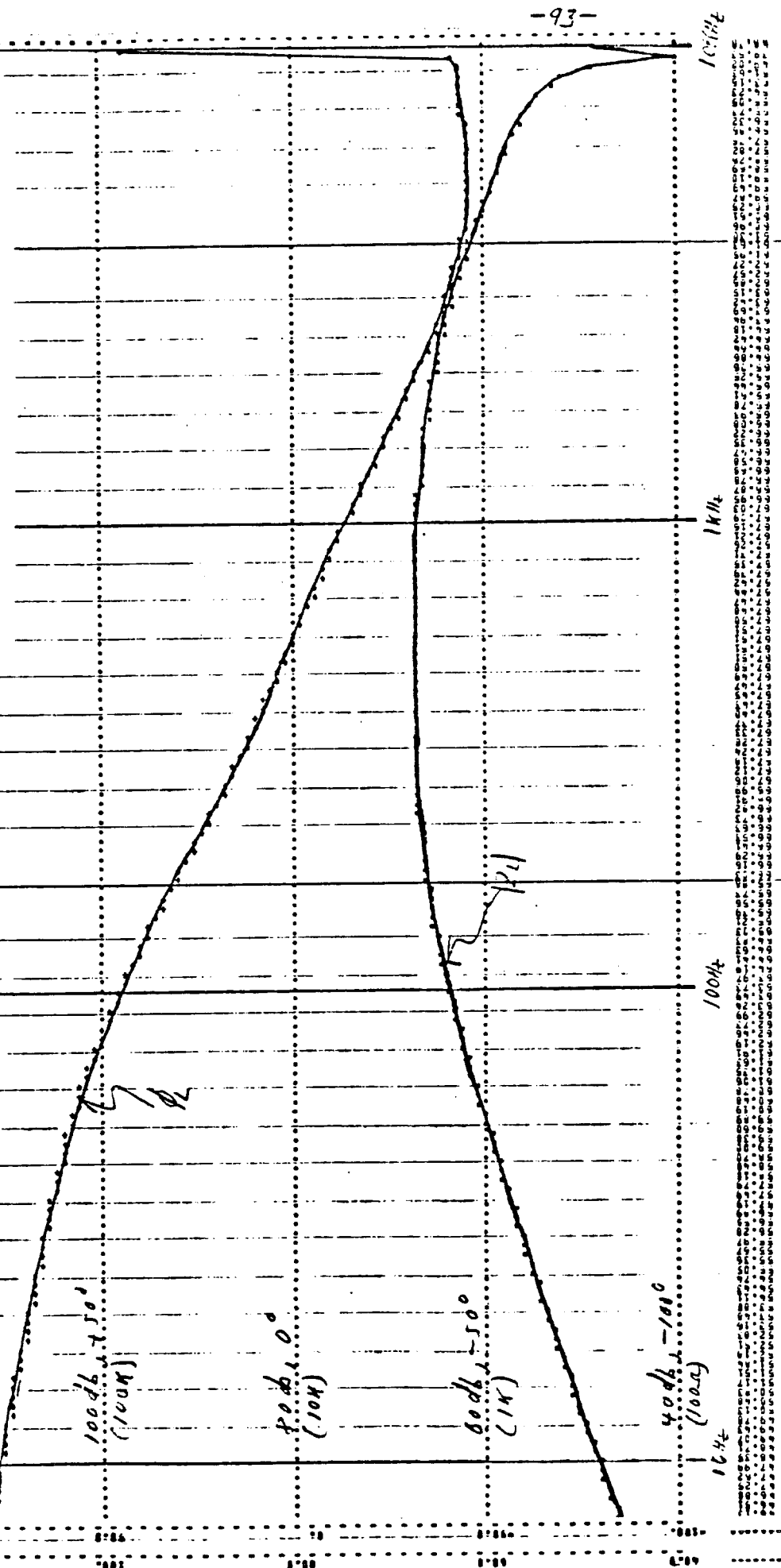
TRANSISTOR FET STANAG 2

TRANSISTOR IGBT STANAG 2

TRANSISTOR MOSFET STANAG 2

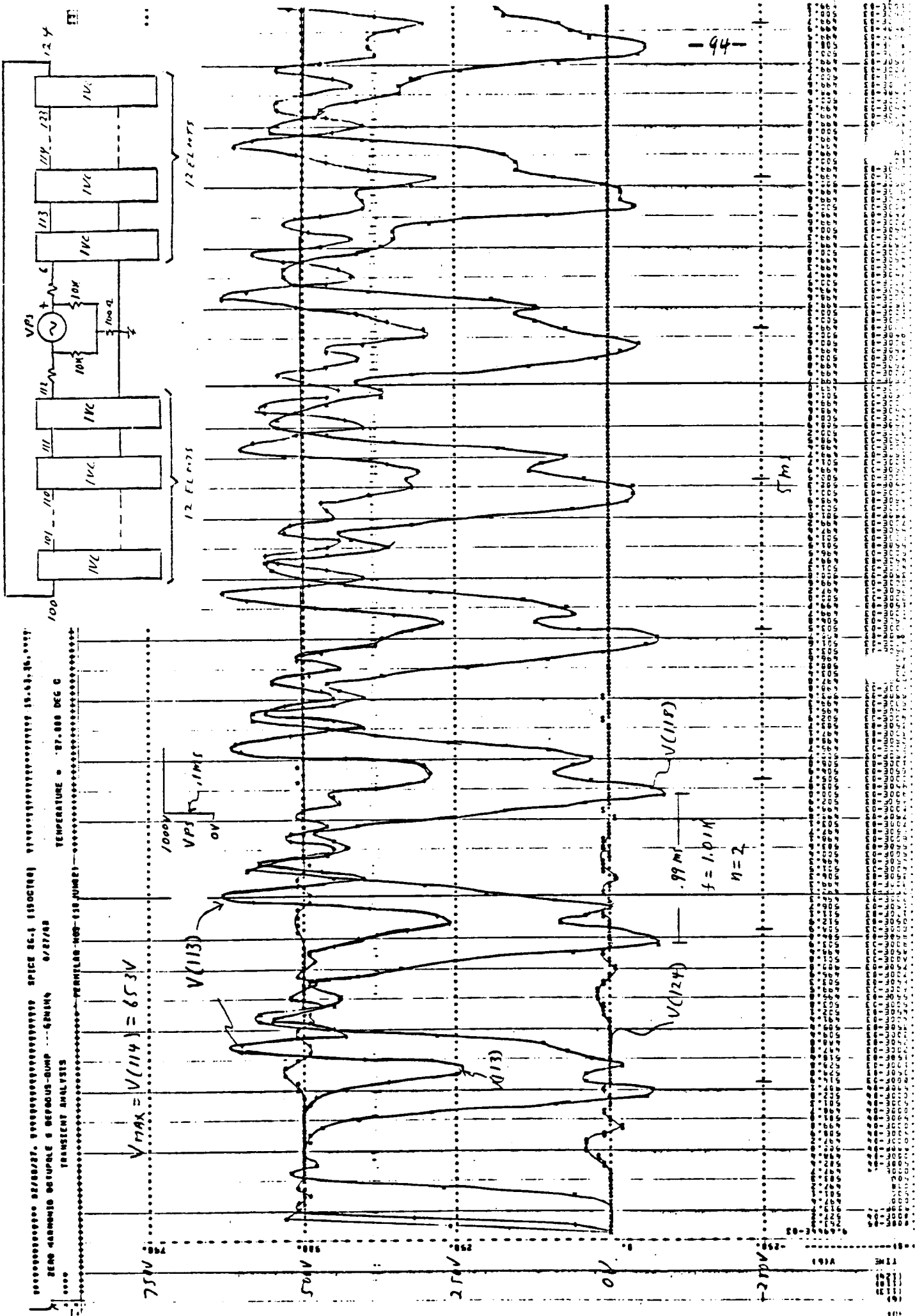


-93-

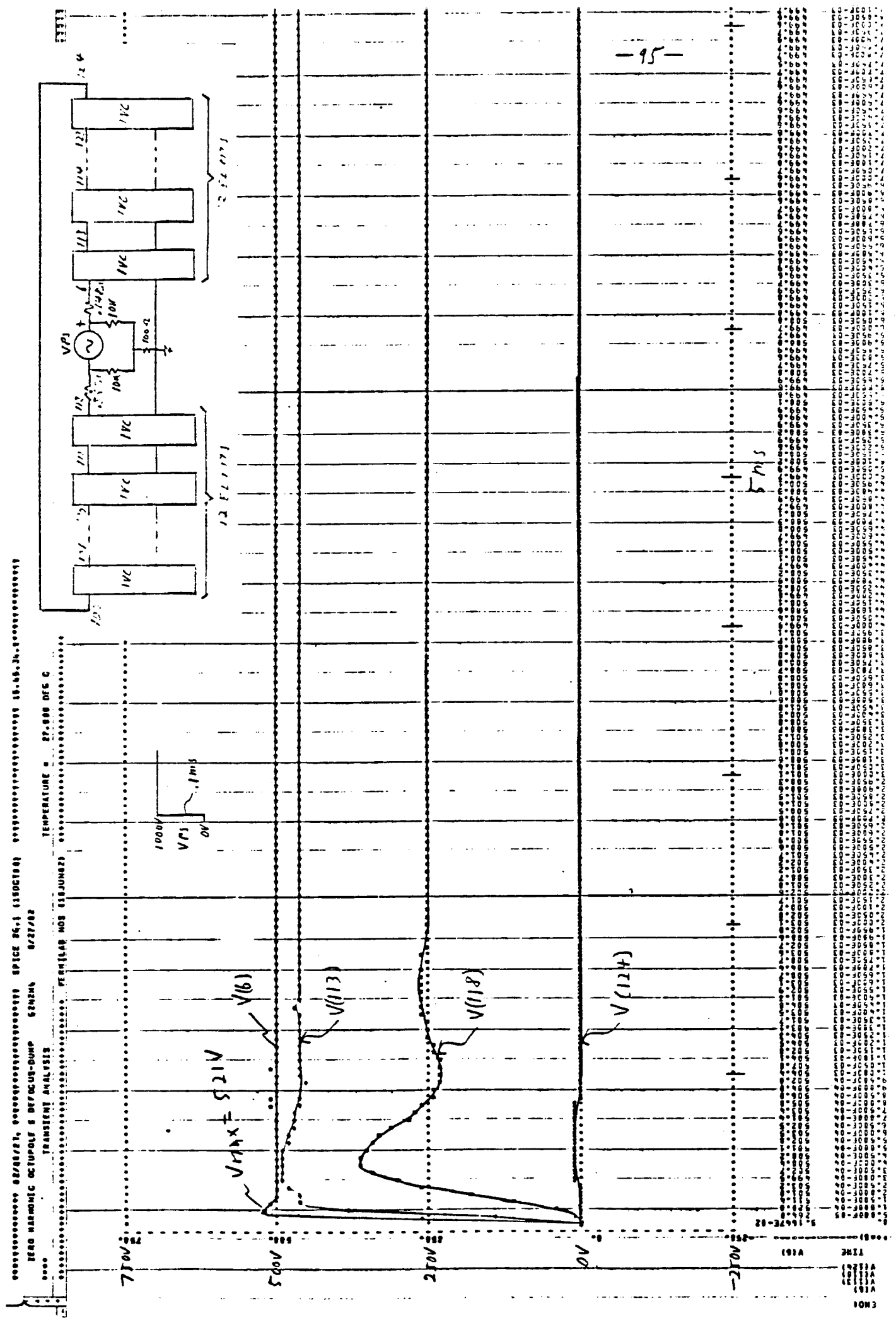


RECORDED BY [unclear]
DATE [unclear]
TIME [unclear]

ZERO HARMONIC OCTUPOLE AT DEFOCUSING LOC.: DUMP W/ RAMP = OPEN



ZERO HARMONIC OCTAPOLE AT DEFOCUSED OC: DIVERGE W NO AMP = 14



ENERGY DEPOSITION IN DOUBLER MAGNETS

DUE TO SCATTERING FROM

ES WIRE SEPTUM

1000 GEV

SEPTUM DOWNSTREAM OF THE FIRST MAGNET OF
A 4-MAGNET BEAM BUMP (VERTICAL BUMP)

PLUG: 5 CM (H) \times 3 CM (V)

COIL RADIAL RANGE: 3.81 TO 4.40 CM

ϕ ANGULAR RANGE:

○ 0.000 TO 0.100 RADIANS

● 3.042 TO 3.142 RADIANS

- ENERGY DENSITY, GEV / CM³ • INCIDENT PROTON)

10⁻²

9

8

7

6

5

4

3

2

1

0

10⁻³

9

8

7

6

5

4

3

2

1

0

10⁻⁴

9

8

7

6

5

4

3

2

1

0

10⁻⁵

9

8

7

6

5

4

3

2

1

0

10⁻⁶

9

8

7

6

5

4

3

2

1

0

10⁻⁷

0

20

40

DISTANCE FROM UPSTREAM END OF MAGNET (M)

Figure S33.